

STATIC AXIALLY SYMMETRIC EINSTEIN-YANG-MILLS-DILATON SOLUTIONS: I.REGULAR SOLUTIONS

Burkhard Kleihaus, and Jutta Kunz

Fachbereich Physik, Universität Oldenburg, Postfach 2503
D-26111 Oldenburg, Germany

We discuss the static axially symmetric regular solutions, obtained recently in Einstein-Yang-Mills and Einstein-Yang-Mills-dilaton theory [1]. These asymptotically flat solutions are characterized by the winding number $n > 1$ and the node number k of the purely magnetic gauge field. The well-known spherically symmetric solutions have winding number $n = 1$. The axially symmetric solutions satisfy the same relations between the metric and the dilaton field as their spherically symmetric counterparts. Exhibiting a strong peak along the ρ -axis, the energy density of the matter fields of the axially symmetric solutions has a torus-like shape. For fixed winding number n with increasing node number k the solutions form sequences. The sequences of magnetically neutral non-abelian axially symmetric regular solutions with winding number n tend to magnetically charged abelian spherically symmetric limiting solutions, corresponding to “extremal” Einstein-Maxwell-dilaton solutions for finite values of γ and to extremal Reissner-Nordström solutions for $\gamma = 0$, with n units of magnetic charge.

arXiv:gr-qc/9707045v1 19 Jul 1997

Preprint gr-qc/9707045

I. INTRODUCTION

SU(2) Einstein-Yang-Mills (EYM) and Einstein-Yang-Mills-dilaton (EYMD) theory possess a rich variety of solutions. Recently, we have constructed static axially symmetric regular and black hole solutions in these theories [1,2]. These solutions represent generalizations of the spherically symmetric regular and black hole solutions, known since several years [3–5]. All these solutions are characterized by two integers, the node number k of the gauge field function(s) and their winding number n with respect to the azimuthal angle ϕ , since the fields wind n times around while ϕ covers the full trigonometric circle once. The spherically symmetric solutions have winding number $n = 1$, a winding number $n > 1$ leads to axially symmetric solutions.

All these EYM and EYMD solutions are asymptotically flat and have non-trivial magnetic gauge field configurations, but no global charge. To every regular spherically symmetric solution there exists a corresponding family of black hole solutions with regular event horizon $x_H > 0$ [4,5]. The same holds true for the axially symmetric solutions [2]. Outside their event horizon these black hole solutions possess non-abelian hair. Therefore they represent counterexamples to the “no-hair” conjecture. The axially symmetric black hole solutions additionally contradict the expectation, that static black hole solutions are spherically symmetric. The spherically symmetric EYM and EYMD solutions are unstable [6,5], and there is all reason to believe, that the axially symmetric solutions are unstable, too.

For fixed n and increasing k the solutions form sequences, tending to limiting solutions. Although all solutions of a given sequence are neutral, the limiting solution is charged, and the winding number n of the solutions represents the charge of the limiting solution. The limiting solutions are spherically symmetric and abelian, representing Einstein-Maxwell-dilaton (EMD) [7] or Reissner-Nordström (RN) solutions for EYMD and EYM theory, respectively. In particular, the limiting solutions of the sequences of regular solutions correspond to extremal EMD and RN solutions.

The regular axially symmetric solutions have a torus-like shape. With the z -axis as symmetry axis, the energy density has a strong peak along the ρ -axis and decreases monotonically along the z -axis [1]. It has the same shape known from axially symmetric multimonopoles [8,9], from axially symmetric multiskyrmions [10] and from multisphalerons [11,12]. The energy density of the axially symmetric black hole solutions looks torus-like only for small horizon radii, for larger horizon radii it changes shape [2].

In EYMD theory the dilaton coupling constant γ represents a parameter. In the limit $\gamma \rightarrow 0$ the dilaton decouples and EYM theory is obtained, for $\gamma = 1$ contact with the low energy effective action of string theory is made, and in the limit $\gamma \rightarrow \infty$ gravity decouples and Yang-Mills-dilaton (YMD) theory is obtained. The YMD limit is of particular interest, since YMD theory also possesses static spherically symmetric and axially symmetric solutions [13,12]. In fact, the axially symmetric YMD solutions serve as starting configurations in our numerical construction of the regular EYMD and EYM solutions.

This paper is the first of two papers on static axially symmetric solutions in EYM and EYMD theory and presents a detailed account of the regular solutions [1]. The second paper will give a detailed account of the axially symmetric black hole solutions [2,14]. In section II of this paper we present the action, the axially symmetric ansatz in isotropic spherical coordinates and the boundary conditions. Further we derive relations between the metric and the dilaton field and expressions for the mass. In section III we recall the spherically symmetric solutions, presenting them in isotropic coordinates. In section IV we discuss the properties of the axially symmetric regular EYM and EYMD solutions and the convergence of the sequences of regular non-abelian solutions to limiting abelian solutions. We present our conclusions in section V. In Appendix A we formulate the ansatz in cylindrical coordinates. We present the equations of motion in Appendix B and the expansion of the functions at the origin and at infinity in Appendix C. Finally, in Appendix D we discuss some technical aspects concerning the construction of the axially symmetric solutions.

II. EINSTEIN-YANG-MILLS-DILATON EQUATIONS OF MOTION

A. Einstein-Yang-Mills-dilaton action

We consider the SU(2) Einstein-Yang-Mills-dilaton action

$$S = \int \left(\frac{R}{16\pi G} + L_M \right) \sqrt{-g} d^4x \quad (1)$$

with the matter Lagrangian

$$L_M = -\frac{1}{2} \partial_\mu \Phi \partial^\mu \Phi - e^{2\kappa\Phi} \frac{1}{2} \text{Tr}(F_{\mu\nu} F^{\mu\nu}), \quad (2)$$

the field strength tensor

$$F_{\mu\nu} = \partial_\mu A_\nu - \partial_\nu A_\mu + ie [A_\mu, A_\nu] , \quad (3)$$

the gauge field

$$A_\mu = \frac{1}{2} \tau^a A_\mu^a , \quad (4)$$

the dilaton field Φ , and the Yang-Mills and dilaton coupling constants e and κ , respectively.

Variation of the action (1) with respect to the metric $g^{\mu\nu}$ leads to the Einstein equations

$$G_{\mu\nu} = R_{\mu\nu} - \frac{1}{2} g_{\mu\nu} R = 8\pi G T_{\mu\nu} \quad (5)$$

with stress-energy tensor

$$\begin{aligned} T_{\mu\nu} &= g_{\mu\nu} L_M - 2 \frac{\partial L_M}{\partial g^{\mu\nu}} \\ &= \partial_\mu \Phi \partial_\nu \Phi - \frac{1}{2} g_{\mu\nu} \partial_\alpha \Phi \partial^\alpha \Phi + 2e^{2\kappa\Phi} \text{Tr}(F_{\mu\alpha} F_{\nu\beta} g^{\alpha\beta} - \frac{1}{4} g_{\mu\nu} F_{\alpha\beta} F^{\alpha\beta}) . \end{aligned} \quad (6)$$

Variation with respect to the gauge field A_μ and the dilaton field Φ leads to the matter field equations.

B. Static axially symmetric ansatz

We here formulate the ansatz in terms of spherical coordinates [2]. The equivalent formulation in terms of cylindrical coordinates [1] is given in Appendix A.

Instead of the Schwarzschild-like coordinates, used for the spherically symmetric EYM and EYMD solutions [3–5] (see section III), we adopt isotropic coordinates to obtain the static axially symmetric solutions. In terms of the spherical coordinates r , θ and ϕ the isotropic metric reads [15]

$$ds^2 = -f dt^2 + \frac{m}{f} dr^2 + \frac{mr^2}{f} d\theta^2 + \frac{lr^2 \sin^2 \theta}{f} d\phi^2 , \quad (7)$$

where the metric functions f , m and l are only functions of the coordinates r and θ . The z -axis ($\theta = 0$) represents the symmetry axis. Regularity on this axis requires [16]

$$m|_{\theta=0} = l|_{\theta=0} . \quad (8)$$

We take a purely magnetic gauge field, $A_0 = 0$, and choose for the gauge field the ansatz [8,11,12,1,2]

$$A_\mu dx^\mu = \frac{1}{2er} [\tau_\phi^n (H_1 dr + (1 - H_2) r d\theta) - n (\tau_r^n H_3 + \tau_\theta^n (1 - H_4)) r \sin \theta d\phi] . \quad (9)$$

Here the symbols τ_r^n , τ_θ^n and τ_ϕ^n denote the dot products of the cartesian vector of Pauli matrices, $\vec{\tau} = (\tau_x, \tau_y, \tau_z)$, with the spatial unit vectors

$$\begin{aligned} \vec{e}_r^n &= (\sin \theta \cos n\phi, \sin \theta \sin n\phi, \cos \theta) , \\ \vec{e}_\theta^n &= (\cos \theta \cos n\phi, \cos \theta \sin n\phi, -\sin \theta) , \\ \vec{e}_\phi^n &= (-\sin n\phi, \cos n\phi, 0) , \end{aligned} \quad (10)$$

respectively. Since the fields wind n times around, while the azimuthal angle ϕ covers the full trigonometric circle once, we refer to the integer n as the winding number of the solutions. The four gauge field functions H_i and the dilaton function Φ depend only on the coordinates r and θ . For $n = 1$ and $H_1 = H_3 = 0$, $H_2 = H_4 = w(r)$ and $\Phi = \Phi(r)$, the spherically symmetric ansatz of ref. [5] is recovered.

The ansatz (9) is axially symmetric in the sense, that a rotation around the z -axis can be compensated by a gauge rotation. The most general axially symmetric ansatz would contain nine gauge field functions (when $A_0 = 0$). By requiring additional discrete symmetries this number is reduced. The ansatz (9) respects the discrete mirror

symmetry $M_{xz} \otimes C$, where the first factor represents reflection through the xz -plane and the second factor denotes charge conjugation [17,11,18].

The ansatz is form-invariant under the abelian gauge transformation [17,11,12]

$$U = \exp\left(\frac{i}{2}\tau_\phi^n \Gamma(r, \theta)\right). \quad (11)$$

The functions H_1 and H_2 transform inhomogeneously under this gauge transformation,

$$\begin{aligned} H_1 &\rightarrow H_1 - r\partial_r\Gamma, \\ H_2 &\rightarrow H_2 + \partial_\theta\Gamma, \end{aligned} \quad (12)$$

like a 2-dimensional gauge field. The functions H_3 and H_4 combine to form a scalar doublet, $(H_3 + \text{ctg}\theta, H_4)$. The choice of an appropriate gauge leading to regular solutions presents a non-trivial problem [17,19]. We therefore fix the gauge by choosing the same gauge condition as previously [17,11,12,1]. In terms of the functions H_i it reads

$$r\partial_r H_1 - \partial_\theta H_2 = 0. \quad (13)$$

With the ansatz (7)-(9) and the gauge condition (13) we obtain the set of EYMD field equations. These are given in Appendix B. Here we only present the energy density of the matter fields $\epsilon = -T_0^0 = -L_M$

$$\begin{aligned} -T_0^0 &= \frac{f}{2m} \left[(\partial_r\Phi)^2 + \frac{1}{r^2}(\partial_\theta\Phi)^2 \right] + e^{2\kappa\Phi} \frac{f^2}{2e^2 r^4 m} \left\{ \frac{1}{m} (r\partial_r H_2 + \partial_\theta H_1)^2 \right. \\ &\quad + \frac{n^2}{l} \left[(r\partial_r H_3 - H_1 H_4)^2 + (r\partial_r H_4 + H_1 (H_3 + \text{ctg}\theta))^2 \right. \\ &\quad \left. \left. + (\partial_\theta H_3 - 1 + \text{ctg}\theta H_3 + H_2 H_4)^2 + (\partial_\theta H_4 + \text{ctg}\theta (H_4 - H_2) - H_2 H_3)^2 \right] \right\}, \end{aligned} \quad (14)$$

where the first gauge field term derives from $F_{r\theta}$, the second and third derive from $F_{r\phi}$ and the fourth and fifth from $F_{\theta\phi}$.

C. Boundary conditions

To obtain asymptotically flat solutions which are globally regular and possess the proper symmetries, we must impose certain boundary conditions [1,2]. Here we are looking for solutions with parity reflection symmetry. Therefore we need to consider the solutions only in the region $0 \leq \theta \leq \pi/2$, imposing boundary conditions along the ρ - and z -axis (i.e. for $\theta = \pi/2$ and $\theta = 0$). The complete solutions then follow from the symmetries. In the following we discuss the boundary conditions for the regular solutions, which possess axial and parity reflection symmetry. The expansions of the functions at the origin (in powers of r) and at infinity (in powers of $1/r$) are given in Appendix C.

Boundary conditions at infinity

Asymptotic flatness imposes for the metric functions of the regular solutions at infinity ($r = \infty$) the boundary conditions

$$f|_{r=\infty} = m|_{r=\infty} = l|_{r=\infty} = 1. \quad (15)$$

For the dilaton function we require

$$\Phi|_{r=\infty} = 0, \quad (16)$$

since any finite value of the dilaton field at infinity can always be transformed to zero via $\Phi \rightarrow \Phi - \Phi(\infty)$, $r \rightarrow r e^{-\kappa\Phi(\infty)}$. For magnetically neutral solutions, the gauge field functions H_i must satisfy

$$H_2|_{r=\infty} = H_4|_{r=\infty} = \pm 1, \quad H_1|_{r=\infty} = H_3|_{r=\infty} = 0. \quad (17)$$

Boundary conditions at the origin

Requiring the solutions to be regular at the origin ($r = 0$) leads to the boundary conditions for the metric functions

$$\partial_r f|_{r=0} = \partial_r m|_{r=0} = \partial_r l|_{r=0} = 0. \quad (18)$$

Analogously, the dilaton function must satisfy

$$\partial_r \Phi|_{r=0} = 0 , \quad (19)$$

and the set of gauge field functions H_i satisfies

$$H_2|_{r=0} = H_4|_{r=0} = 1, \quad H_1|_{r=0} = H_3|_{r=0} = 0 . \quad (20)$$

As for the spherically symmetric solutions [3–5], this choice of boundary conditions for the gauge field functions is always possible, because of the symmetry with respect to $H_i \rightarrow -H_i$. Solutions with an even number of nodes then have $H_2(\infty) = H_4(\infty) = 1$, whereas solutions with an odd number of nodes have $H_2(\infty) = H_4(\infty) = -1$.

Boundary conditions along the axes

The boundary conditions along the ρ - and z -axis ($\theta = \pi/2$ and $\theta = 0$) are determined by the symmetries. The metric functions satisfy along the axes

$$\begin{aligned} \partial_\theta f|_{\theta=0} &= \partial_\theta m|_{\theta=0} = \partial_\theta l|_{\theta=0} = 0 , \\ \partial_\theta f|_{\theta=\pi/2} &= \partial_\theta m|_{\theta=\pi/2} = \partial_\theta l|_{\theta=\pi/2} = 0 , \end{aligned} \quad (21)$$

in addition to the condition (8) along the z -axis. Likewise the dilaton function satisfies

$$\begin{aligned} \partial_\theta \Phi|_{\theta=0} &= 0 , \\ \partial_\theta \Phi|_{\theta=\pi/2} &= 0 \end{aligned} \quad (22)$$

along the axes. For the gauge field functions H_i symmetry considerations lead to the boundary conditions

$$\begin{aligned} H_1|_{\theta=0} &= H_3|_{\theta=0} = 0 , & \partial_\theta H_2|_{\theta=0} &= \partial_\theta H_4|_{\theta=0} = 0 , \\ H_1|_{\theta=\pi/2} &= H_3|_{\theta=\pi/2} = 0 , & \partial_\theta H_2|_{\theta=\pi/2} &= \partial_\theta H_4|_{\theta=\pi/2} = 0 \end{aligned} \quad (23)$$

along the axes.

D. Dimensionless Quantities

It is convenient to introduce dimensionless quantities. We introduce the dimensionless coordinate x ,

$$x = \frac{e}{\sqrt{4\pi G}} r , \quad (24)$$

the dimensionless dilaton function φ ,

$$\varphi = \sqrt{4\pi G} \Phi , \quad (25)$$

and the dimensionless dilaton coupling constant γ ,

$$\gamma = \frac{1}{\sqrt{4\pi G}} \kappa . \quad (26)$$

The value $\gamma = 1$ corresponds to string theory.

The dimensionless mass μ is related to the mass M via

$$\mu = \frac{eG}{\sqrt{4\pi G}} M . \quad (27)$$

E. Relations between metric and dilaton field

We now derive two relations between metric and dilaton field for static axially symmetric solutions of EYMD theory with purely magnetic gauge fields and a general gauge group. These relations are known to hold for the spherically symmetric solutions [20].

Let us return to eq. (2) and introduce the gauge field Lagrangian L_A

$$L_A = -\frac{1}{2}\text{Tr}(F_{\mu\nu}F^{\mu\nu}) . \quad (28)$$

From the action (1) we obtain the equation of motion for the dilaton field

$$\partial_\mu (\sqrt{-g}\partial^\mu\Phi) = -2\kappa\sqrt{-g}e^{2\kappa\Phi}L_A . \quad (29)$$

Our aim now is to replace the matter field functions on the r.h.s. of this equation by metric functions alone. Therefore we consider the matter lagrangian

$$L_M = -\frac{1}{2}\partial_\mu\Phi\partial^\mu\Phi + e^{2\kappa\Phi}L_A .$$

We replace L_M on the l.h.s. with help of the (00) component of the Einstein equations

$$G_{00} = 8\pi GT_{00} = 8\pi Gg_{00}L_M ,$$

and we replace the dilaton term on the r.h.s. with help of the contracted Einstein equations,

$$R = -8\pi GT_\mu{}^\mu = 8\pi G\partial_\mu\Phi\partial^\mu\Phi . \quad (30)$$

(For purely magnetic gauge fields the contracted gauge field stress energy tensor vanishes.) This gives for the matter part on the r.h.s. of eq. (29)

$$2e^{2\kappa\Phi}L_A = 2g^{00}T_{00} - g^{\mu\nu}T_{\mu\nu} = \frac{1}{8\pi G}(2g^{00}G_{00} + R) = \frac{1}{4\pi G}g^{00}R_{00} , \quad (31)$$

and the dilaton field equation becomes

$$\partial_\mu (\sqrt{-g}\partial^\mu\Phi) = -\frac{\kappa}{4\pi G}\sqrt{-g}g^{00}R_{00} . \quad (32)$$

By evaluating R_{00} explicitly for the metric (7), we find

$$-\sqrt{-g}g^{00}R_{00} = \frac{1}{2}\partial_\mu (\sqrt{-g}\partial^\mu \ln f) . \quad (33)$$

The dilaton equation then becomes

$$\partial_\mu \left(\sqrt{-g}\partial^\mu \left[\Phi - \frac{\kappa}{8\pi G} \ln f \right] \right) = 0 . \quad (34)$$

The derivation of the relations between metric and dilaton field is based on this equation.

Abbreviating the expression in square brackets in eq. (34) by B ,

$$B = \Phi - \frac{\kappa}{8\pi G} \ln f , \quad (35)$$

we now show that the regular static axially symmetric solutions satisfy $B = 0$. Therefore we multiply eq. (34) by B and integrate over r and θ . When integrating by parts, the surface terms vanish, (the boundary conditions eq. (15) and (16) give $B(\infty) = 0$.) and the integral becomes

$$\int_0^\infty \int_0^\pi (r^2(\partial_r B)^2 + (\partial_\theta B)^2) \sin\theta \sqrt{l} dr d\theta = 0 . \quad (36)$$

Since the integrand is positive this implies that B is constant. With $B(\infty) = 0$ this implies $B \equiv 0$, yielding the first relation between metric and dilaton field,

$$\Phi = \frac{\kappa}{8\pi G} \ln f . \quad (37)$$

Using dimensionless quantities, this relation reads

$$\varphi = \frac{\gamma}{2} \ln f = \frac{\gamma}{2} \ln(-g_{00}) , \quad (38)$$

representing the same relation obtained in the case of regular spherically symmetric solutions [20].

The second relation is either obtained by integrating eq. (34) over r and θ , or directly from eq. (37), which yields

$$\lim_{r \rightarrow \infty} r^2 \partial_r \Phi = \frac{\kappa}{8\pi G} \lim_{r \rightarrow \infty} r^2 \partial_r f , \quad (39)$$

since $f(\infty) = 1$. Changing to dimensionless quantities we find

$$\lim_{x \rightarrow \infty} x^2 \partial_x \varphi = \frac{\gamma}{2} \lim_{x \rightarrow \infty} x^2 \partial_x f . \quad (40)$$

The l.h.s. of eq. (40) defines the dilaton charge

$$D = \lim_{x \rightarrow \infty} x^2 \partial_x \varphi . \quad (41)$$

The r.h.s. of eq. (40) is proportional to the dimensionless mass μ

$$\mu = \frac{1}{2} \lim_{x \rightarrow \infty} x^2 \partial_x f , \quad (42)$$

as shown below. Together this yields the second relation

$$D = \gamma \mu , \quad (43)$$

which also holds for regular spherically symmetric solutions [20].

F. Mass

The mass M of the static axially symmetric solutions can be obtained directly from the total energy-momentum “tensor” $\tau^{\mu\nu}$ of matter and gravitation [21]

$$M = \int \tau^{00} d^3 r . \quad (44)$$

Adopting the procedure of [21], we start from the metric $g_{\mu\nu}$ in isotropic coordinates, eq. (7). We then change to quasi-Minkowskian coordinates, in the sense that the metric $\tilde{g}_{\mu\nu}$ approaches the Minkowski metric $\eta_{\mu\nu}$ at great distances, i.e. we introduce $h_{\mu\nu}$

$$\tilde{g}_{\mu\nu} = \eta_{\mu\nu} + h_{\mu\nu} \quad (45)$$

such that $h_{\mu\nu}$ vanishes at infinity. Identifying $h_{\mu\nu}$ from the metric equation, eq. (7), and employing the coordinates

$$x^1 = r \sin \theta \cos \phi , \quad x^2 = r \sin \theta \sin \phi , \quad x^3 = r \cos \theta , \quad (46)$$

we obtain

$$h_{\mu\nu} = \begin{pmatrix} -f + 1 & 0 & 0 & 0 \\ 0 & \frac{m}{f} \cos^2 \phi + \frac{l}{f} \sin^2 \phi - 1 & \left(\frac{m}{f} - \frac{l}{f}\right) \sin \phi \cos \phi & 0 \\ 0 & \left(\frac{m}{f} - \frac{l}{f}\right) \sin \phi \cos \phi & \frac{m}{f} \sin^2 \phi + \frac{l}{f} \cos^2 \phi - 1 & 0 \\ 0 & 0 & 0 & \frac{m}{f} - 1 \end{pmatrix} . \quad (47)$$

Indeed, $h_{\mu\nu}$ vanishes at infinity.

The exact Einstein equations can be written as

$$R_{\mu\nu}^{(1)} - \frac{1}{2}\eta_{\mu\nu}R^{(1)\lambda}_{\lambda} = -8\pi G(T_{\mu\nu} + t_{\mu\nu}) , \quad (48)$$

where $R_{\mu\nu}^{(1)}$ is the part of the Ricci tensor linear in $h_{\mu\nu}$. Interpreting the quantity

$$\tau^{\alpha\beta} = \eta^{\alpha\mu}\eta^{\beta\nu}(T_{\mu\nu} + t_{\mu\nu}) \quad (49)$$

as the total energy-momentum “tensor” of matter and gravitation, the mass is given as the volume integral over τ^{00} . Transforming this integral to a surface integral yields for the mass [21]

$$M = -\frac{1}{16\pi G} \int \left(\frac{\partial h_{jj}}{\partial x^i} - \frac{\partial h_{ij}}{\partial x^j} \right) \frac{x_i}{r} r^2 \sin\theta d\theta d\phi , \quad (50)$$

where x^i are the coordinates, eq. (46), and the integral is taken over a large sphere of radius $r \rightarrow \infty$. Evaluating the integrand, we obtain

$$M = -\frac{1}{16\pi G} \int \left(\frac{\partial}{\partial r} \left(\frac{m+l}{f} \right) + \frac{m-l}{rf} \right) r^2 \sin\theta d\theta d\phi . \quad (51)$$

Since the term in square brackets is independent of the angle for $r \rightarrow \infty$, the integration is trivial, yielding

$$M = -\frac{1}{4G} \lim_{r \rightarrow \infty} \left(\frac{\partial}{\partial r} \left(\frac{m+l}{f} \right) + \frac{m-l}{rf} \right) r^2 = \frac{1}{2G} \lim_{r \rightarrow \infty} r^2 \partial_r f , \quad (52)$$

where the last step makes use of the asymptotic behaviour of the metric functions (see Appendix C)

$$f = 1 + \frac{\tilde{f}_1}{r} + O\left(\frac{1}{r^2}\right) , \quad m = 1 + O\left(\frac{1}{r^2}\right) , \quad l = 1 + O\left(\frac{1}{r^2}\right) . \quad (53)$$

In dimensionless quantities, eq. (52) yields the desired relation for the mass, eq. (42).

We next show, that the mass of the regular axially symmetric solutions can also be obtained from

$$M = - \int_0^\infty \int_0^\pi \int_0^{2\pi} \sqrt{-g} (2T_0^0 - T_\mu^\mu) dr d\theta d\phi . \quad (54)$$

We start from the dilaton field equation (32)

$$\partial_\mu (\sqrt{-g} \partial^\mu \Phi) = \frac{\kappa}{4\pi G} \sqrt{-g} \frac{R_{00}}{f} \quad (55)$$

and replace the r.h.s with help of eq. (31)

$$\partial_\mu (\sqrt{-g} \partial^\mu \Phi) = -\kappa \sqrt{-g} (2T_0^0 - T_\mu^\mu) . \quad (56)$$

Integrating both sides over r , θ and ϕ , we obtain

$$4\pi \lim_{r \rightarrow \infty} r^2 \partial_r \Phi = -\kappa \int_0^\infty \int_0^\pi \int_0^{2\pi} \sqrt{-g} (2T_0^0 - T_\mu^\mu) dr d\theta d\phi = \kappa M , \quad (57)$$

where the last equality makes use of relation (39) together with eq. (52).

III. SPHERICALLY SYMMETRIC SOLUTIONS

The spherically symmetric EYM and EYMD solutions were obtained previously in Schwarzschild-like coordinates with metric [3,5,20]

$$ds^2 = -A^2 N dt^2 + \frac{1}{N} d\tilde{r}^2 + \tilde{r}^2 (d\theta^2 + \sin^2\theta d\phi^2) , \quad (58)$$

where the metric functions A and N are only functions of the radial coordinate \tilde{r} , and

$$N(\tilde{r}) = 1 - \frac{2\tilde{m}(\tilde{r})}{\tilde{r}} . \quad (59)$$

Since we here construct the static axially symmetric solutions in isotropic coordinates, we briefly review the spherical solutions in isotropic coordinates, derive the coordinate transformation between both sets of coordinates and discuss the limiting solutions.

A. Coordinate transformation

By requiring $l = m$ and the metric functions f and m to be only functions of the coordinate r , the axially symmetric isotropic metric (7) reduces to the spherically symmetric isotropic metric

$$ds^2 = -f dt^2 + \frac{m}{f} (dr^2 + r^2 (d\theta^2 + \sin^2 \theta d\phi^2)) . \quad (60)$$

Comparison with the metric (58) yields

$$\frac{m(r)}{f(r)} = \frac{\tilde{r}^2}{r^2} \quad (61)$$

and, with (61),

$$\frac{dr}{r} = \frac{1}{\sqrt{N(\tilde{r})}} \frac{d\tilde{r}}{\tilde{r}} . \quad (62)$$

The function $N(\tilde{r})$ (or equivalently the mass function $\tilde{m}(\tilde{r})$) is only known numerically. Therefore the coordinate function $r(\tilde{r})$ can only be obtained numerically from eq. (62). To obtain the coordinate transformation, we switch to dimensionless coordinates x and \tilde{x} and introduce the function β ,

$$\beta = \frac{x}{\tilde{x}} . \quad (63)$$

Rewriting eq. (62) in terms of β ,

$$\frac{d\ln\beta}{d\tilde{x}} = \frac{1}{\tilde{x}} \left(\frac{1}{\sqrt{N}} - 1 \right) , \quad (64)$$

we find

$$\beta(\tilde{x}) = \exp \left[- \int_{\tilde{x}}^{\infty} \frac{1}{\tilde{x}'} \left(\frac{1}{\sqrt{N}} - 1 \right) d\tilde{x}' \right] , \quad (65)$$

with

$$N(\tilde{x}) = 1 - \frac{2\mu(\tilde{x})}{\tilde{x}} . \quad (66)$$

The integrand is well behaved at the origin, since $\mu(\tilde{x}) \sim \tilde{x}^3$, and the integration constant is adjusted such that at infinity $\beta = 1$, i.e. $x = \tilde{x}$.

Fig. 1 demonstrates the coordinate transformation for the spherically symmetric EYMD solutions, for $\gamma = 1$ and $k = 1 - 4$. Figs. 2a,b show the metric functions f and m , and Figs. 3a,b show the gauge field function w and the dilaton function φ . These solutions satisfy relation (38), $\varphi = (\gamma/2)\ln f$ and relation (43), $D = \gamma\mu$, where $\mu = \mu(\infty)$ represents the dimensionless mass.

Fig. 4 demonstrates the coordinate transformation for the spherically symmetric EYM solutions, for $k = 1 - 4$. Figs. 5a,b show the metric functions f and m .

B. Limiting solutions

For fixed dilaton coupling constant γ , the sequence of neutral regular spherically symmetric EYMD solutions converges to a limiting solution [5,20]. This limiting solution is the ‘‘extremal’’ EMD solution [7] with horizon $\tilde{x} = 0$, charge $P = 1$, mass

$$\mu = P/\sqrt{1 + \gamma^2} \quad (67)$$

and dilaton charge $D = \gamma\mu$ (38). For $\gamma = 1$ the coordinate transformation for the limiting solution

$$x = \frac{1}{\sqrt{2}} \left(\sqrt{P^2 + 2\tilde{x}^2} - P \right) \quad (68)$$

is also shown in Fig. 1, the metric functions f and m of the limiting solution

$$ds^2 = - \left(\frac{x}{\sqrt{2P+x}} \right) dt^2 + \left(\frac{\sqrt{2P+x}}{x} \right) (dx^2 + x^2 (d\theta^2 + \sin^2 \theta d\phi^2)) \quad (69)$$

are also shown in Figs. 2, and the dilaton function φ of the limiting solution,

$$e^{2\varphi_\infty} = \frac{x}{\sqrt{2P+x}}, \quad (70)$$

is also shown in Fig. 3. The gauge field function of the limiting solution is trivial, $w_\infty = 0$. The limiting functions for f and φ are reached uniformly. In contrast, the function m approaches the limiting function $m_\infty = 1$ non-uniformly, since it tends to a constant $m(0) \neq 1$ at $x = 0$. Likewise the function w approaches the limiting function $w_\infty = 0$ non-uniformly, since the boundary conditions require $w(0) \neq 0$ as well as $w(\infty) \neq 0$.

The sequence of spherically symmetric regular EYM solutions also approaches a limiting solution [22]. In Schwarzschild-like coordinates this limiting solution consists of two parts. A non-trivial part for $\tilde{x} < 1$, representing an oscillating solution, and a simple part for $\tilde{x} > 1$, representing the exterior of an extremal RN solution with mass $\mu = 1$, horizon radius $\tilde{x}_H = 1$ and charge $P = 1$.

From Fig. 4 we observe, that with increasing k the interval $0 < \tilde{x} < 1$ is mapped to an ever smaller interval $0 < x < x_m$, with x_m tending to zero for $k \rightarrow \infty$. Therefore the limiting solution becomes rather simple in isotropic coordinates. The non-trivial part of the solution in Schwarzschild-like coordinates is mapped to zero, and the limiting solution corresponds to the exterior of an extremal RN solution with mass $\mu = 1$, horizon $x_H = 0$ and charge $P = 1$. The coordinate transformation for this limiting RN solution,

$$x = \tilde{x} - P, \quad (71)$$

is also shown in Fig. 4, and the metric functions f_∞ and m_∞ , given by the metric

$$ds^2 = - \left(\frac{x}{P+x} \right)^2 dt^2 + \left(\frac{P+x}{x} \right)^2 (dx^2 + x^2 (d\theta^2 + \sin^2 \theta d\phi^2)) \quad (72)$$

(i.e. $m_\infty = 1$), are also shown in Figs. 5. Again, the gauge field function of the limiting solution is trivial, $w_\infty = 0$, and the functions m and w approach the limiting functions non-uniformly.

IV. AXIALLY SYMMETRIC SOLUTIONS

Beginning with a short discription of the numerical technique, we here give a detailed description of the numerically constructed axially symmetric regular solutions. We discuss the properties of these solutions and the convergence of the various sequences of solutions to limiting solutions. Some technical aspects concerning the construction of the axially symmetric solutions are discussed in Appendix D.

A. Numerical technique

Subject to the above boundary conditions, we solve the system of coupled non-linear partial differential equations numerically. We employ the radial coordinate

$$\bar{x} = \frac{x}{1+x} \quad (73)$$

instead of x , to map spatial infinity to the finite value $\bar{x} = 1$ (see also Appendix B). The numerical calculations are performed with help of the program FIDISOL, which is extensively documented in [23]. The equations are discretized on a non-equidistant grid in \bar{x} and θ . Typical grids used have sizes 150×30 , covering the integration region $0 \leq \bar{x} \leq 1$ and $0 \leq \theta \leq \pi/2$.

The numerical method is based on the Newton-Raphson method, an iterative procedure to find a good approximation to the exact solution. Let us put the partial differential equations into the form $P(u) = 0$, where u denotes the unknown functions (and their derivatives). For an approximate solution $u^{(1)}$, $P(u^{(1)})$ does not vanish. If we could find a small

correction Δu , such that $u^{(1)} + \Delta u$ is the exact solution, $P(u^{(1)} + \Delta u) = 0$ should hold. Approximately the expansion in Δu gives

$$0 = P(u^{(1)} + \Delta u) \approx P(u^{(1)}) + \frac{\partial P}{\partial u}(u^{(1)})\Delta u .$$

The equation $P(u^{(1)}) = -\frac{\partial P}{\partial u}(u^{(1)})\Delta u$ can be solved to determine the correction $\Delta u^{(1)} = \Delta u$. $u^{(2)} = u^{(1)} + \Delta u^{(1)}$ will not be the exact solution but an improved approximate solution. Repeating the calculations iteratively, the approximate solutions will converge to the exact solution, provided the initial guess solution is close enough to the exact solution. The iteration stops after i steps if the Newton residual $P(u^{(i)})$ is smaller than a prescribed tolerance. Therefore it is essential to have a good first guess, to start the iteration procedure. Our strategy therefore is to use a known solution as guess and then vary some parameter to produce the next solution. To construct regular axially symmetric EYMD and EYM solutions, we have used the known regular axially symmetric YMD solutions [12] as starting solutions, corresponding to the limit $\gamma \rightarrow \infty$. Beginning with large values of the parameter γ , γ is slowly decreased, until EYMD solutions with $\gamma = 1$ and EYM solutions ($\gamma = 0$) are obtained. A second procedure, also employed, is to start from the spherically symmetric regular solutions with $n = 1$, and then increase the ‘parameter’ n slowly, to obtain the desired EYMD and EYM solutions at integer values of n .

For a numerical solution it is important to have information about its quality, i. e. to have an error estimate. The error originates from the discretization of the system of partial differential equations. It depends on the number of gridpoints and on the order of consistency of the differential formulae for the derivatives. FIDISOL provides an error estimate for each unknown function, corresponding to the maximum of the discretization error divided by the maximum of the function. For the solutions presented here the estimations of the relative error for the functions are on the order of 10^{-3} and 10^{-2} for $k < 4$ and $k = 4$, respectively.

B. Properties of the solutions

For the static axially symmetric solutions constructed here, the functions depend on two variables, the radial coordinate x and the angle θ . In the following we either present the functions in three-dimensional plots, employing the compactified coordinates $\bar{\rho} = \bar{x} \sin \theta$ and $\bar{z} = \bar{x} \cos \theta$ (with \bar{x} given in eq. (73)), or we present the functions in two-dimensional plots exhibiting the x -dependence for three fixed angles, $\theta = 0$, $\theta = \pi/4$ and $\theta = \pi/2$. While the three-dimensional plots give a good qualitative picture of the solutions, the two-dimensional plots are better for a quantitative analysis of the solutions and in particular for a comparison of solutions with differing values of n , k or γ .

We begin with a description of the lowest axially symmetric regular solution of EYMD and EYM theory. This solution has winding number $n = 2$ and node number $k = 1$. The EYMD solution for $\gamma = 1$ is shown in Figs. 6-9. Figs. 6a-c show the metric functions f , m and l . The functions m and l have a rather similar shape. Figs. 7a-d show the gauge field functions H_1 - H_4 . The single (non-trivial) node of the functions H_2 , H_3 and H_4 is seen in Fig. 7e. The lines representing the position of the node of H_2 and H_4 are close together. The non-trivial node of the function H_3 is located farther outwards. Interestingly, the nodal lines of the functions H_2 - H_4 are almost spherical. The function H_1 does not possess a non-trivial node. Fig. 8 shows the dilaton function φ , which is related to the metric function f via (38). Fig. 9 presents the energy density of the matter fields ϵ , showing a pronounced peak along the ρ -axis and decreasing monotonically along the z -axis. Thus equal density contours reveal a torus-like shape of the solutions. The maximum of the energy density ϵ_{\max} and the location ρ_{\max} of the maximum of the energy density are shown in Table 1 along with the mass of the solution.

The corresponding EYM solution looks very similar to the EYMD solution. We therefore exhibit only the energy density of the matter fields for this solution in Fig. 10. The mass of the solution is shown in Table 2 along with the maximum of the energy density ϵ_{\max} and the location ρ_{\max} of the maximum of the energy density.

Let us now consider the lowest solutions for higher winding number. To see the change of the functions for node number $k = 1$ with increasing winding number n , we exhibit in Figs. 11-14 the EYMD solutions for $\gamma = 1$ with $n = 1$, 2 and 4. Figs. 11a-c show the metric functions, Figs. 12a-d the gauge field functions, Fig. 13 the dilaton function and Fig. 14 the energy density of the matter fields. Obviously, the angle-dependence of the metric and matter functions increases strongly with n . The location of the biggest angular splitting of the metric and the matter field functions moves further outward with increasing n along with the location of the nodes of the gauge field functions H_2 - H_4 . At the same time the peak of the energy density along the ρ -axis shifts outward with increasing n and decreases in height. At the origin the values of the metric functions increase with n , while the central energy density decreases. The nodal line of the functions H_2 - H_4 remains almost spherical with increasing n , and H_1 remains nodeless. (Note, that H_1 and H_3 are zero on the axes in Figs. 12a,c.)

By decreasing γ from one to zero, we obtain the corresponding EYM solutions, shown in Figs. 15-17. Qualitatively the EYM solutions look like their EYMD counterparts. But there are a number of quantitative differences. The metric functions of the EYM solutions are considerably smaller at the origin, the gauge field functions have their peaks and nodes shifted inwards, and the energy density of the matter fields has slightly higher peaks, which are also shifted inwards, as compared to the EYMD solutions. The masses increase with decreasing γ , as seen in Tables 1-3.

We now consider the radially excited solutions. To see the change of the functions for fixed winding number n with increasing node number k , we exhibit in Figs. 18-21 the EYMD solutions for $\gamma = 1$ winding number $n = 2$ and node number $k = 1 - 4$. Figs. 18a-c show the metric functions, Figs. 19a-d the gauge field functions, Fig. 20 the dilaton function and Fig. 21 the energy density of the matter fields. The magnitude of the angular dependence of the metric and matter functions stays roughly the same with increasing k in these figures. The peak of the energy density of the matter fields moves inward with increasing k and at the same time increases strongly in height, along with the central density. The gauge field functions H_2 and H_4 have precisely k nodes, the gauge field function H_1 has $k - 1$ nodes, and the gauge field function H_3 has one node.

Again, the corresponding EYM solutions are similar to these EYMD solutions. We exhibit only the metric functions in Figs. 22 and the energy density of the matter fields in Fig. 23. Again, the metric functions of the EYM solutions are considerably smaller at the origin, and the gauge field functions have their peaks and nodes shifted inwards, as compared to the EYMD solutions. But the energy density of the matter fields increases only moderately with k , indicating a finite limit for the energy density of the EYM solutions. In contrast, the dramatic increase of the energy density of the matter fields of the EYMD solutions with increasing k indicates a diverging limit.

The masses of the EYMD solutions with $\gamma = 1$ are shown in Table 1, and the masses of the EYM solutions are shown in Table 2. The EYMD solutions for other values of γ are similar to these solutions. For comparison, Table 3 presents the masses of the solutions with $n = 3$ and $k = 1 - 4$ for several values of γ . In the limit $\gamma \rightarrow 0$ the EYM solutions are obtained, and in the limit $\gamma \rightarrow \infty$ the corresponding YMD solutions [1,12].

C. Limiting solutions

Let us now consider the limiting solutions of the sequences of axially symmetric solutions with fixed winding number n , dilaton coupling constant γ and increasing node number k . For $n > 1$ the pattern of convergence is similar to the one observed in the spherically symmetric case, $n = 1$, considered in section III.

For fixed winding number n and dilaton coupling constant γ , we consider the solutions with $k = 1 - 4$, shown in Figs. 18-23 and Tables 1-3, and extrapolate to the limit $k \rightarrow \infty$, to obtain the limiting solution, also shown. For finite γ this limiting solution is an “extremal” EMD solution with mass $\mu_\infty = n/\sqrt{1 + \gamma^2}$ (67), charge $P = n$ and metric (69). For $\gamma = 0$ it represents the exterior solution of an extremal RN solution with mass $\mu_\infty = n$, horizon $x_H = 0$, charge $P = n$ and metric (71). So we find, that this limiting solution is spherically symmetric, although the solutions of the sequence are axially symmetric, and that this limiting solution carries charge n , although the solutions of the sequence are magnetically neutral.

The limiting values for the mass represent upper bounds for the sequences. The convergence of the mass μ_k to the mass of the corresponding limiting solution μ_∞ is exponential. This is demonstrated in Figs. 24, where we show the deviation of the mass of the k -th solution from the mass of the limiting solution, $\Delta\mu_k$,

$$\Delta\mu_k = \mu_\infty(\infty) - \mu_k(\infty) , \quad (74)$$

for fixed winding number n , $n = 1 - 4$, and $\gamma = 1$ (Fig. 24a) as well as $\gamma = 0$ (Fig. 24b). As required for an exponential convergence, the logarithm of the deviation $\Delta\mu_k$ is a straight line as a function of k . The slope of this straight line decreases with increasing n , thus the larger n the slower is the convergence to the limiting solution.

The convergence of the functions of the axially symmetric solutions is less rapid than the convergence of the mass. The metric function f , the gauge field functions H_1 and H_3 and the dilaton function φ converge uniformly to the corresponding functions f_∞ , $H_{1,\infty}$, $H_{3,\infty}$ and φ_∞ of the limiting solution. For instance we observe from Fig. 20, that the dilaton function φ deviates from φ_∞ only in an inner region, which decreases exponentially with k . The metric functions m and l also deviate from the limiting functions $m_\infty = 1$ and $l_\infty = 1$ only in an exponentially decreasing inner region. But the metric functions m and l as well as the gauge field functions H_2 and H_4 converge non-uniformly to the corresponding limiting functions. The metric functions m and l tend to constants $m(0) \neq 1$ and $l(0) \neq 1$ at the origin, while the gauge field functions H_2 and H_4 differ from the value zero of the limiting solution both at the origin and at infinity because of their boundary conditions.

V. CONCLUSIONS

We have given strong numerical evidence, that both EYMD and EYM theory possess sequences of regular static axially symmetric solutions, in addition to the known static spherically symmetric solutions. These sequences are characterized by the winding number $n > 1$, and the solutions within each sequence by the node number k . (For $n = 1$ the spherically symmetric solutions are recovered.) To rigorously establish the existence of these solutions a formal existence proof is desirable, analogous to the proof given for the spherically symmetric solutions [24].

For fixed n and $\gamma > 0$ ($\gamma = 0$) the sequences of regular axially symmetric solutions tend to limiting solutions. These are the “extremal” EMD solutions [7] (the exterior solutions of the extremal RN solutions) with magnetic charge n and the same γ . This generalizes the corresponding observation for the sequences of spherically symmetric solutions [5,20]. For the YMD solutions the limiting solutions are magnetic monopoles with n units of charge [12].

The regular axially symmetric solutions have a torus-like shape. Otherwise, many properties of the axially symmetric solutions are similar to those of their spherically symmetric counterparts. In particular, there is all reason to believe, that these static regular axially symmetric EYMD and EYM solutions are unstable. Since we can also associate the Chern-Simons number $N_{CS} = n/2$ [11,18] (for odd k [25]) with these solutions, we interpret them as *gravitating multisphalerons*.

Having constructed the axially symmetric solutions in EYMD and EYM theory, it appears straightforward to construct analogous solutions in other non-abelian theories. For instance, we expect to find gravitating axially symmetric multimonopoles in SU(2) Einstein-Yang-Mills-Higgs (EYMH) theory with a Higgs triplet, gravitating axially symmetric multisphalerons in SU(2) EYMH theory with a Higgs doublet, or gravitating axially symmetric multiskyrmions in SU(2) Einstein-Skyrme (ES) theory. In particular we expect, that the lowest gravitating axially symmetric $n = 2$ multimonopole and multiskyrmion solutions are stable.

We expect, that the axially symmetric solutions represent only the simplest type of non-spherical gravitating regular solutions in EYMD and EYM theory as well as in other non-abelian theories. We conjecture, that there are gravitating regular solutions with much more complex shapes and only discrete symmetries left. Such solutions arise in flat space for instance in SU(2) Skyrme theory [26,27] and in SU(2) Yang-Mills-Higgs theory [28], representing multiskyrmions with higher baryon number and multimonopoles with higher charge, respectively.

But EYMD and EYM theory also possess black hole solutions. The non-abelian spherically symmetric black hole solutions may be regarded as black holes inside sphalerons [25]. The axially symmetric black hole solutions in EYM and EYMD theory [2], corresponding to black holes inside multisphalerons, will be discussed in detail in [14]. We expect analogous black hole solutions in EYMH and ES theory. Indeed, a perturbative calculation has revealed not only axially symmetric EYMH black holes, but also black holes without rotational symmetry [29].

We would like to thank the RRZN in Hannover for computing time.

- [1] B. Kleihaus and J. Kunz, Static axially symmetric solutions of Einstein-Yang-Mills-dilaton theory, Phys. Rev. Lett. 78 (1997) 2527.
- [2] B. Kleihaus and J. Kunz, Static black hole solutions with axial symmetry, gr-qc/9704060.
- [3] R. Bartnik and J. McKinnon, Particlelike solutions of the Einstein-Yang-Mills equations, Phys. Rev. Lett. 61 (1988) 141.
- [4] M. S. Volkov and D. V. Gal'tsov, Black holes in Einstein-Yang-Mills theory, Sov. J. Nucl. Phys. 51 (1990) 747;
P. Bizon, Colored black holes, Phys. Rev. Lett. 64 (1990) 2844;
H. P. Künzle and A. K. M. Masoud-ul-Alam, Spherically symmetric static SU(2) Einstein-Yang-Mills fields, J. Math. Phys. 31 (1990) 928.
- [5] E. E. Donets and D. V. Gal'tsov, Stringy sphalerons and non-abelian black holes, Phys. Lett. B302 (1993) 411;
G. Lavrelashvili and D. Maison, Regular and black hole solutions of Einstein-Yang-Mills dilaton theory, Nucl. Phys. B410 (1993) 407;
T. Torii and K. Maeda, Black holes with non-Abelian hair and their thermodynamical properties, Phys. Rev. D48 (1993) 1643;
C. M. O'Neill, Einstein-Yang-Mills theory with a massive dilaton and axion: String-inspired regular and black hole solutions, Phys. Rev. D50 (1994) 865;
P. Bizon, Saddle points of stringy action, Acta Physica Polonica B24 (1993) 1209.
- [6] N. Straumann and Z. H. Zhou, Instability of the Bartnik-McKinnon solutions of the Einstein-Yang-Mills equations, Phys. Lett. B237 (1990) 353;
N. Straumann and Z. H. Zhou, Instability of colored black hole solutions, Phys. Lett. B243 (1990) 33;

- M. S. Volkov and D. V. Gal'tsov, Odd-parity negative modes of Einstein-Yang-Mills black holes and sphalerons, *Phys. Lett.* B341 (1995) 279;
- G. Lavrelashvili, and D. Maison, A remark on the instability of the Bartnik-McKinnon solutions, *Phys. Lett.* B343 (1995) 214;
- M. S. Volkov, O. Brodbeck, G. Lavrelashvili and N. Straumann, The number of sphaleron instabilities of the Bartnik-McKinnon solitons and nonabelian black holes, *Phys. Lett.* B349 (1995) 438.
- [7] G. W. Gibbons and K. Maeda, Black holes and membranes in higher-dimensional theories with dilaton fields, *Nucl. Phys.* B298 (1988) 741;
- D. Garfinkle, G. T. Horowitz and A. Strominger, Charged black holes in string theory, *Phys. Rev.* D43 (1991) 3140.
- [8] C. Rebbi and P. Rossi, Multimono-pole solutions in the Prasad-Sommerfield limit, *Phys. Rev.* D22 (1980) 2010.
- [9] R. S. Ward, A Yang-Mills Higgs monopole of charge 2, *Commun. Math. Phys.* 79 (1981) 317;
- P. Forgacs, Z. Horvath and L. Palla, Exact multimono-pole solutions in the Bogomolny-Prasad-Sommerfield limit, *Phys. Lett* B99 (1981) 232;
- P. Forgacs, Z. Horvath and L. Palla, Non-linear superposition of monopoles, *Nucl. Phys.* B192 (1981) 141.
- [10] V. B. Kopeliovich and B. E. Stern, Exotic Skyrmions, *JETP Lett.* 45 (1987) 203;
- N. S. Manton, Is the B=2 Skyrmion axially symmetric?, *Phys. Lett.* B192 (1987) 177;
- J. J. M. Verbaarschot, Axial symmetry of bound baryon number two solution of the Skyrme model, *Phys. Lett.* B195 (1987) 235.
- [11] B. Kleihaus and J. Kunz, Multisphalerons in the weak interactions, *Phys. Lett.* B329 (1994) 61;
- B. Kleihaus and J. Kunz, Multisphalerons in the Weinberg-Salam theory, *Phys. Rev.* D50 (1994) 5343.
- [12] B. Kleihaus and J. Kunz, Axially symmetric multisphalerons in Yang-Mills-dilaton theory, *Phys. Lett.* B392 (1997) 135.
- [13] G. Lavrelashvili and D. Maison, Static spherically symmetric solutions of a Yang-Mills field coupled to a dilaton, *Phys. Lett.* B295 (1992) 67;
- P. Bizon, Saddle-point solutions in Yang-Mills-dilaton theory, *Phys. Rev.* D47 (1993) 1656.
- [14] B. Kleihaus and J. Kunz, Static axially symmetric Einstein-Yang-Mills-dilaton solutions: II. Black hole solutions, in preparation.
- [15] Another parametrization of the isotropic metric is given in Appendix D.
- [16] see e. g. D. Kramer, H. Stephani, E. Herlt, and M. MacCallum, *Exact Solutions of Einstein's Field Equations*, Ch. 17 (Cambridge University Press, Cambridge, 1980)
- [17] B. Kleihaus, J. Kunz and Y. Brihaye, The electroweak sphaleron at physical mixing angle, *Phys. Lett.* 273B (1991) 100;
- J. Kunz, B. Kleihaus, and Y. Brihaye, Sphalerons at finite mixing angle, *Phys. Rev.* D46 (1992) 3587.
- [18] Y. Brihaye and J. Kunz, Axially symmetric solutions in the electroweak theory, *Phys. Rev.* D50 (1994) 4175.
- [19] Y. Brihaye, B. Kleihaus and J. Kunz, Sphalerons at finite mixing angle and singular gauges, *Phys. Rev.* D47 (1993) 1664.
- [20] B. Kleihaus, J. Kunz and A. Sood, SU(3) Einstein-Yang-Mills-dilaton sphalerons and black holes, *Phys. Lett.* B374 (1996) 289;
- B. Kleihaus, J. Kunz and A. Sood, Sequences of Einstein-Yang-Mills-dilaton black holes, *Phys. Rev.* D54 (1996) 5070.
- [21] S. Weinberg, *Gravitation and Cosmology* (Wiley, New York, 1972)
- [22] J. A. Smoller and A. G. Wasserman, An investigation of the limiting behavior of particle-like solutions to the Einstein-Yang/Mills equations and a new black hole solution, *Commun. Math. Phys.* 161 (1994) 365;
- P. Breitenlohner, P. Forgacs and D. Maison, Static spherically symmetric solutions of the Einstein-Yang-Mills equations, *Commun. Math. Phys.* 163 (1994) 141;
- P. Breitenlohner and D. Maison, On the limiting solution of the Bartnik-McKinnon family, *Commun. Math. Phys.* 171 (1995) 685.
- [23] W. Schönauer and R. Weiß, *J. Comput. Appl. Math.* 27, 279 (1989) 279; M. Schauder, R. Weiß and W. Schönauer, The CADSOL Program Package, Universität Karlsruhe, Interner Bericht Nr. 46/92 (1992).
- [24] J. A. Smoller, A. G. Wasserman, S. T. Yau and J. B. McLeod, Smooth static solutions of the Einstein/Yang-Mills equations, *Commun. Math. Phys.* 143 (1991) 115;
- J. A. Smoller and A. G. Wasserman, Existence of infinitely many smooth, static, global solutions of the Einstein/Yang-Mills equations, *Commun. Math. Phys.* 151 (1993) 303.
- [25] D. V. Gal'tsov and M. S. Volkov, Sphalerons in Einstein-Yang-Mills theory, *Phys. Lett.* B263 (1991) 255.
- [26] E. Braaten, S. Townsend and L. Carson, Novel structure of static multisoliton solutions in the Skyrme model, *Phys. Lett.* B235 (1990) 147.
- [27] R. A. Battye and P. M. Sutcliffe, Symmetric Skyrmions, hep-th/9702089;
- C. J. Houghton, N. S. Manton, P. M. Sutcliffe, Rational Maps, Monopoles and Skyrmions, hep-th/9705151.
- [28] N. J. Hitchin, N. S. Manton and M. K. Murray, Symmetric monopoles, *Nonlinearity* 8 (1995) 661;
- C. J. Houghton and P. M. Sutcliffe, Tetrahedral and cubic monopoles, *Commun. Math. Phys.* 180 (1996) 343;
- C. J. Houghton and P. M. Sutcliffe, Octahedral and dodecahedral monopoles, *Nonlinearity* 9 (1996) 385.
- [29] S. A. Ridgway and E. J. Weinberg, Static black hole solutions without rotational symmetry, *Phys. Rev.* D52 (1995) 3440.
- [30] This form of the isotropic metric, supplemented with a fifth function for the $dtd\phi$ -term was used in the calculation of rotating boson stars [31].

- [31] F. Schunck, Selbstgravitierende bosonische Materie, PhD Thesis, Universität zu Köln (1995) (Cuvillier Verlag, Göttingen, 1996)

VI. APPENDIX A

We here present the ansatz, the gauge condition and the boundary conditions in cylindrical coordinates, as employed in [1]. We also show the relation of the functions H_i , used in this paper, to the functions F_i , employed in [1].

A. Ansatz in cylindrical coordinates

In terms of the cylindrical coordinates ρ and z the metric in isotropic coordinates reads

$$ds^2 = -f dt^2 + \frac{m}{f} (d\rho^2 + dz^2) + \frac{l}{f} \rho^2 d\phi^2, \quad (75)$$

where the metric functions f , m and l are only functions of ρ and z .

The gauge field is parametrized by [8,11,12,1]

$$A_\mu dx^\mu = \frac{1}{2} [\tau_\phi^n (w_1^3 d\rho + w_2^3 dz) + (\tau_\rho^n w_3^1 + \tau_z w_3^2) \rho d\phi], \quad (76)$$

where τ_ϕ^n , τ_ρ^n and τ_z denote the dot products of the cartesian vector of Pauli matrices with the spatial unit vectors

$$\vec{e}_\phi^n = (-\sin n\phi, \cos n\phi, 0), \quad \vec{e}_\rho^n = (\cos n\phi, \sin n\phi, 0), \quad \vec{e}_z = (0, 0, 1), \quad (77)$$

respectively. The four functions w_j^i and the dilaton function Φ depend only on the coordinates ρ and z .

With respect to the gauge transformation (11),

$$U = \exp\left(\frac{i}{2} \tau_\phi^n \Gamma(\rho, z)\right), \quad (78)$$

the functions $(\rho w_3^1, \rho w_3^2 - n/e)$ transform like a scalar doublet, and the functions (w_1^3, w_2^3) transform like a 2-dimensional gauge field. The gauge condition reads [17,11,12,1]

$$\partial_\rho w_1^3 + \partial_z w_2^3 = 0. \quad (79)$$

With the ansatz (75)-(76) and the gauge condition (79) the set of EYMD field equations is obtained. The energy density of the matter fields $\epsilon = -T_0^0 = -L_M$ reads

$$\begin{aligned} -T_0^0 = & \frac{f}{2m} [(\partial_\rho \Phi)^2 + (\partial_z \Phi)^2] + e^{2\kappa\Phi} \frac{f^2}{2m^2} (\partial_\rho w_2^3 - \partial_z w_1^3)^2 \\ & + e^{2\kappa\Phi} \frac{f^2}{2ml} \left[\left(\partial_\rho w_3^1 + \frac{(nw_1^3 + w_3^1)}{\rho} - ew_1^3 w_3^2 \right)^2 + \left(\partial_\rho w_3^2 + \frac{w_3^2}{\rho} + ew_1^3 w_3^1 \right)^2 \right. \\ & \left. + \left(\partial_z w_3^1 + \frac{nw_2^3}{\rho} - ew_2^3 w_3^2 \right)^2 + (\partial_z w_3^2 + ew_2^3 w_3^1)^2 \right]. \end{aligned} \quad (80)$$

Transforming to spherical coordinates r and θ ($\rho = r \sin \theta$, $z = r \cos \theta$), the gauge field functions $F_i(r, \theta)$ are introduced via [11,12,1]

$$\begin{aligned} w_1^3 &= \frac{1}{er} (1 - F_1) \cos \theta, & w_2^3 &= -\frac{1}{er} (1 - F_2) \sin \theta, \\ w_3^1 &= -\frac{n}{er} (1 - F_3) \cos \theta, & w_3^2 &= \frac{n}{er} (1 - F_4) \sin \theta. \end{aligned} \quad (81)$$

The spherically symmetric ansatz of ref. [5] is recovered for $F_1 = F_2 = F_3 = F_4 = w(r)$, $\Phi = \Phi(r)$ and $n = 1$.

B. Boundary conditions

At infinity the boundary conditions for the metric functions and the dilaton functions are given by eqs. (15)-(16), whereas the gauge field functions F_i satisfy

$$F_1|_{r=\infty} = F_2|_{r=\infty} = F_3|_{r=\infty} = F_4|_{r=\infty} = \pm 1 . \quad (82)$$

At the origin the boundary conditions for the metric functions and the dilaton functions are given by eqs. (18)-(19), and the set of gauge field functions F_i satisfies

$$F_1|_{r=0} = F_2|_{r=0} = F_3|_{r=0} = F_4|_{r=0} = 1 . \quad (83)$$

Along the ρ - and z -axis, the boundary conditions for the metric functions and the dilaton function are given by eqs. (21)-(22), and for the gauge field functions F_i by

$$\begin{aligned} \partial_\theta F_1|_{\theta=0} &= \partial_\theta F_2|_{\theta=0} = \partial_\theta F_3|_{\theta=0} = \partial_\theta F_4|_{\theta=0} = 0 \\ \partial_\theta F_1|_{\theta=\pi/2} &= \partial_\theta F_2|_{\theta=\pi/2} = \partial_\theta F_3|_{\theta=\pi/2} = \partial_\theta F_4|_{\theta=\pi/2} = 0 \end{aligned} \quad (84)$$

with the exception of $F_2(r, \theta)$ for $n = 2$, which has

$$\partial_\theta F_2(r, \theta)|_{\theta=0} \neq 0 \quad (\text{for } n = 2) . \quad (85)$$

C. Relation between H_i and F_i

The functions F_i are related to the functions $H_i(r, \theta)$ via

$$\begin{aligned} H_1 &= \sin \theta \cos \theta (F_2 - F_1) , \\ H_3 &= \sin \theta \cos \theta (F_4 - F_3) , \\ H_2 &= \cos^2 \theta F_1 + \sin^2 \theta F_2 , \\ H_4 &= \cos^2 \theta F_3 + \sin^2 \theta F_4 . \end{aligned} \quad (86)$$

Note, that the boundary conditions on the z -axis for the functions F_i , eqs. (84), imply the boundary conditions for the functions H_i , eqs. (23), but not vice versa. The boundary conditions (23) allow for $\partial_\theta F_2(r, \theta)|_{\theta=0} \neq 0$ i. e. they properly incorporate the case $n = 2$ with condition (85).

VII. APPENDIX B

We here derive the equations of motion in isotropic spherical coordinates.

A. Tensors $F_{\mu\nu}$, $T_{\mu\nu}$, $G_{\mu\nu}$

We expand the field strength tensor with respect to the Pauli matrices τ_λ^n , ($\lambda = r, \theta, \phi$, see eq. (10))

$$F_{\mu\nu} = F_{\mu\nu}^{(\lambda)} \frac{\tau_\lambda^n}{2} .$$

Inserting ansatz (9) for the gauge field, we obtain the non-vanishing coefficients $F_{\mu\nu}^{(\lambda)}$,

$$\begin{aligned} F_{r\theta}^{(\phi)} &= -\frac{1}{r} (H_{1,\theta} + rH_{2,r}) , \\ F_{r\phi}^{(r)} &= -n \frac{\sin \theta}{r} (rH_{3,r} - H_1 H_4) , \\ F_{r\phi}^{(\theta)} &= n \frac{\sin \theta}{r} (rH_{4,r} + H_1 H_3 + \cot \theta H_1) , \\ F_{\theta\phi}^{(r)} &= -n \sin \theta (H_{3,\theta} - 1 + H_2 H_4 + \cot \theta H_3) , \\ F_{\theta\phi}^{(\theta)} &= n \sin \theta (H_{4,\theta} - H_2 H_3 - \cot \theta (H_2 - H_4)) , \end{aligned} \quad (87)$$

and $F_{\mu\nu}^{(\lambda)} = -F_{\nu\mu}^{(\lambda)}$. It is convenient to define

$$\begin{aligned} F_{r\theta}^2 &= \left(F_{r\theta}^{(\phi)}\right)^2 + \frac{1}{r^2} (rH_{1,r} - H_{2,\theta})^2, \\ F_{r\phi}^2 &= \left(F_{r\phi}^{(r)}\right)^2 + \left(F_{r\phi}^{(\theta)}\right)^2, \\ F_{\theta\phi}^2 &= \left(F_{\theta\phi}^{(r)}\right)^2 + \left(F_{\theta\phi}^{(\theta)}\right)^2, \end{aligned} \tag{88}$$

where the second term in the definition of $F_{r\theta}^2$ represents the gauge fixing term.

With the ansatz for the metric (7) we obtain the Lagrange densities

$$\begin{aligned} L_F &= -\frac{f}{2m} \left(\frac{f}{r^2 m} F_{r\theta}^2 + \frac{f}{r^2 \sin^2 \theta l} (F_{r\phi}^2 + \frac{1}{r^2} F_{\theta\phi}^2) \right), \\ L_\Phi &= -\frac{f}{2m} \left(\Phi_{,r}^2 + \frac{1}{r^2} \Phi_{,\theta}^2 \right), \\ L_M &= L_\Phi + e^{2\kappa\Phi} L_F, \end{aligned} \tag{89}$$

and the non-vanishing components of the stress energy tensor,

$$\begin{aligned} T_{00} &= \frac{f^2}{2m} \left(\Phi_{,r}^2 + \frac{1}{r^2} \Phi_{,\theta}^2 + e^{2\kappa\Phi} \left[\frac{f}{r^2 m} F_{r\theta}^2 + \frac{f}{r^2 \sin^2 \theta l} (F_{r\phi}^2 + \frac{1}{r^2} F_{\theta\phi}^2) \right] \right), \\ T_{rr} &= \frac{1}{2} \left(\Phi_{,r}^2 - \frac{1}{r^2} \Phi_{,\theta}^2 + e^{2\kappa\Phi} \left[\frac{f}{r^2 m} F_{r\theta}^2 + \frac{f}{r^2 \sin^2 \theta l} (F_{r\phi}^2 - \frac{1}{r^2} F_{\theta\phi}^2) \right] \right), \\ T_{\theta\theta} &= \frac{r^2}{2} \left(-\Phi_{,r}^2 + \frac{1}{r^2} \Phi_{,\theta}^2 + e^{2\kappa\Phi} \left[\frac{f}{r^2 m} F_{r\theta}^2 + \frac{f}{r^2 \sin^2 \theta l} (-F_{r\phi}^2 + \frac{1}{r^2} F_{\theta\phi}^2) \right] \right), \\ T_{\phi\phi} &= \frac{r^2 \sin \theta l}{2m} \left(-\Phi_{,r}^2 - \frac{1}{r^2} \Phi_{,\theta}^2 + e^{2\kappa\Phi} \left[-\frac{f}{r^2 m} F_{r\theta}^2 + \frac{f}{r^2 \sin^2 \theta l} (F_{r\phi}^2 + \frac{1}{r^2} F_{\theta\phi}^2) \right] \right), \\ T_{r\theta} &= \Phi_{,r} \Phi_{,\theta} + e^{2\kappa\Phi} \frac{f}{r^2 \sin^2 \theta l} (F_{r\phi}^{(r)} F_{\theta\phi}^{(r)} + F_{r\phi}^{(\theta)} F_{\theta\phi}^{(\theta)}). \end{aligned} \tag{90}$$

The Einstein tensor has the non-vanishing components

$$\begin{aligned} G_{00} &= -\frac{f^2}{4r^2 m} \\ &\left(2 \left(\frac{m_{,\theta,\theta} + r^2 m_{,r,r} + r m_{,r}}{m} - \left(\frac{m_{,\theta}}{m} \right)^2 - \left(\frac{r m_{,r}}{m} \right)^2 \right) + \left(2 \frac{l_{,\theta,\theta} + r^2 l_{,r,r} + 3 r l_{,r}}{l} - \left(\frac{l_{,\theta}}{l} \right)^2 - \left(\frac{r l_{,r}}{l} \right)^2 \right) \right. \\ &- 4 \frac{f_{,\theta,\theta} + r^2 f_{,r,r}}{f} + 5 \left(\left(\frac{f_{,\theta}}{f} \right)^2 + \left(\frac{r f_{,r}}{f} \right)^2 \right) \\ &\left. - 2 \left(\left(4 + \frac{r l_{,r}}{l} \right) \frac{r f_{,r}}{f} + \frac{l_{,\theta}}{l} \frac{f_{,\theta}}{f} \right) + 4 \left(\frac{l_{,\theta}}{l} - \frac{f_{,\theta}}{f} \right) \cot \theta \right), \\ G_{rr} &= \frac{1}{4r^2} \left(2 \frac{l_{,\theta,\theta}}{l} - \left(\frac{l_{,\theta}}{l} \right)^2 + 2 \left(\frac{r l_{,r}}{l} + \frac{r m_{,r}}{m} \right) + \frac{r m_{,r}}{m} \frac{r l_{,r}}{l} - \frac{m_{,\theta}}{m} \frac{l_{,\theta}}{l} + \left(\frac{f_{,\theta}}{f} \right)^2 - \left(\frac{r f_{,r}}{f} \right)^2 \right. \\ &\left. - 2 \left(\frac{m_{,\theta}}{m} - 2 \frac{l_{,\theta}}{l} \right) \cot \theta \right), \\ G_{\theta\theta} &= \frac{1}{4} \left(2 \frac{r^2 l_{,r,r}}{l} - \left(\frac{r l_{,r}}{l} \right)^2 + 4 \frac{r l_{,r}}{l} - 2 \frac{r m_{,r}}{m} - \frac{r m_{,r}}{m} \frac{r l_{,r}}{l} + \frac{m_{,\theta}}{m} \frac{l_{,\theta}}{l} + \left(\frac{r f_{,r}}{f} \right)^2 - \left(\frac{f_{,\theta}}{f} \right)^2 + 2 \frac{m_{,\theta}}{m} \cot \theta \right), \end{aligned}$$

$$\begin{aligned}
G_{\phi\phi} &= \frac{l \sin^2 \theta}{4m} \left(2 \left(\frac{r^2 m_{,r,r} + r m_{,r} + m_{,\theta,\theta}}{m} - \left(\frac{m_{,\theta}}{m} \right)^2 - \left(\frac{r m_{,r}}{m} \right)^2 \right) + \left(\frac{f_{,\theta}}{f} \right)^2 + \left(\frac{r f_{,r}}{f} \right)^2 \right), \\
G_{r\theta} &= \frac{1}{4r} \left(-2 \frac{r l_{,r,\theta}}{l} + \frac{r l_{,r}}{l} \frac{l_{,\theta}}{l} + \frac{r m_{,r}}{m} \frac{l_{,\theta}}{l} + \frac{r l_{,r}}{l} \frac{m_{,\theta}}{m} + 2 \frac{m_{,\theta}}{m} - 2 \frac{r f_{,r}}{f} \frac{f_{,\theta}}{f} + 2 \left(\frac{r m_{,r}}{m} - \frac{r l_{,r}}{l} \right) \cot \theta \right).
\end{aligned} \tag{91}$$

With these results at hand we now derive the equations of motion.

B. Matter equations

The equations of motion for the gauge field functions and for the dilaton function are obtained from the variation of the matter part of the action (1),

$$\begin{aligned}
0 &= \left(r^2 H_{1,r,r} + H_{1,\theta,\theta} + H_{2,\theta} - n^2 \frac{m}{l} (r H_{4,r} H_3 - r H_{3,r} H_4 + (H_3^2 + H_4^2 - 1) H_1) \right) \sin^2 \theta \\
&\quad + \left(r H_{2,r} + H_{1,\theta} - n^2 \frac{m}{l} (2 H_1 H_3 + r H_{4,r}) \right) \sin \theta \cos \theta - n^2 \frac{m}{l} H_1 \\
&\quad + \sin^2 \theta [H_{1,\theta} + r H_{2,r}] \ln \left(\Sigma \frac{l}{m} \right)_{,\theta} + \sin^2 \theta [r H_{1,r} - H_{2,\theta}] r \ln \left(\Sigma \frac{l}{m} \right)_{,r}
\end{aligned} \tag{92}$$

$$\begin{aligned}
0 &= \left(-r^2 H_{2,r,r} + H_{2,\theta,\theta} - H_{1,\theta} \right) + n^2 \frac{m}{l} (H_4 H_{3,\theta} - H_3 H_{4,\theta} + (H_3^2 + H_4^2 - 1) H_2) \sin^2 \theta \\
&\quad + \left(r H_{1,r} - H_{2,\theta} + n^2 \frac{m}{l} (2 H_2 H_3 - H_{4,\theta}) \right) \sin \theta \cos \theta + n^2 \frac{m}{l} (H_2 - H_4) \\
&\quad + \sin^2 \theta [r H_{1,r} - H_{2,\theta}] \ln \left(\Sigma \frac{l}{m} \right)_{,\theta} - \sin^2 \theta [H_{1,\theta} + r H_{2,r}] r \ln \left(\Sigma \frac{l}{m} \right)_{,r}
\end{aligned} \tag{93}$$

$$\begin{aligned}
0 &= \left(r^2 H_{3,r,r} + H_{3,\theta,\theta} - H_3 (H_1^2 + H_2^2) + H_1 (H_4 - 2r H_{4,r}) - H_4 (r H_{1,r} - H_{2,\theta}) + 2 H_2 H_{4,\theta} \right) \sin^2 \theta \\
&\quad + (H_{3,\theta} + H_2 H_4 - H_1^2 - H_2^2) \sin \theta \cos \theta - H_3 \\
&\quad + \sin^2 \theta [H_{3,\theta} - 1 + H_2 H_4 + \cot \theta H_3] \ln (\Sigma)_{,\theta} + \sin^2 \theta [r H_{3,r} - H_1 H_4] r \ln (\Sigma)_{,r}
\end{aligned} \tag{94}$$

$$\begin{aligned}
0 &= \left(-r^2 H_{4,r,r} - H_{4,\theta,\theta} + H_4 (H_1^2 + H_2^2) + H_1 H_3 - H_2 (1 - 2 H_{3,\theta}) - 2r H_{3,r} H_1 - H_3 (r H_{1,r} - H_{2,\theta}) \right) \sin^2 \theta \\
&\quad + (H_2 H_3 + H_1 - r H_{1,r} + H_{2,\theta} - H_{4,\theta}) \sin \theta \cos \theta - (H_2 - H_4) \\
&\quad - \sin^2 \theta [H_{4,\theta} - H_3 H_2 - (H_2 - H_4) \cot \theta] \ln (\Sigma)_{,\theta} - \sin^2 \theta [r H_{4,r} + H_1 H_3 + \cot \theta H_1] r \ln (\Sigma)_{,r}
\end{aligned} \tag{95}$$

$$\begin{aligned}
0 &= \Phi_{,r,r} + \frac{1}{r^2} \Phi_{,\theta,\theta} - \kappa e^{2\kappa\Phi} \left(\frac{f}{r^2 m} F_{r\theta}^2 + \frac{f}{r^2 \sin^2 \theta l} (F_{r\phi}^2 + \frac{1}{r^2} F_{\theta\phi}^2) \right) \\
&\quad + \ln(\sin \theta \sqrt{l r^2})_{,r} \Phi_{,r} + \frac{1}{r^2} \ln(\sin \theta \sqrt{l r^2})_{,\theta} \Phi_{,\theta}
\end{aligned} \tag{96}$$

with $\Sigma = e^{2\kappa\Phi} \frac{f}{\sqrt{l}}$. The differential equations for the gauge field functions and the dilaton function are diagonal in the second derivatives with respect to the variable r .

C. Metric equations

The equations for the metric functions are the Einstein equations

$$8\pi G T_{\mu\nu} = G_{\mu\nu} . \tag{97}$$

They represent five differential equations for three metric functions. Two of these equations are redundant and can be used to achieve a convenient form of the three equations to be solved numerically (see Appendix D).

We diagonalize the Einstein equations with respect to the set of derivatives $(f_{,r,r}, m_{,r,r}, l_{,r,r}, l_{,\theta,\theta}, l_{,r,\theta})$. Except for the (00) equation, these equations are already diagonal. The resulting equation for the (00) component is

$$8\pi G \frac{m}{f} (T_\mu^\mu - 2T_0^0) = \frac{1}{r^2} \left(\frac{r^2 f_{,r,r} + f_{,\theta,\theta} + 2r f_{,r}}{f} - \left(\left(\frac{f_{,\theta}}{f} \right)^2 + \left(\frac{r f_{,r}}{f} \right)^2 \right) + \cot \theta \frac{f_{,\theta}}{f} + \frac{1}{2} \left(\frac{r f_{,r}}{f} \frac{r l_{,r}}{l} + \frac{f_{,\theta}}{f} \frac{l_{,\theta}}{l} \right) \right). \quad (98)$$

Then we solve the (rr) component for $(\frac{r f_{,r}}{f})^2$ and substitute this expression into the $(\phi\phi)$ and $(\theta\theta)$ components, yielding

$$8\pi G \frac{m}{f} (T_r^r + T_\phi^\phi) = \frac{1}{4r^2} \left(2 \left(\frac{r^2 m_{,r,r} + r m_{,r} + m_{,\theta,\theta}}{m} - \left(\frac{m_{,\theta}}{m} \right)^2 - \left(\frac{r m_{,r}}{m} \right)^2 \right) + 2 \frac{l_{,\theta,\theta}}{l} + 2 \left(\frac{f_{,\theta}}{f} \right)^2 - \left(\frac{l_{,\theta}}{l} \right)^2 + 2 \left(\frac{r l_{,r}}{l} + \frac{r m_{,r}}{m} \right) + \frac{r m_{,r}}{m} \frac{r l_{,r}}{l} - \frac{m_{,\theta}}{m} \frac{l_{,\theta}}{l} - 2 \left(\frac{m_{,\theta}}{m} - 2 \frac{l_{,\theta}}{l} \right) \cot \theta \right), \quad (99)$$

$$8\pi G \frac{m}{f} (T_r^r + T_\theta^\theta) = \frac{1}{4r^2} \left(2 \frac{r^2 l_{,r,r} + l_{,\theta,\theta}}{l} - \left(\frac{l_{,\theta}}{l} \right)^2 - \left(\frac{r l_{,r}}{l} \right)^2 + 6 \frac{r l_{,r}}{l} + 4 \frac{l_{,\theta}}{l} \cot \theta \right). \quad (100)$$

The differential equations (92)-(96) and (98)-(100) are then diagonal in the second derivatives with respect to the radial variable r .

Finally we change to dimensionless quantities x , φ and γ , (eqs. (24)-(26)) and furthermore to the radial variable \bar{x} , (eq. (73)), thus mapping the infinite interval of the variable x onto the finite interval $[0, 1]$ of the variable \bar{x} . For the derivatives this leads to the substitutions

$$r F_{,r} \longrightarrow \bar{x} (1 - \bar{x}) F_{,\bar{x}}, \quad (101)$$

$$r^2 F_{,r,r} \longrightarrow \bar{x}^2 \left((1 - \bar{x})^2 F_{,\bar{x},\bar{x}} - 2(1 - \bar{x}) F_{,\bar{x}} \right) \quad (102)$$

for any function F in the differential equations. In this form we have solved the system of differential equations numerically.

VIII. APPENDIX C

Here we present the expansion of the functions at the origin in powers of x and at infinity in powers of $1/x$.

A. Expansion at the origin

Expanding the gauge field functions, the dilaton function and the metric functions at the origin up to the second order in x we obtain

$$\begin{aligned} H_1 &= x^2 \sin \theta \cos \theta H_{11} + O(x^3), \\ H_2 &= 1 - x^2 \frac{H_{11}}{2} (1 - 2 \sin^2 \theta) + O(x^3), \\ H_3 &= x^2 \sin \theta \cos \theta H_{31} + O(x^3), \\ H_4 &= 1 - x^2 \left(\frac{H_{11}}{2} - H_{31} \sin^2 \theta \right) + O(x^3), \\ \varphi &= \varphi_0 - x^2 \left((1 - 3 \cos^2 \theta) \frac{\varphi_1}{2} - n^2 \gamma \sin^2 \theta \frac{f_0}{4l_0} e^{2\gamma\varphi_0} (H_{11} - 2H_{31})^2 \right) + O(x^3), \end{aligned} \quad (103)$$

$$\begin{aligned}
f &= f_0 \left(1 - x^2 \left(\frac{f_1}{2} (1 - 3 \cos^2 \theta) - n^2 \sin^2 \theta \frac{f_0}{2l_0} e^{2\gamma\varphi_0} (H_{11} - 2H_{31})^2 \right) \right) + O(x^3) , \\
m &= l_0 \left(1 - x^2 \left(l_1 (1 - 2 \cos^2 \theta) - n^2 \sin^2 \theta \frac{f_0}{l_0} e^{2\gamma\varphi_0} (H_{11} - 2H_{31})^2 \right) \right) + O(x^3) , \\
l &= l_0 \left(1 - x^2 \frac{l_1}{3} (1 - 4 \cos^2 \theta) \right) + O(x^3) ,
\end{aligned}$$

where H_{11} , H_{31} , φ_0 , φ_1 , f_0 , f_1 , l_0 and l_1 are constants.

B. Expansion at infinity

Expanding the gauge field functions, the dilaton function and the metric functions at infinity in powers of $\frac{1}{x}$ we obtain

$$\begin{aligned}
H_1 &= \frac{1}{x^2} \bar{H}_{12} \sin \theta \cos \theta + O\left(\frac{1}{x^3}\right) , \\
H_2 &= \pm 1 + \frac{1}{2x^2} \bar{H}_{12} (\cos^2 \theta - \sin^2 \theta) + O\left(\frac{1}{x^3}\right) , \\
H_3 &= \frac{1}{x} \sin \theta \cos \theta \bar{H}_{31} + \frac{1}{4x^2} \sin \theta \cos \theta (\pm 2\bar{H}_{12} + \bar{H}_{31} (\bar{f}_1 + 2\gamma\bar{\varphi}_1)) + O\left(\frac{1}{x^3}\right) , \\
H_4 &= \pm \left(1 + \frac{1}{x} \bar{H}_{31} \sin^2 \theta - \frac{1}{4x^2} \sin^2 \theta (\pm 2\bar{H}_{12} + \bar{H}_{31} (\bar{f}_1 + 2\gamma\bar{\varphi}_1)) \right) + O\left(\frac{1}{x^3}\right) , \\
\varphi &= \frac{1}{x} \bar{\varphi}_1 + O\left(\frac{1}{x^3}\right) , \\
f &= 1 + \frac{1}{x} \bar{f}_1 + \frac{1}{2x^2} \bar{f}_1^2 + O\left(\frac{1}{x^3}\right) , \\
m &= 1 + \frac{1}{x^2} \bar{l}_2 + \frac{1}{x^2} \sin^2 \theta \bar{m}_2 + O\left(\frac{1}{x^3}\right) , \\
l &= 1 + \frac{1}{x^2} \bar{l}_2 + O\left(\frac{1}{x^3}\right) ,
\end{aligned} \tag{104}$$

with constants \bar{H}_{12} , \bar{H}_{31} , \bar{f}_1 , $\bar{\varphi}_1$, \bar{m}_2 and \bar{l}_2 .

IX. APPENDIX D

Here we discuss some technical aspects concerning the construction of the axially symmetric solutions.

A. Metric

Prior to the metric (7) we have employed the isotropic metric in the form [30]

$$ds^2 = -f dt^2 + e^{\bar{\mu}} (dr^2 + r^2 d\theta^2) + \bar{l} r^2 \sin^2 \theta d\phi^2 , \tag{105}$$

where the metric functions f , $\bar{\mu}$ and \bar{l} are functions of the coordinates r and θ . At infinity, the functions satisfy

$$\begin{aligned}
f &= 1 + \frac{1}{x} \bar{f}_1 + O\left(\frac{1}{x^2}\right) , \\
\bar{\mu} &= -\frac{1}{x} \bar{f}_1 + O\left(\frac{1}{x^2}\right) ,
\end{aligned}$$

$$l = 1 - \frac{1}{x} \bar{f}_1 + O\left(\frac{1}{x^2}\right), \quad (106)$$

$$(107)$$

with constant \bar{f}_1 . We have also replaced the function $\bar{\mu}$ by the new function \bar{m} ,

$$\bar{m} = e^{\bar{\mu}}. \quad (108)$$

Our final choice of metric parametrization with

$$\bar{m} = \frac{m}{f} \quad \text{and} \quad \bar{l} = \frac{l}{f}, \quad (109)$$

has the advantage that it does lead to a faster convergence of the metric functions m and l to their limiting values (see Appendix C).

B. Einstein equations

We have diagonalized the Einstein equations with respect to the second derivatives in r of the metric functions. But this diagonalization is ambiguous, since only 3 of 5 equations are needed. In the earliest calculations we followed the diagonalization scheme employed in ref. [31]. However, these calculations did not properly produce the asymptotic behaviour of the derivative $\partial_x \bar{\mu}$. Using another linear combination of the equations, the problem was shifted to the asymptotic behaviour of the derivative $\partial_x f$. The problem persisted even for the spherical solutions, indicating that its origin resided in the program package FIDISOL. Therefore we looked for a combination of the equations which FIDISOL would deal with properly. We realized, that eliminating the square of the first derivatives of f , $(\partial_r f)^2$, from the metric equations, would precisely do this. Eqs. (99) and (100) then become identical in the spherically symmetric case, $n = 1$. In this form the computations with FIDISOL give the correct behaviour of the functions for $n = 1$ and also for $n > 1$. This motivates our final choice of the equations, (98)-100).

C. Regularity condition

Regularity on the z -axis requires the condition (8) to be satisfied. When the numerical calculations do not impose this condition, it is not exactly satisfied. Typical values for the ratio m/l are 0.995 instead of precisely one. To strictly satisfy the regularity condition (8) we have introduced a new function

$$g = \frac{m}{l}, \quad (110)$$

imposing condition (8) as boundary condition for this function. The resulting solutions respect the regularity condition and are otherwise in excellent agreement with the solutions obtained before.

μ				
k/n	1	2	3	4
1	0.577	0.961	1.297	1.607
2	0.685	1.262	1.770	2.239
3	0.703	1.365	1.976	2.549
4	0.707	1.399	2.063	2.698
–	0.707	1.414	2.121	2.828
$\epsilon_{max}(\rho_{max})$				
k/n	1	2	3	4
1	1.075 (0.)	0.177 (0.90)	0.098 (1.59)	0.072 (2.37)
2	11.63 (0.)	0.910 (0.30)	0.380 (0.66)	0.235 (1.10)
3	79.70 (0.)	3.443 (0.09)	1.124 (0.28)	0.601 (0.51)
4	498.2 (0.)	12.01 (0.03)	3.064 (0.11)	1.435 (0.24)

Table 1

The dimensionless mass μ , the maximum of the energy density ϵ_{max} and the location ρ_{max} of the maximum of the energy density of the EYMD solutions of the sequences $n = 1 - 4$ with node numbers $k = 1 - 4$ and $\gamma = 1$. For comparison, the mass of the limiting solutions is also shown. Note, that μ/n decreases with n for fixed finite k .

μ				
k/n	1	2	3	4
1	.829	1.385	1.870	2.319
2	.971	1.796	2.527	3.197
3	.995	1.935	2.805	3.621
4	.999	1.980	2.921	3.824
–	1.	2.	3.	4.
$\epsilon_{max}(\rho_{max})$				
k/n	1	2	3	4
1	1.23 (0.)	0.26 (0.7)	0.16 (1.3)	0.12 (1.8)
2	2.55 (0.)	0.49 (0.2)	0.26 (0.5)	0.19 (0.8)
3	2.92 (0.)	0.62 (0.07)	0.35 (0.2)	0.25 (0.4)
4	2.98 (0.)	0.68 (0.02)	0.40 (0.1)	0.28 (0.2)

Table 2

The dimensionless mass μ , the maximum of the energy density ϵ_{max} and the location ρ_{max} of the maximum of the energy density of the EYM solutions of the sequences $n = 1 - 4$ with node numbers $k = 1 - 4$. For comparison, the mass of the limiting solutions is also shown. Note, that μ/n decreases with n for fixed finite k .

k/γ	<i>EYM</i>	<i>EYMD</i>			<i>YMD</i>
	0	0.5	1.0	2.0	∞
1	1.870	1.659	1.297	0.811	1.800
2	2.524	2.250	1.770	1.114	2.482
3	2.805	2.505	1.976	1.247	2.785
4	2.922	2.611	2.063	1.304	2.913
—	3	2.683	2.121	1.342	3

Table 3

The dimensionless mass μ of the EYMD solutions with winding number $n = 3$ and up to 4 nodes for several values of the dilaton coupling constant γ . For comparison, the last row gives the mass of the limiting solutions, the first column gives the mass of the EYM solutions, and the last column the scaled mass of the corresponding YMD solutions [12].

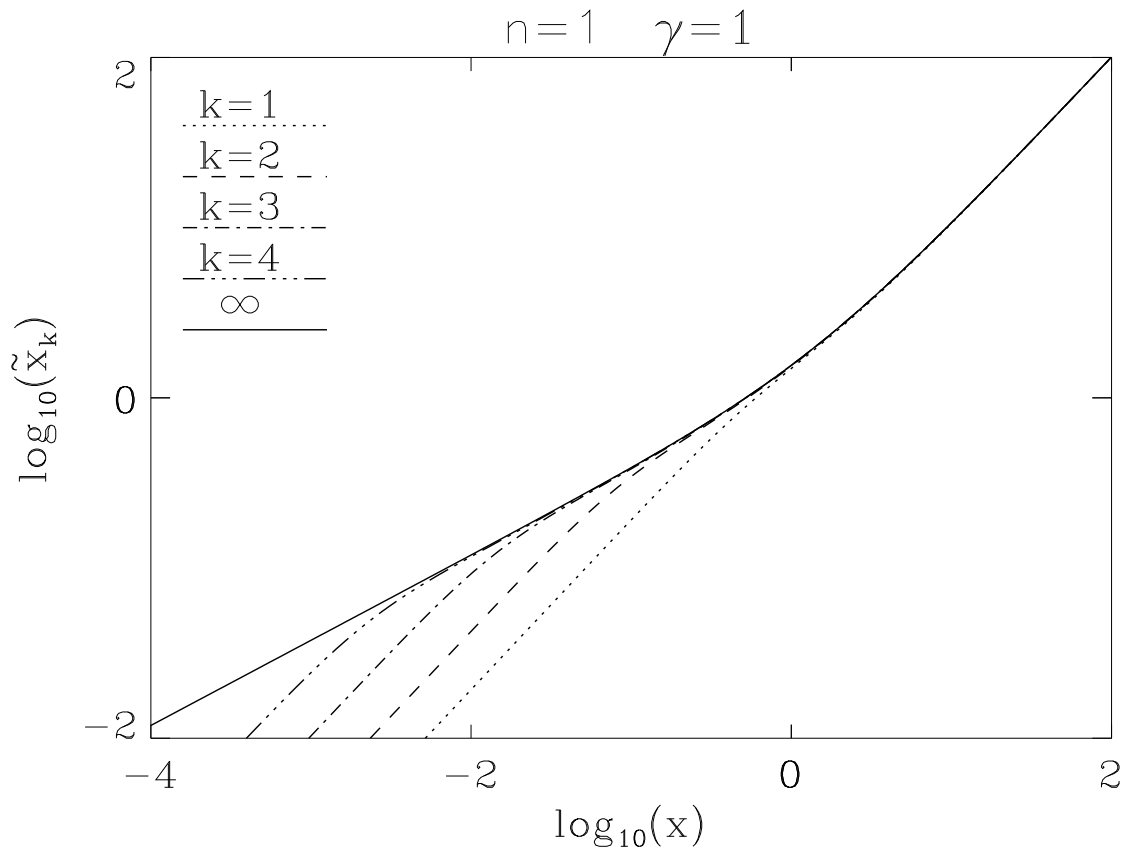


Fig. 1

The coordinate transformation between the isotropic coordinate x and the Schwarzschild-like coordinate \tilde{x} is shown for the spherically symmetric solutions ($n = 1$) of EYMD theory with $\gamma = 1$ and $k = 1 - 4$. Also shown is the coordinate transformation for the limiting EMD solution.

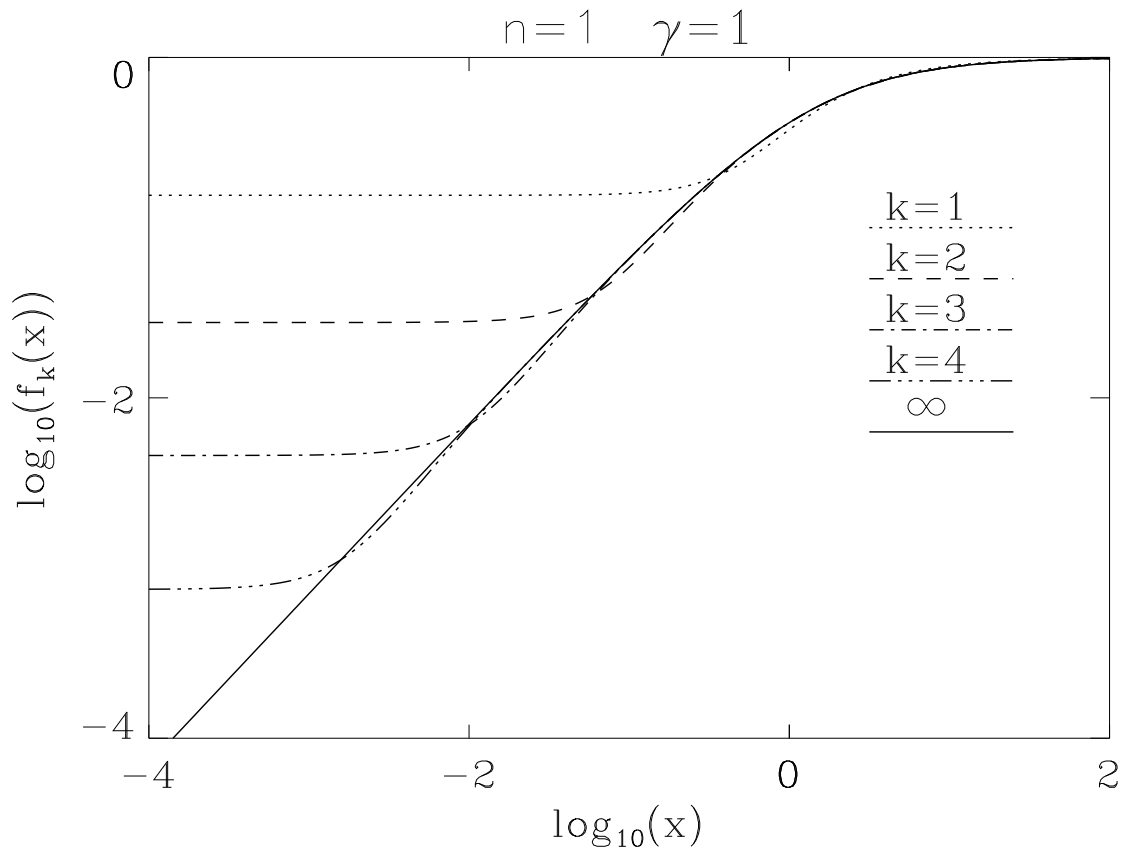


Fig. 2a

The metric function f is shown for the spherically symmetric solutions ($n = 1$) of EYMD theory with $\gamma = 1$ and $k = 1 - 4$. Also shown is the metric function of the limiting EMD solution.

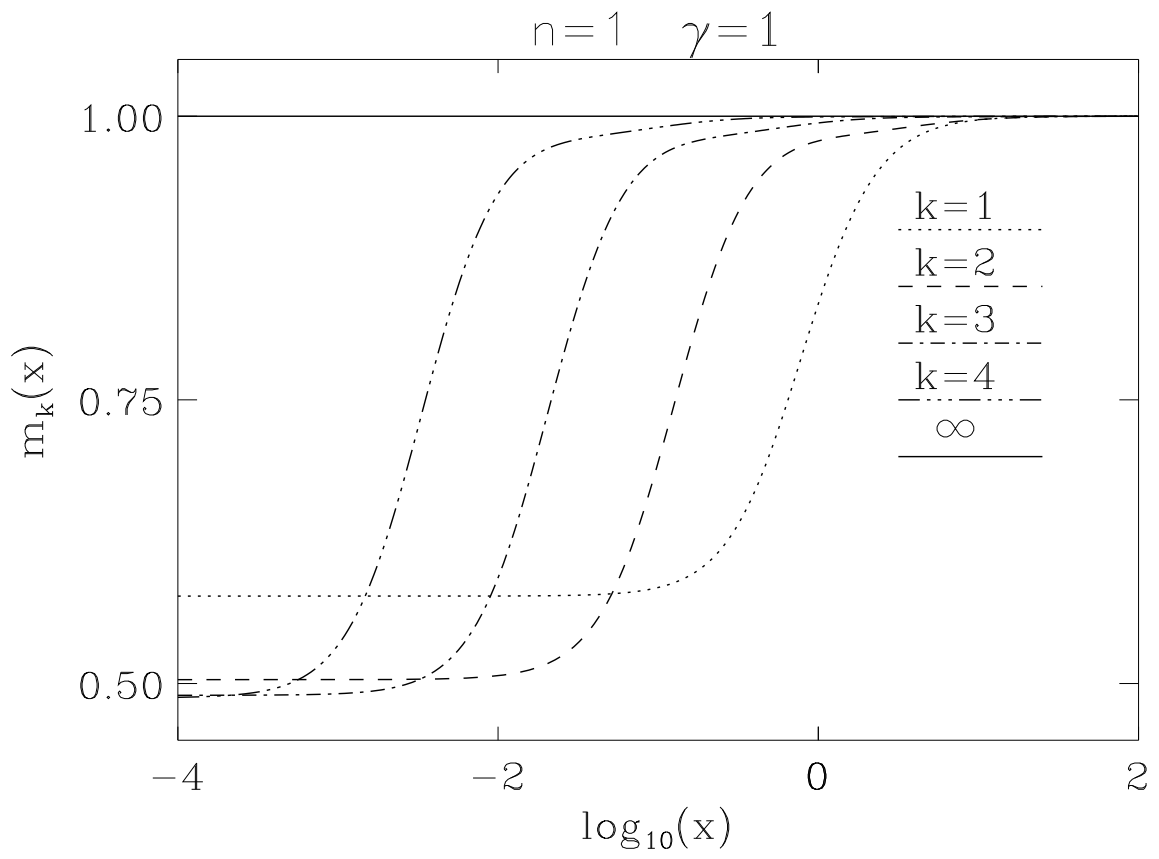


Fig. 2b
Same as Fig. 2a for the metric function m .

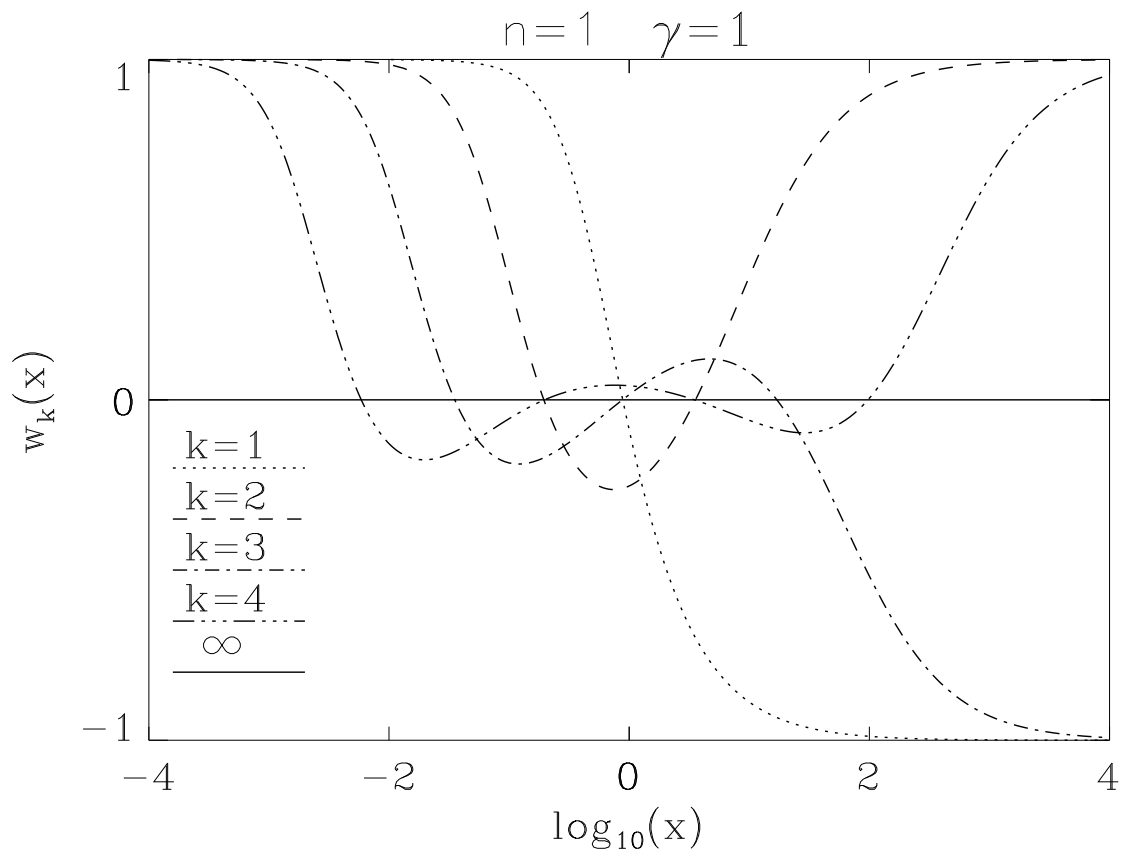


Fig. 3a
Same as Fig. 2a for the gauge field function w .

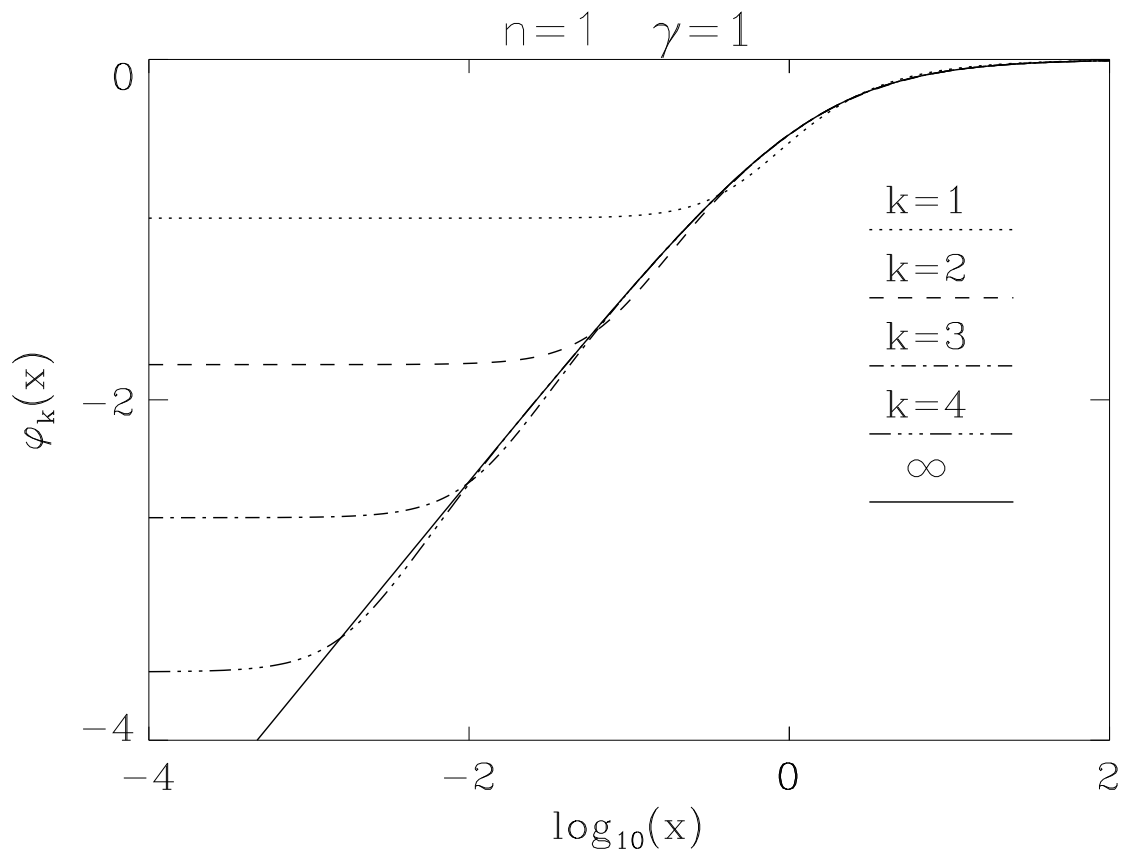


Fig. 3b
Same as Fig. 2a for the dilaton function φ .

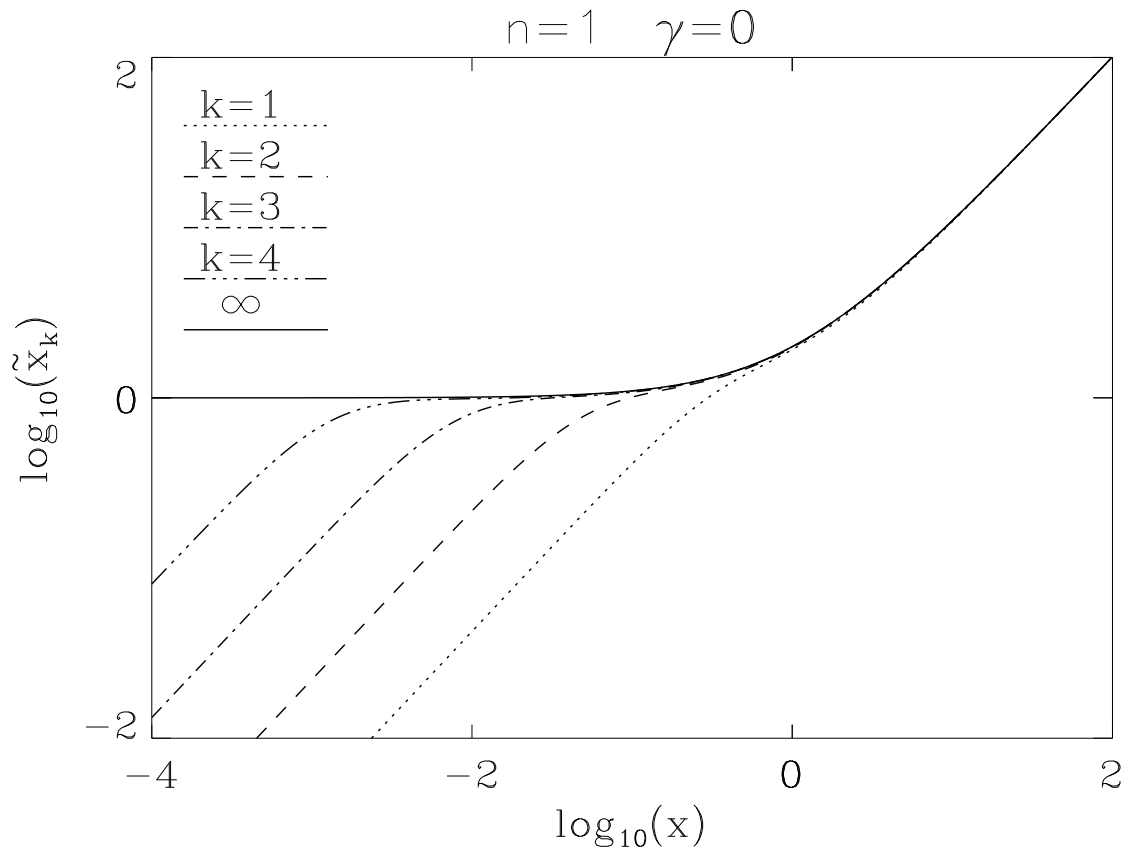


Fig. 4

The coordinate transformation between the isotropic coordinate x and the Schwarzschild-like coordinate \tilde{x} is shown for the spherically symmetric solutions ($n = 1$) of EYM theory with $k = 1 - 4$. Also shown is the coordinate transformation for the limiting RN solution.

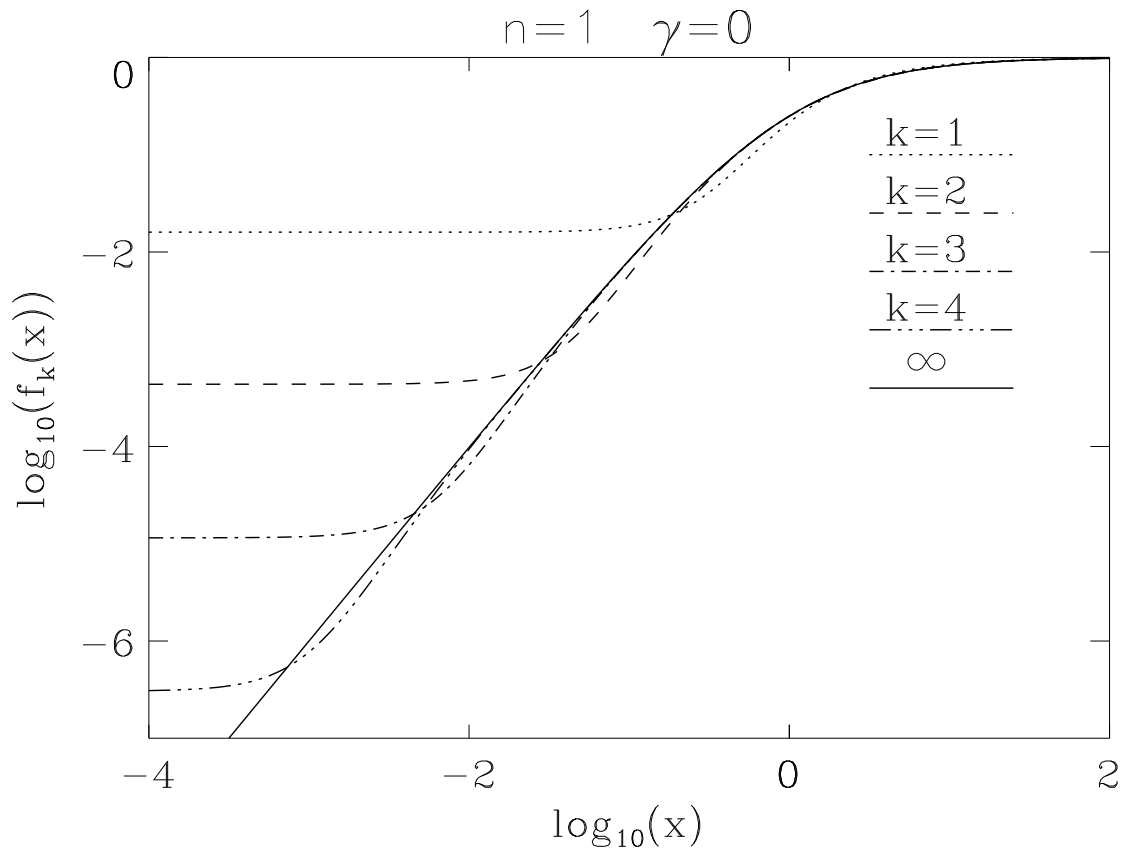


Fig. 5a

The metric function f is shown for the spherically symmetric solutions ($n = 1$) of EYM theory with $k = 1 - 4$. Also shown is the metric function of the limiting RN solution.

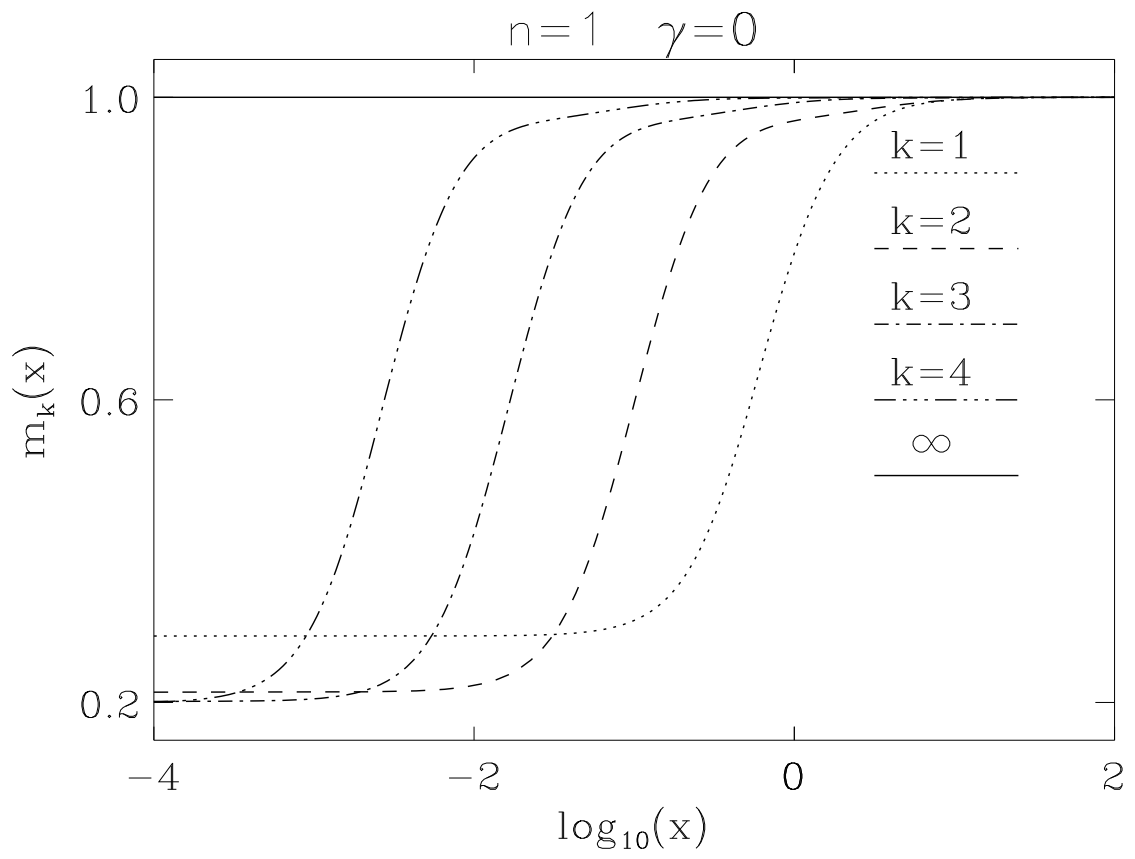


Fig. 5b
Same as Fig. 5a for the metric function m .

$$f(\bar{\rho}, \bar{z}) \quad n=2 \quad k=1 \quad \gamma=1$$

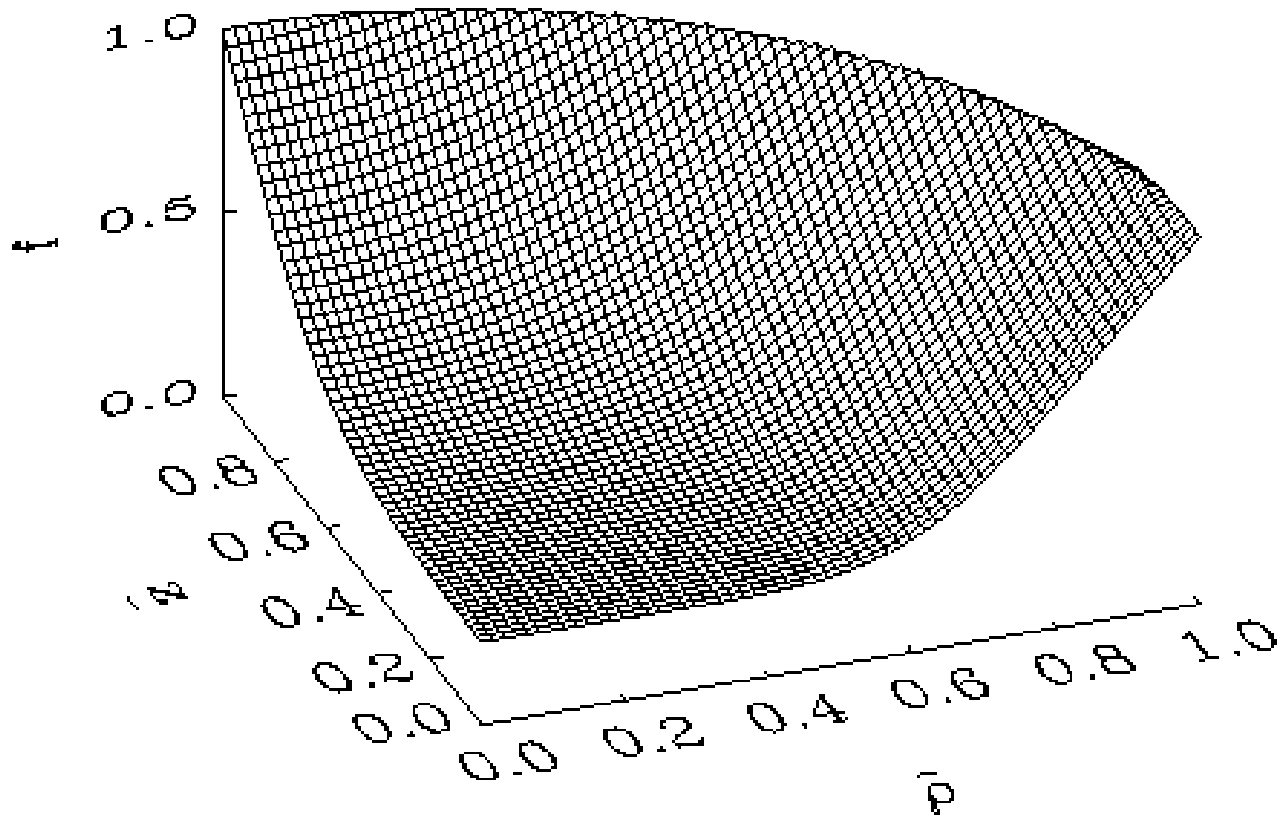


Fig. 6a

The metric function f of the EYMD solution with $\gamma = 1$, $n = 2$, $k = 1$ is shown as a function of the compactified coordinates $\bar{\rho}$ and \bar{z} .

$$m(\bar{\rho}, \bar{z}) \quad n=2 \quad k=1 \quad \gamma=1$$

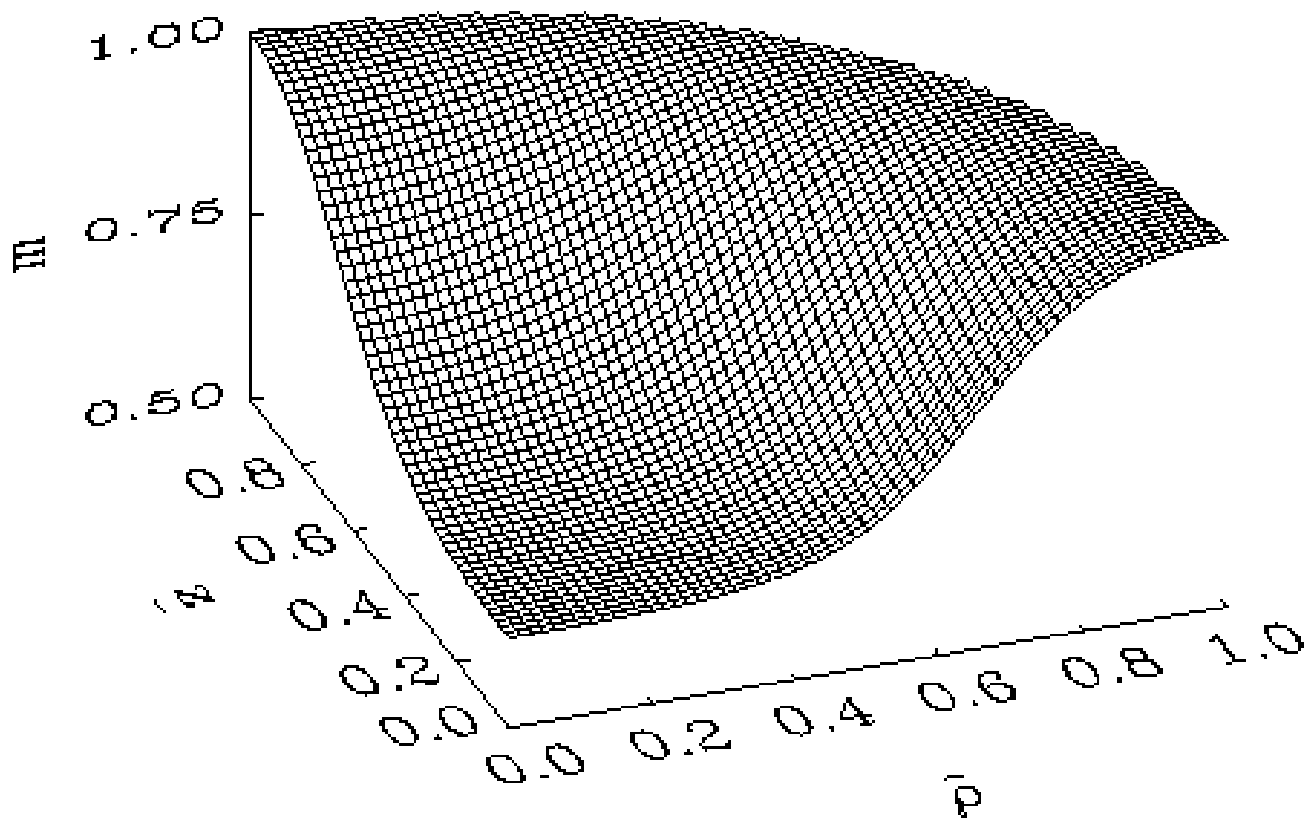


Fig. 6b

Same as Fig. 6a for the metric function m .

$$l(\bar{\rho}, \bar{z}) \quad n=2 \quad k=1 \quad \gamma=1$$

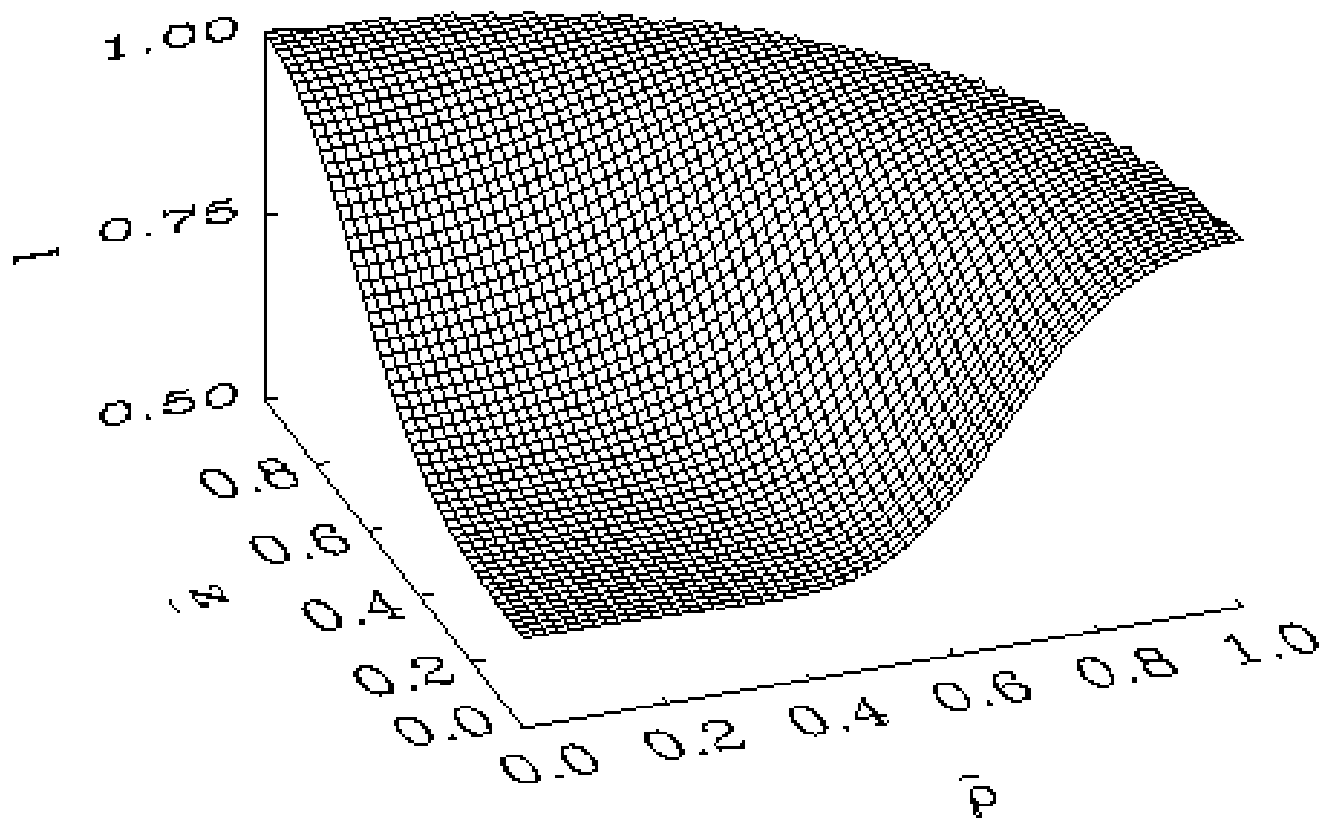


Fig. 6c

Same as Fig. 6a for the metric function l .

$$H_1(\bar{\rho}, \bar{z}) \quad n=2 \quad k=1 \quad \gamma=1$$

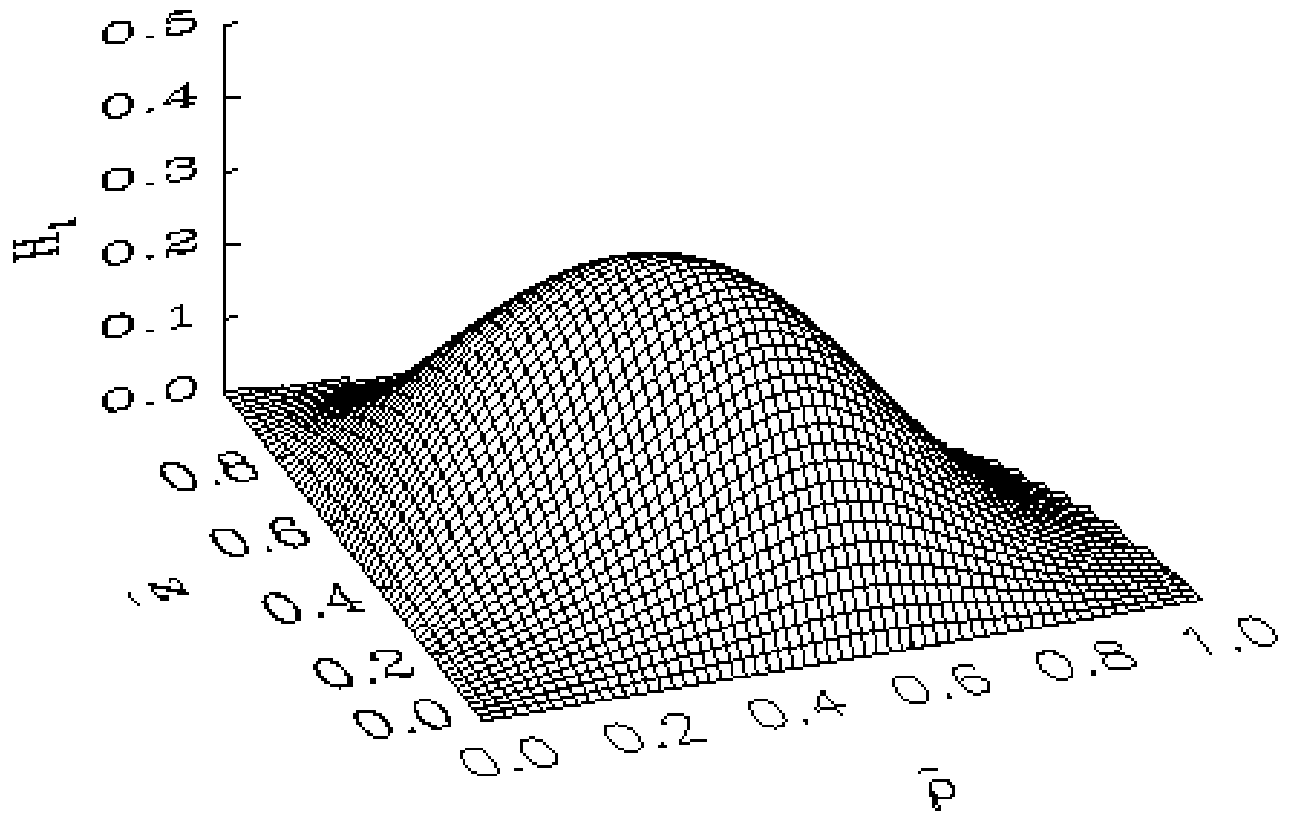


Fig. 7a

Same as Fig. 6a for the gauge field function H_1 .

$$H_2(\bar{\rho}, \bar{z}) \quad n=2 \quad k=1 \quad \gamma=1$$

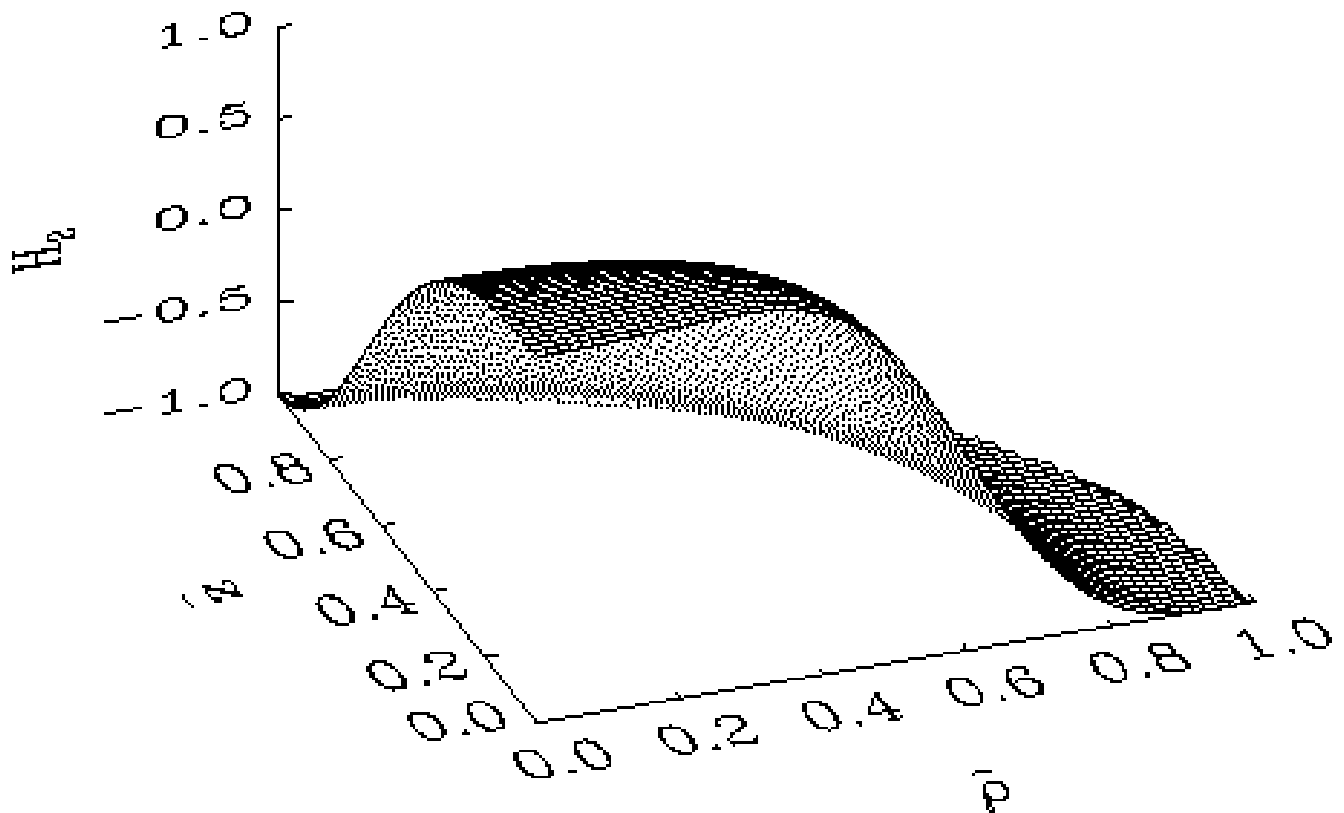


Fig. 7b

Same as Fig. 6a for the gauge field function H_2 .

$$H_3(\bar{\rho}, \bar{z}) \quad n=2 \quad k=1 \quad \gamma=1$$

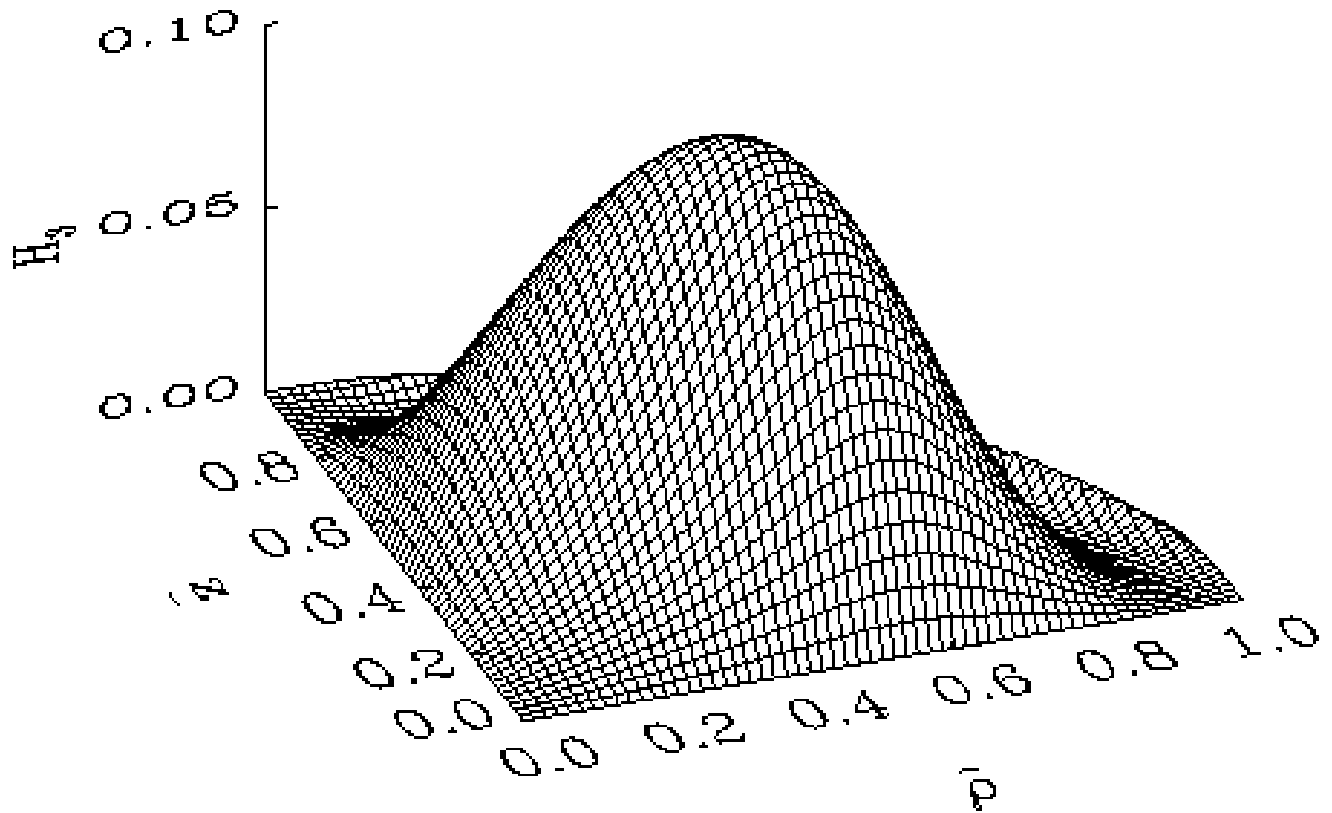


Fig. 7c

Same as Fig. 6a for the gauge field function H_3 .

$$H_4(\bar{\rho}, \bar{z}) \quad n=2 \quad k=1 \quad \gamma=1$$

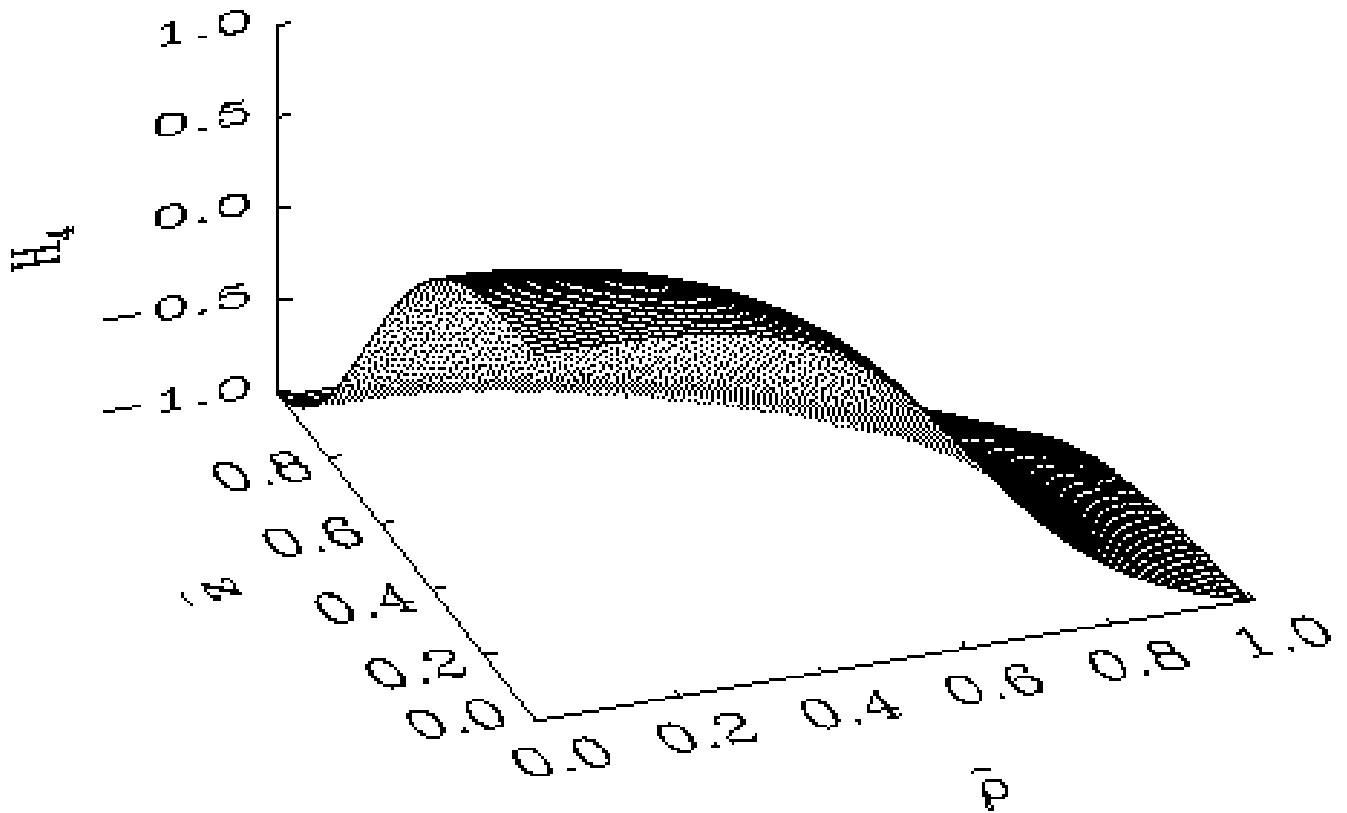


Fig. 7d

Same as Fig. 6a for the gauge field function H_4 .

Nodes $n=2$ $k=1$ $\gamma=1$

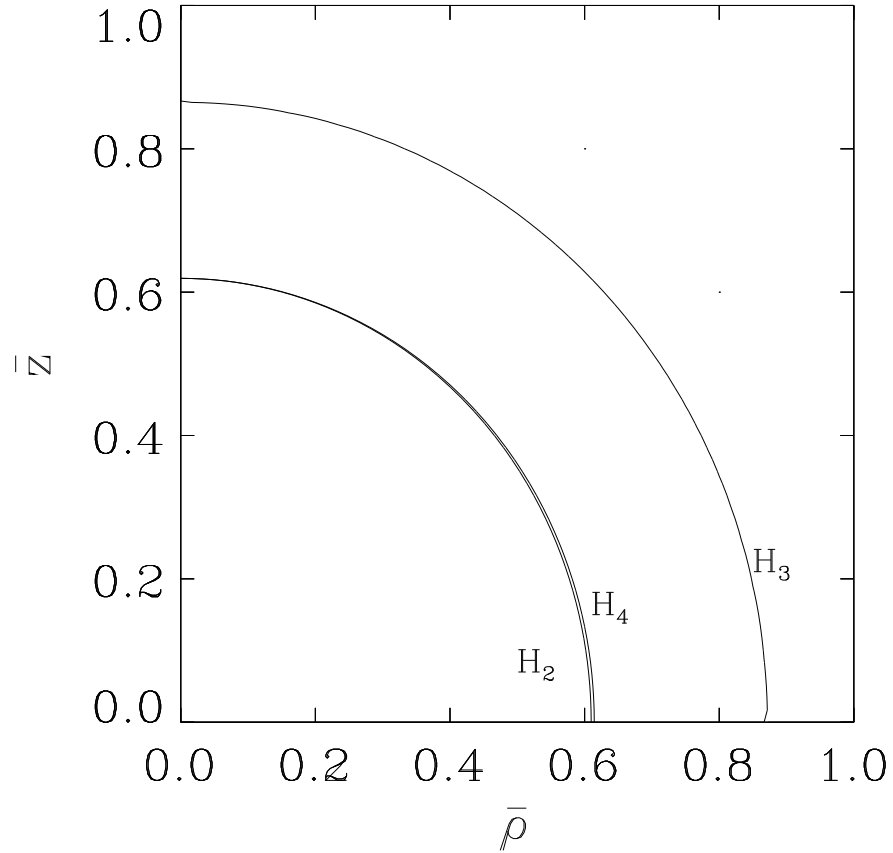


Fig. 7e

Same as Fig. 6a for the nodal lines of the gauge field functions $H_2 - H_4$.

$$\varphi(\bar{\rho}, \bar{z}) \quad n=2 \quad k=1 \quad \gamma=1$$

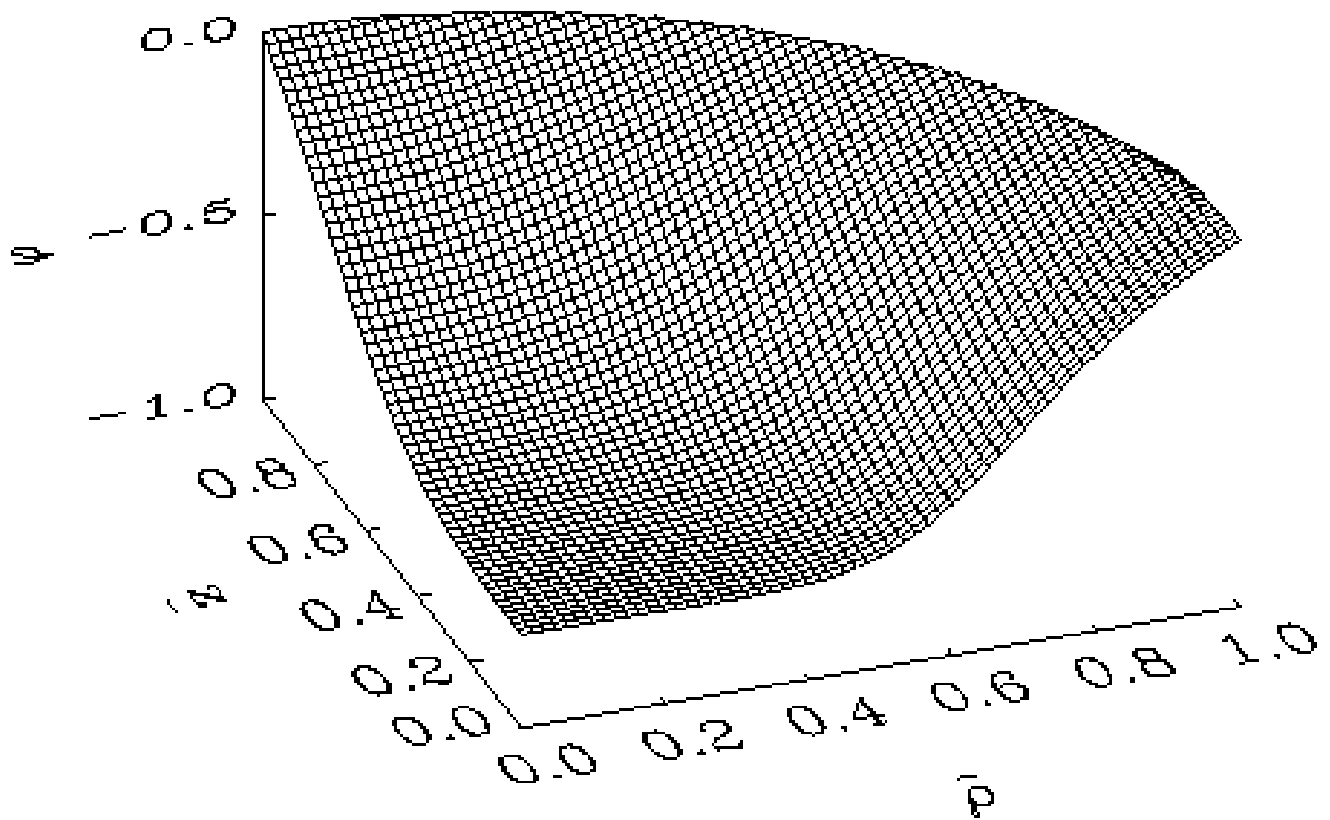


Fig. 8

Same as Fig. 6a for the dilaton function φ .

$$\epsilon(\bar{\rho}, \bar{z}) \quad n=2 \quad k=1 \quad \gamma=1$$

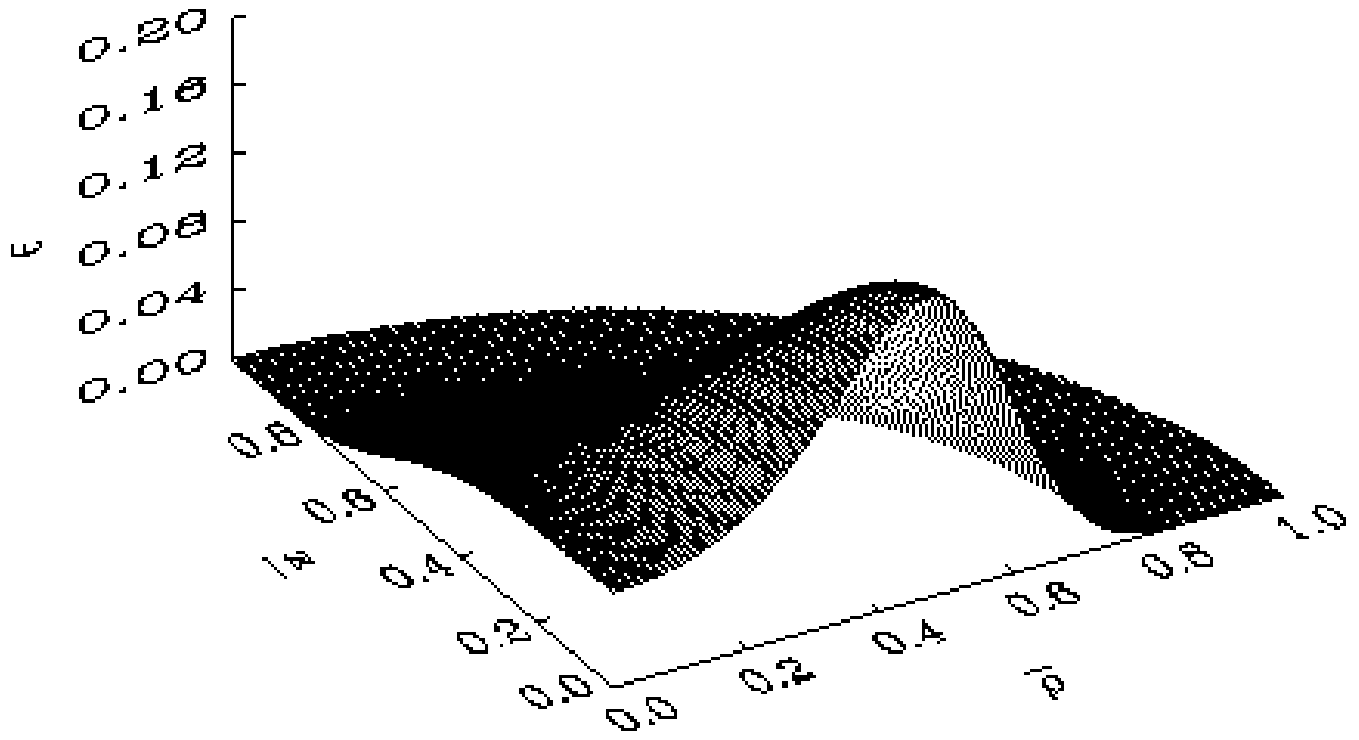


Fig. 9

Same as Fig. 6a for the energy density of the matter fields ϵ .

$$\epsilon(\bar{\rho}, \bar{z}) \quad n=2 \quad k=1 \quad \gamma=0$$

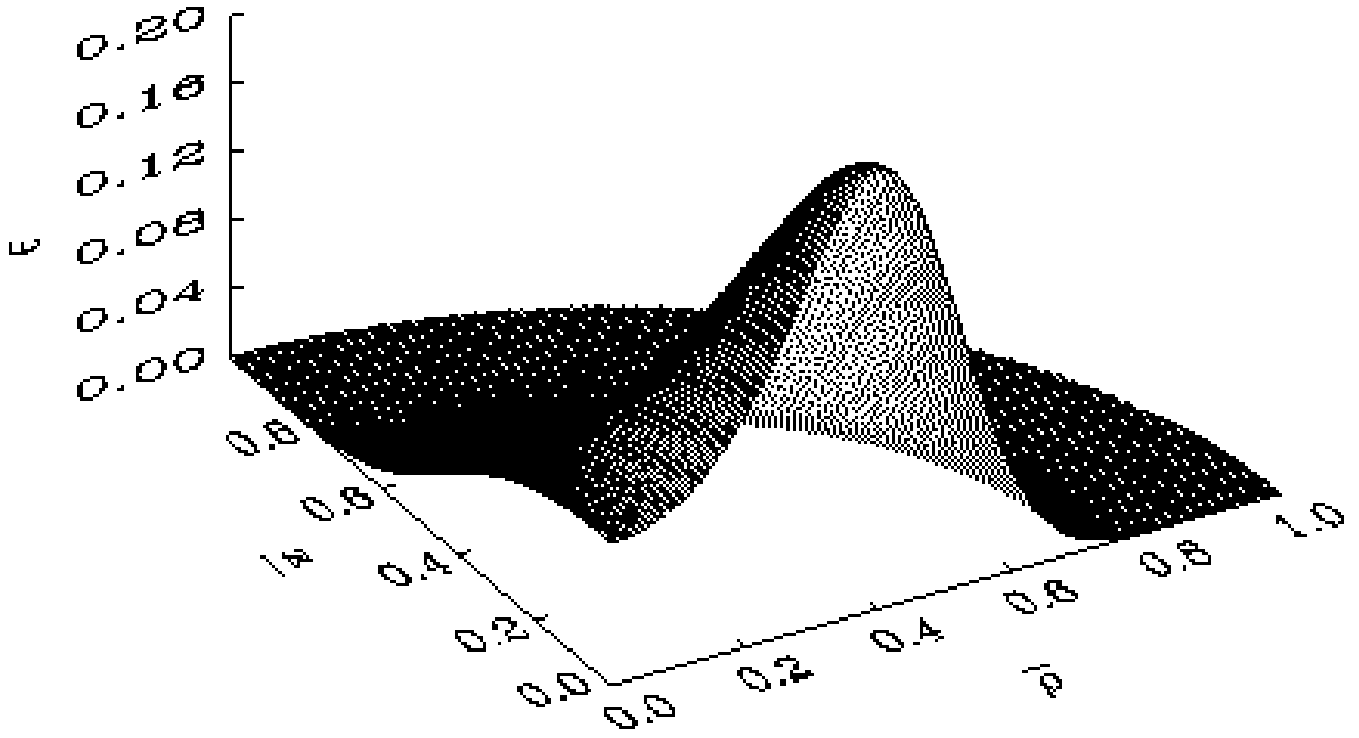


Fig. 10

The energy density of the matter fields ϵ of the EYM solution with $n = 2$, $k = 1$ is shown as a function of the compactified coordinates $\bar{\rho}$ and \bar{z} .

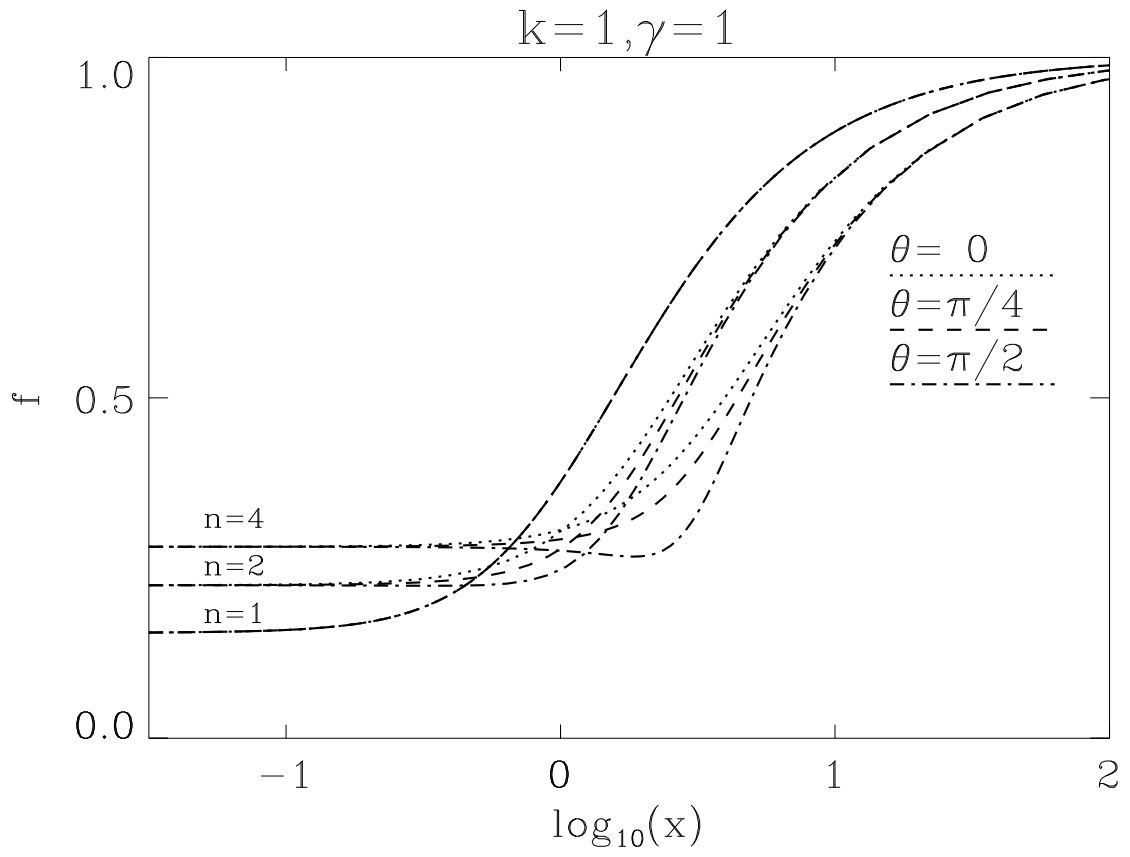


Fig. 11a

The metric function f of the EYMD solutions with $\gamma = 1$, $n = 1, 2$, and 4 and $k = 1$ is shown as a function of the coordinate x for the angles $\theta = 0, \pi/4$ and $\pi/2$.

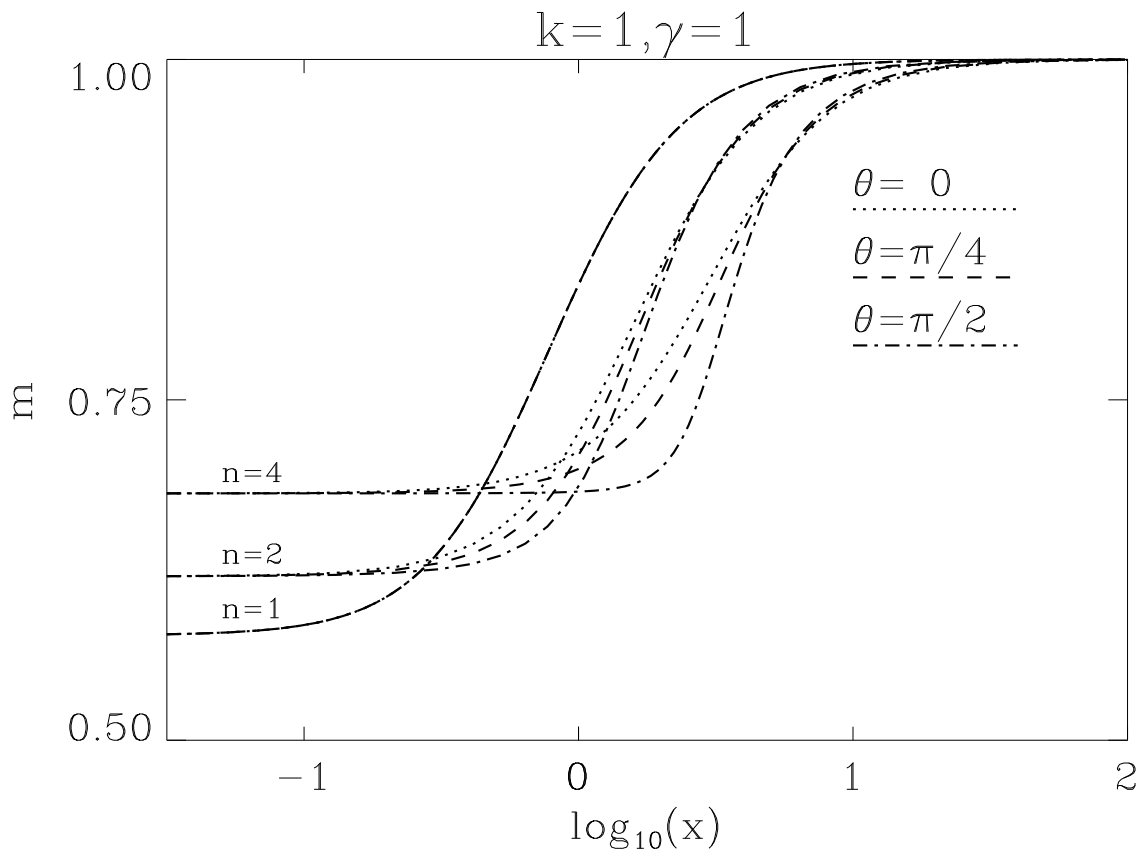


Fig. 11b
Same as Fig. 11a for the metric function m .

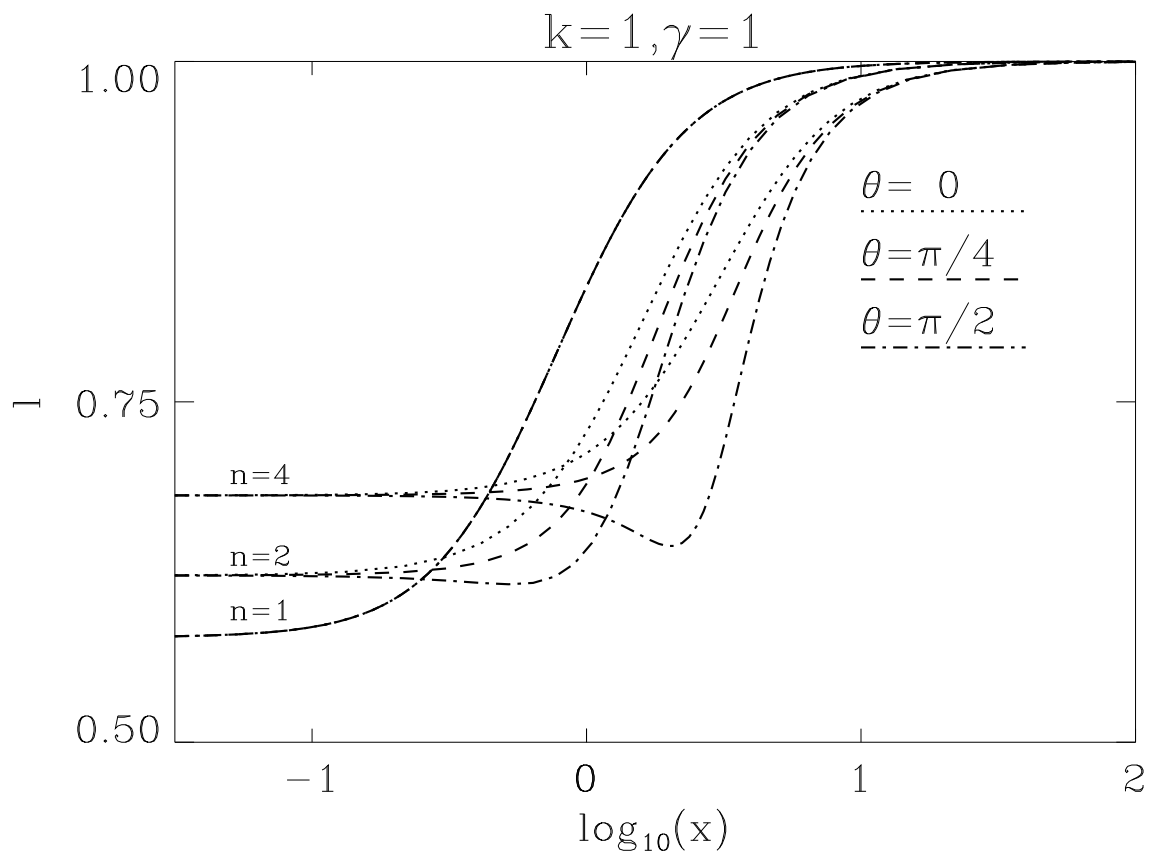


Fig. 11c
Same as Fig. 11a for the metric function l .

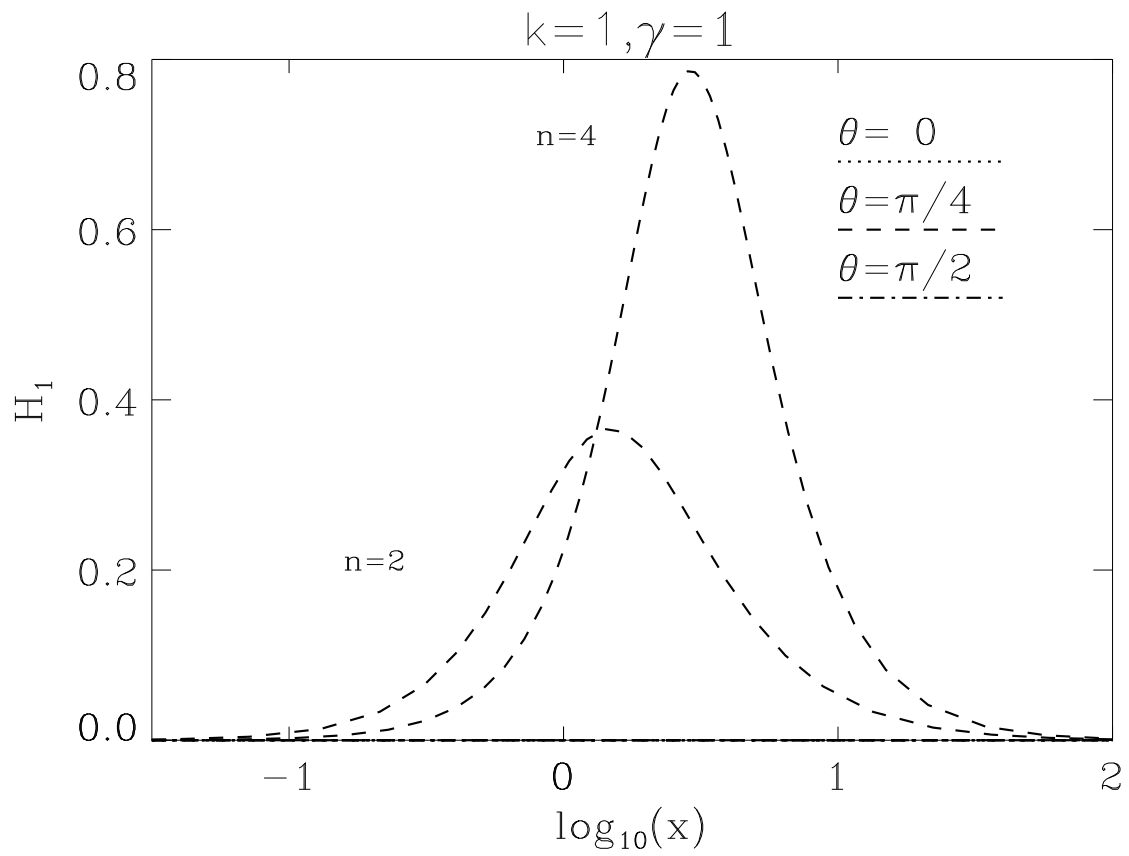


Fig. 12a
 Same as Fig. 11a for the gauge field function H_1 .

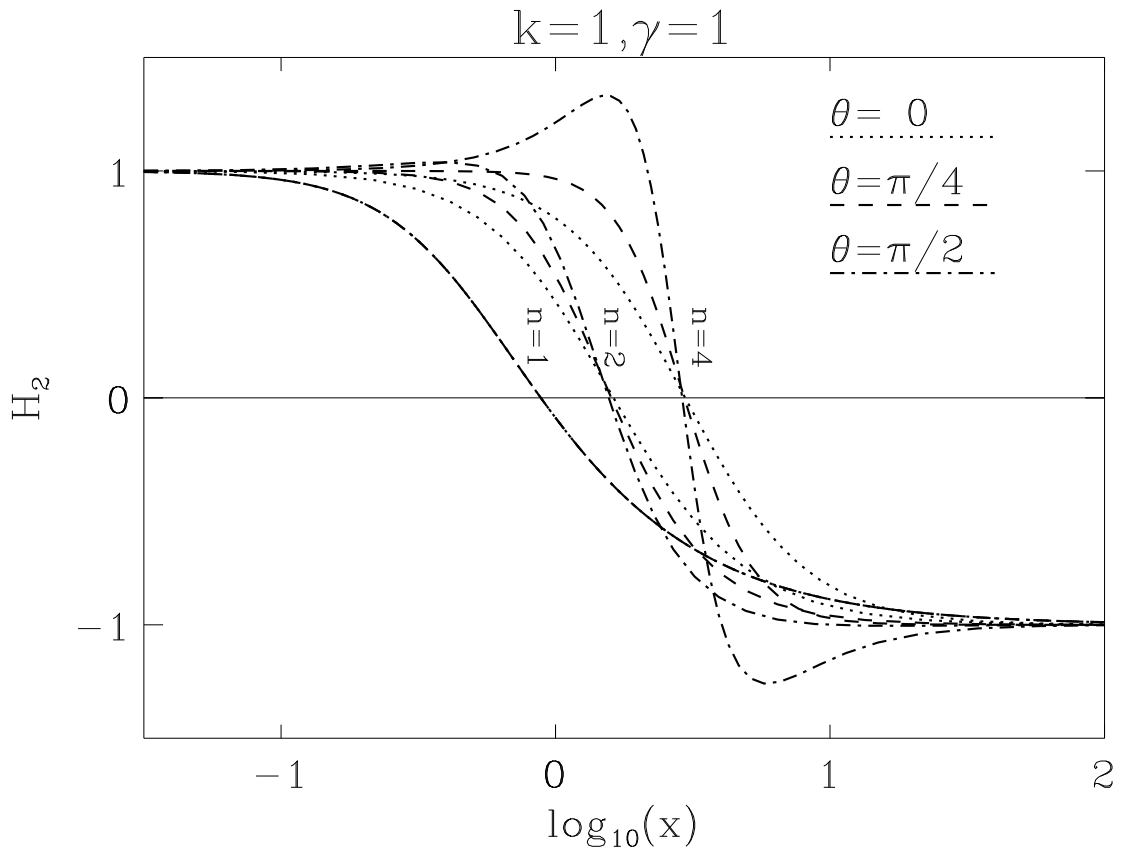


Fig. 12b
 Same as Fig. 11a for the gauge field function H_2 .

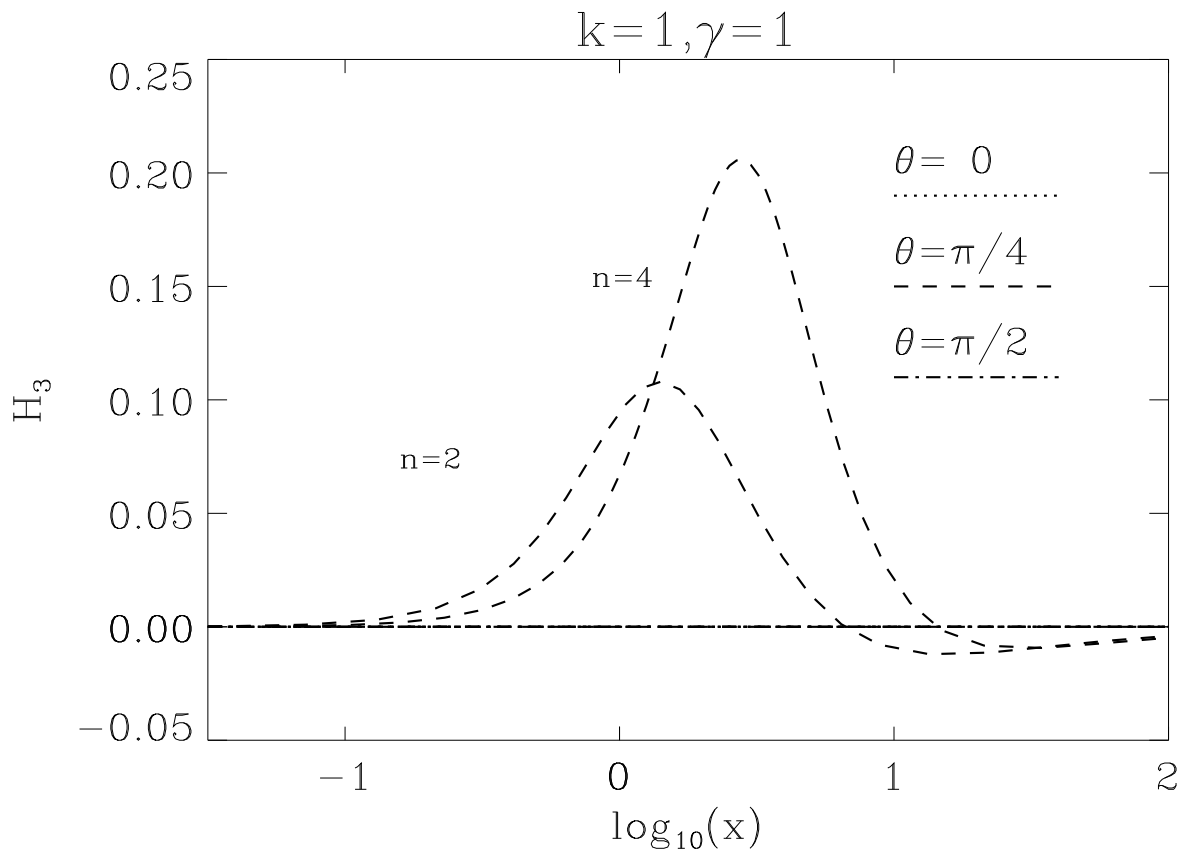


Fig. 12c
 Same as Fig. 11a for the gauge field function H_3 .

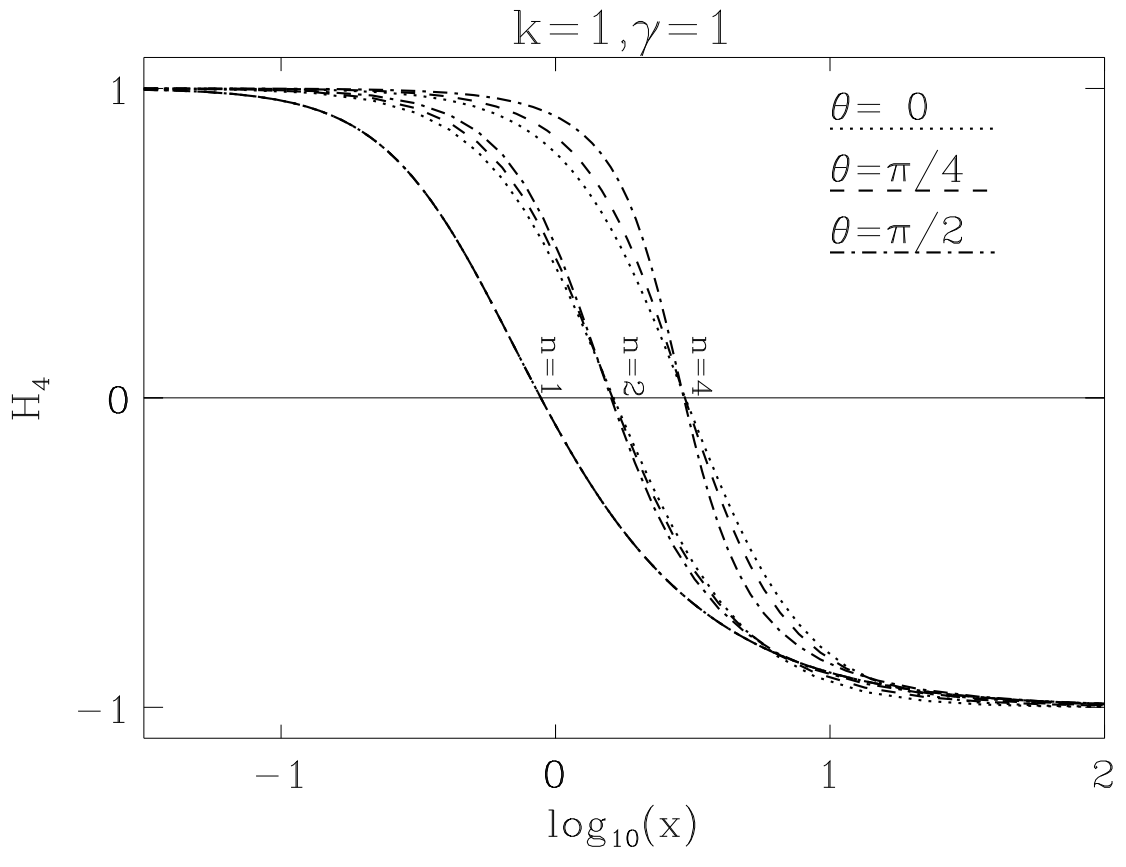


Fig. 12d
Same as Fig. 11a for the gauge field function H_4 .

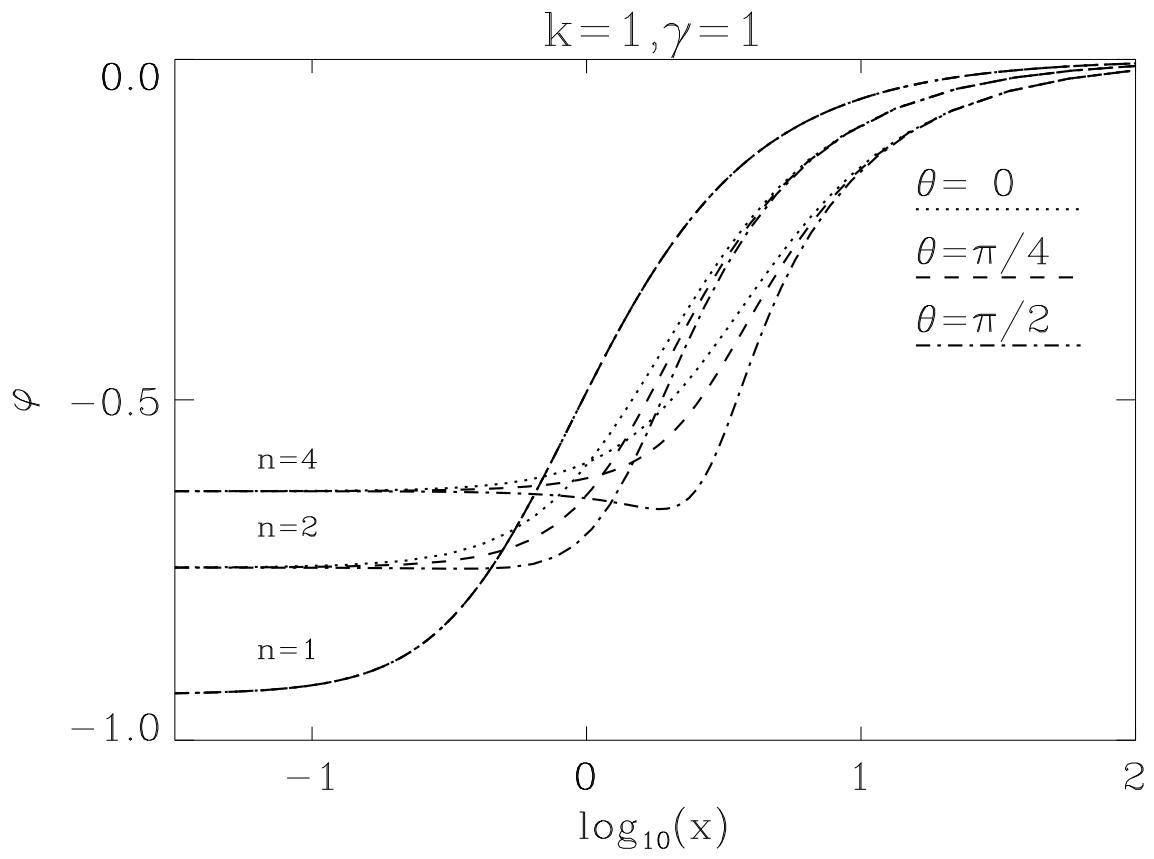


Fig. 13
Same as Fig. 11a for the dilaton function φ .

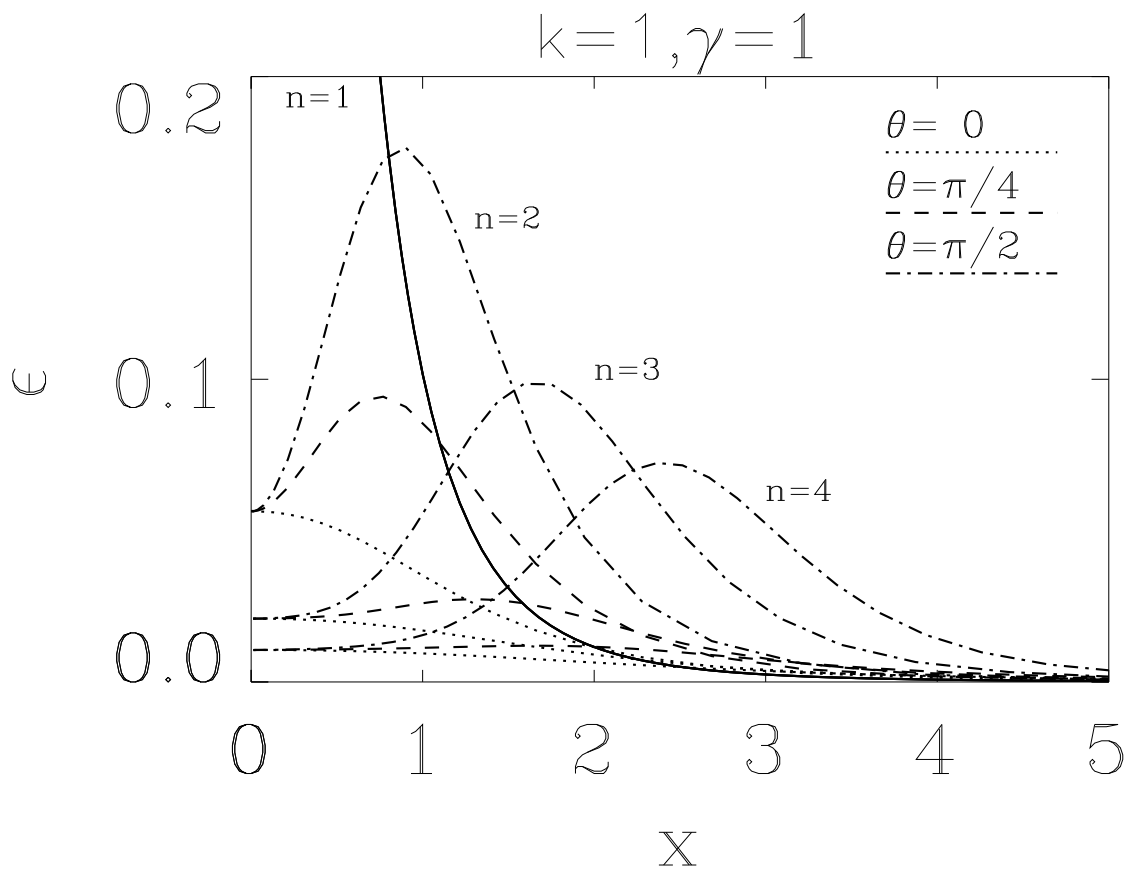


Fig. 14
Same as Fig. 11a for the energy density of the matter fields ϵ .

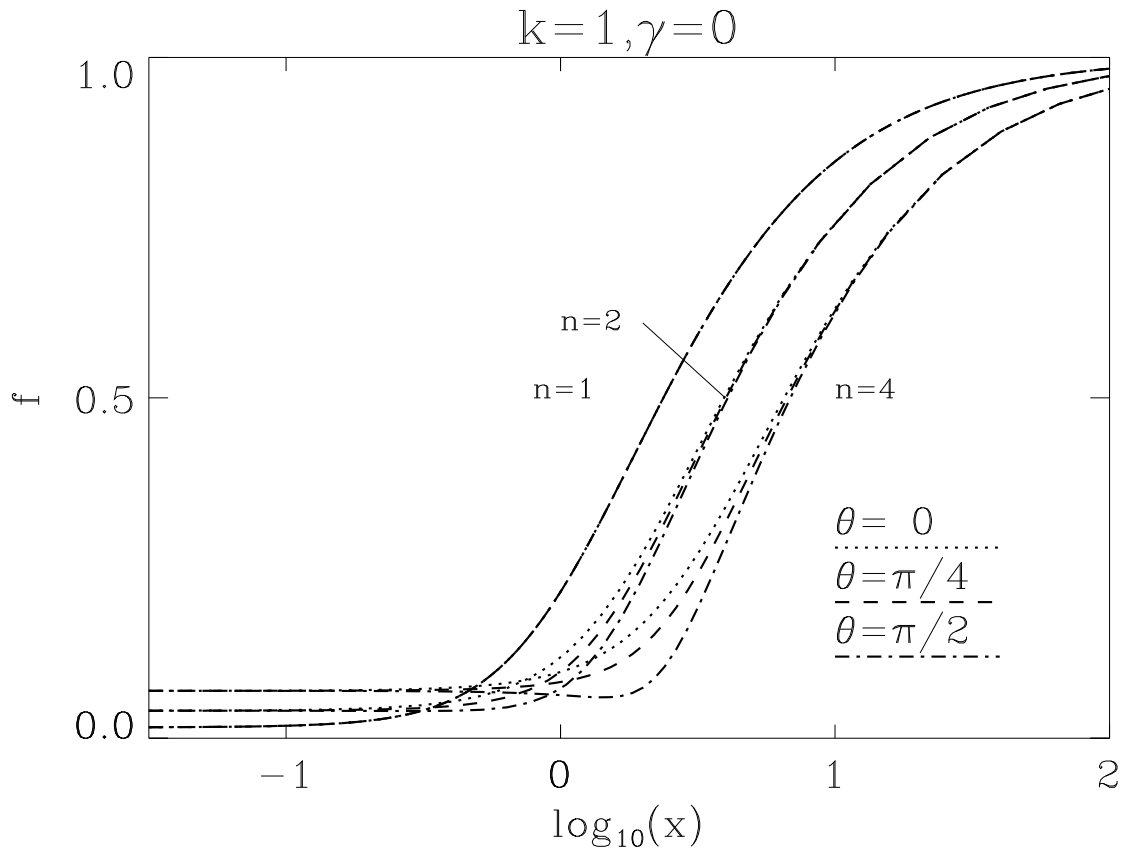


Fig. 15a

The metric function f of the EYM solutions with $n = 1, 2$, and 4 and $k = 1$ is shown as a function of the coordinate x for the angles $\theta = 0, \pi/4$ and $\pi/2$.

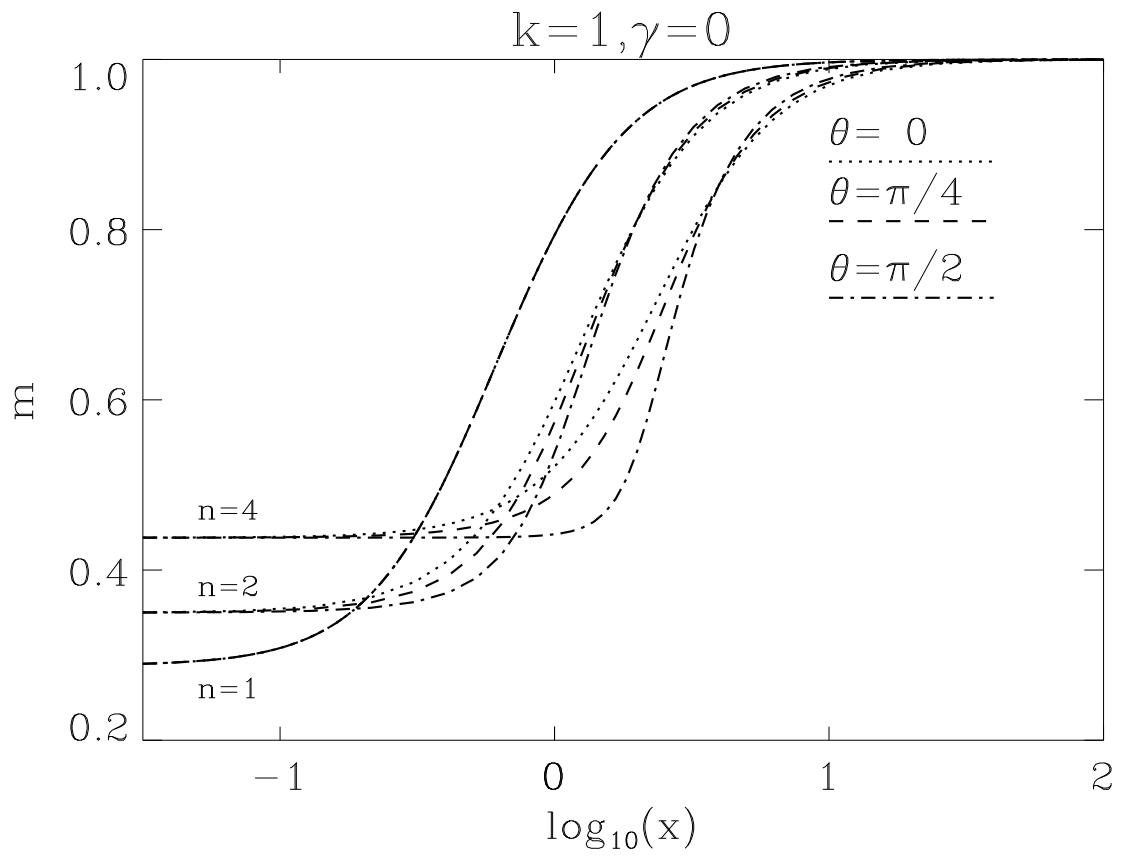


Fig. 15b
Same as Fig. 15a for the metric function m .

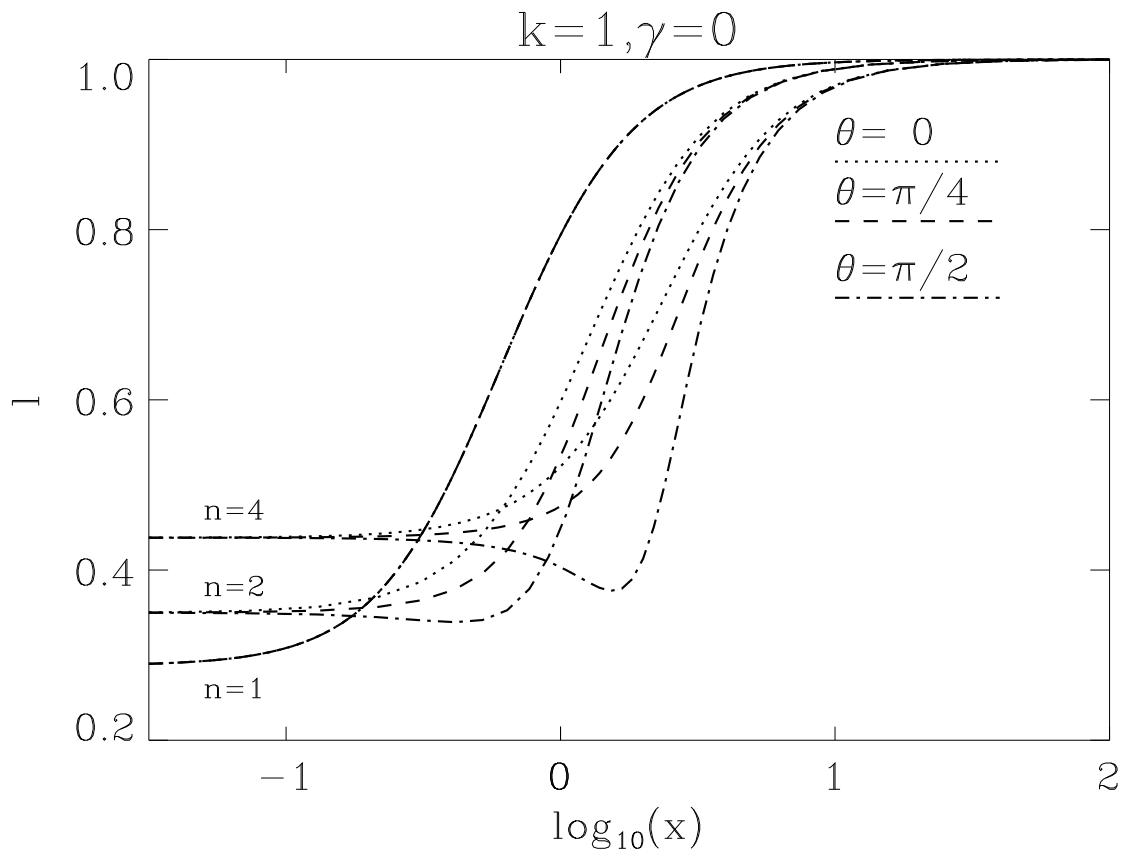


Fig. 15c
Same as Fig. 15a for the metric function l .

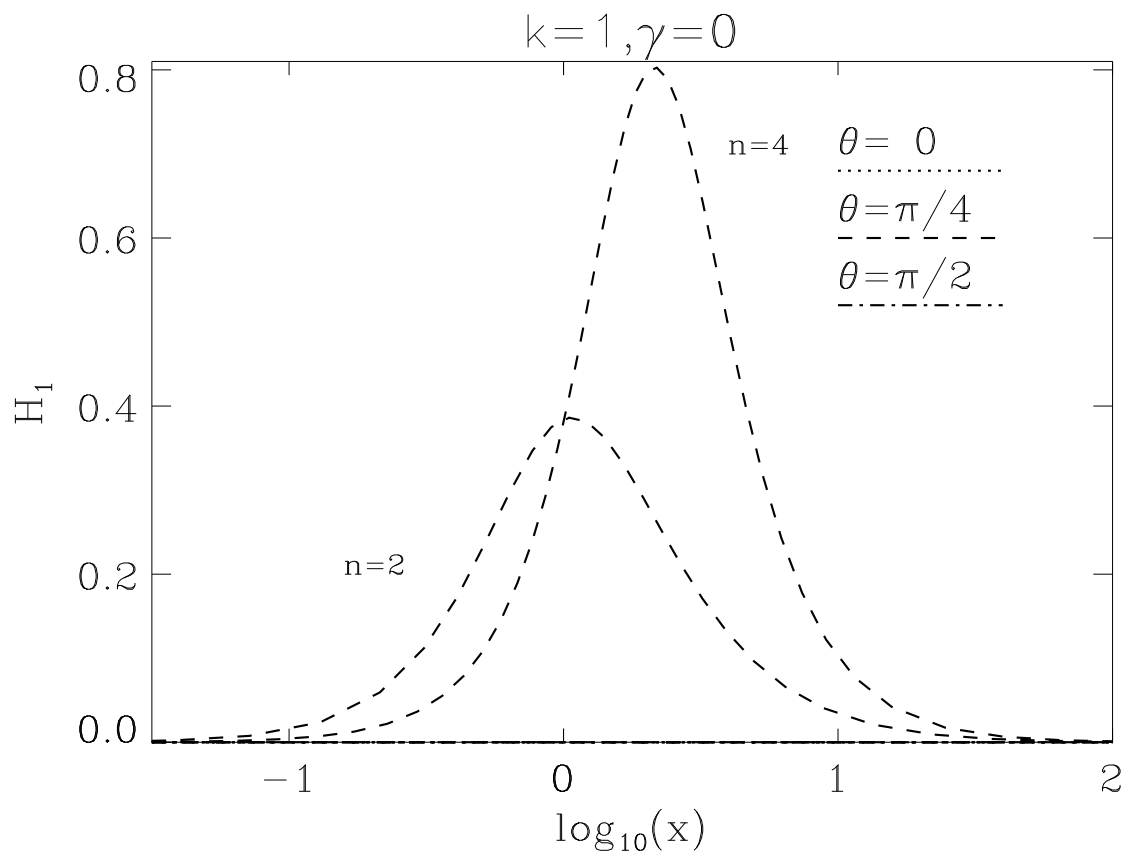


Fig. 16a
Same as Fig. 15a for the gauge field function H_1 .

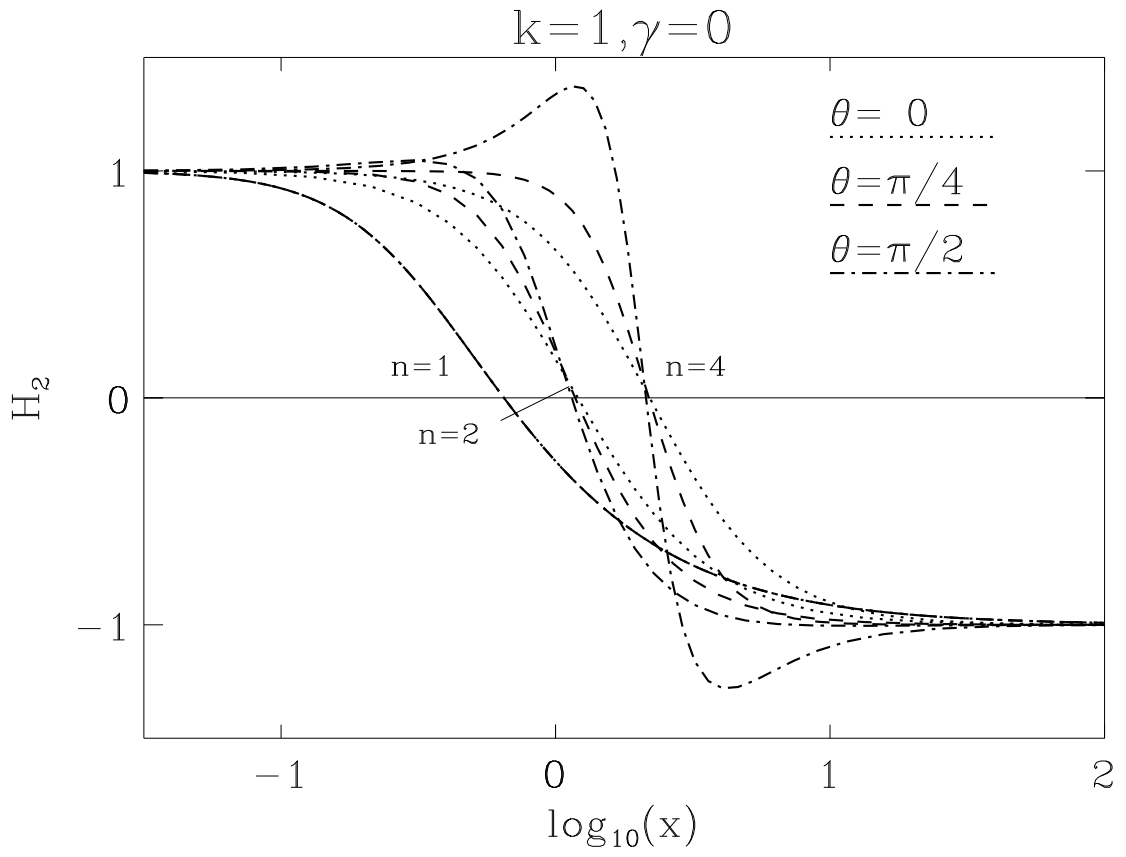


Fig. 16b
Same as Fig. 15a for the gauge field function H_2 .

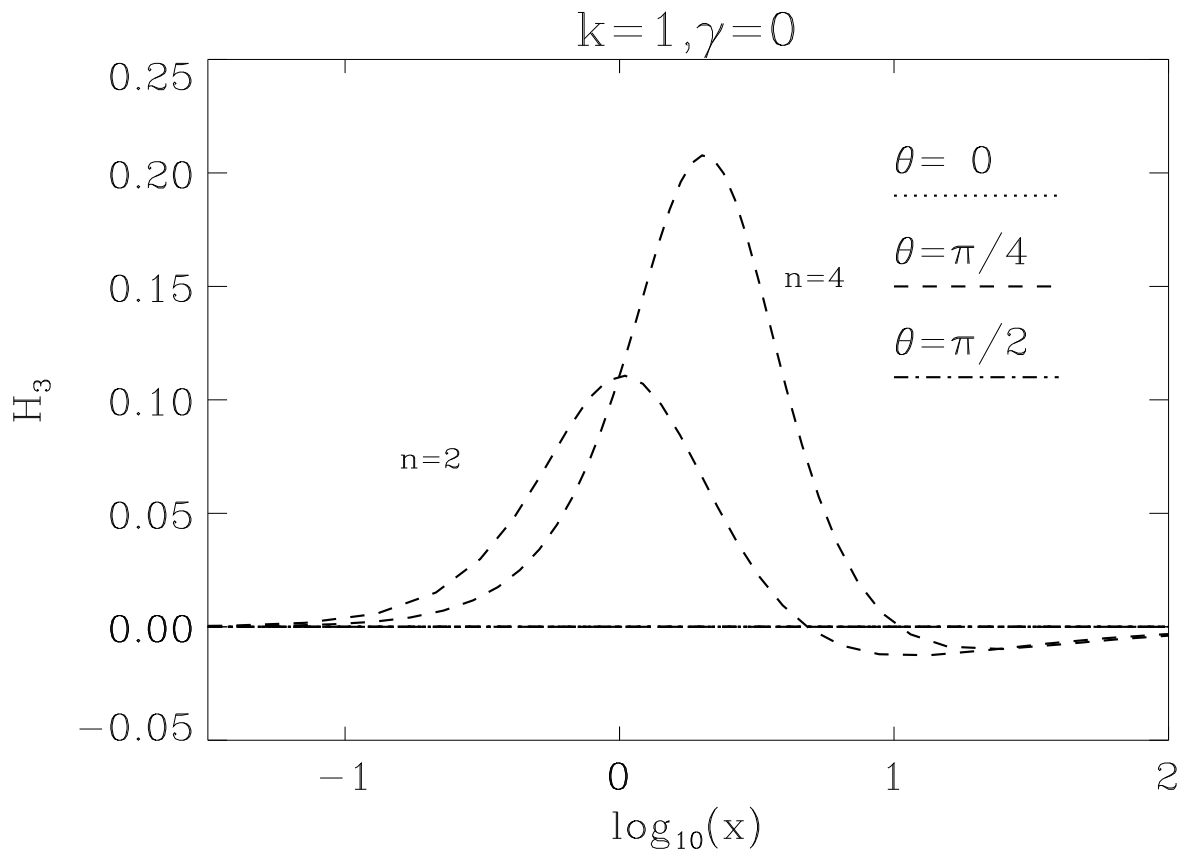


Fig. 16c
 Same as Fig. 15a for the gauge field function H_3 .

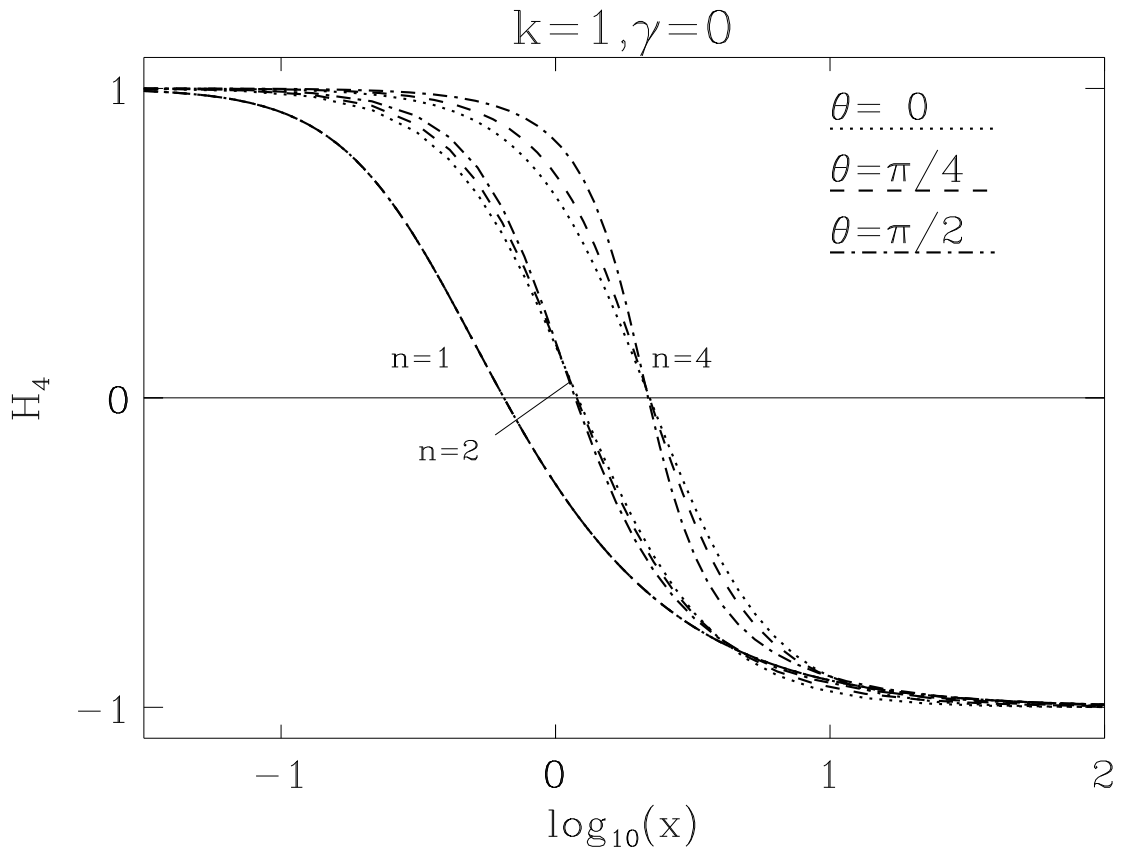


Fig. 16d
 Same as Fig. 15a for the gauge field function H_4 .

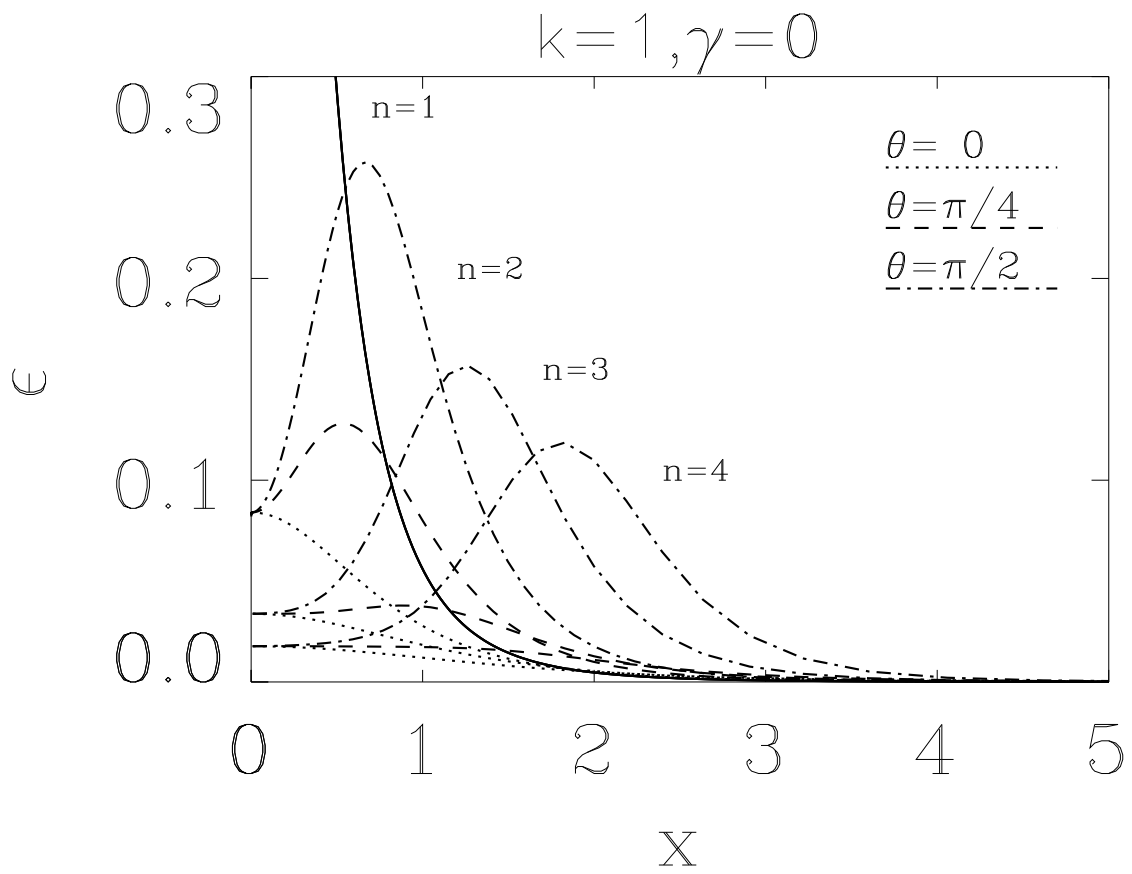


Fig. 17
Same as Fig. 15a for the energy density of the matter fields ϵ .

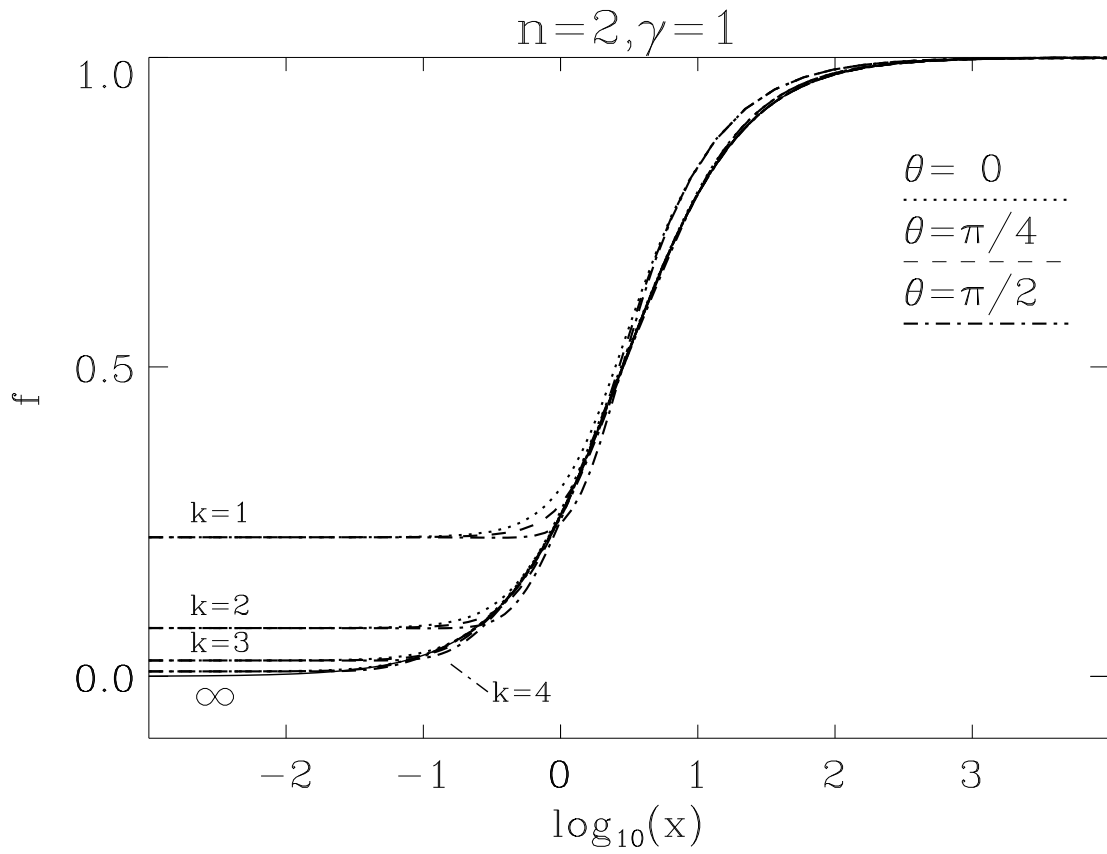


Fig. 18a

The metric function f of the EYMD solutions with $\gamma = 1$, $n = 2$, and $k = 1 - 4$ is shown as a function of the coordinate x for the angles $\theta = 0, \pi/4$ and $\pi/2$. Also shown is the metric function of the limiting EMD solution.

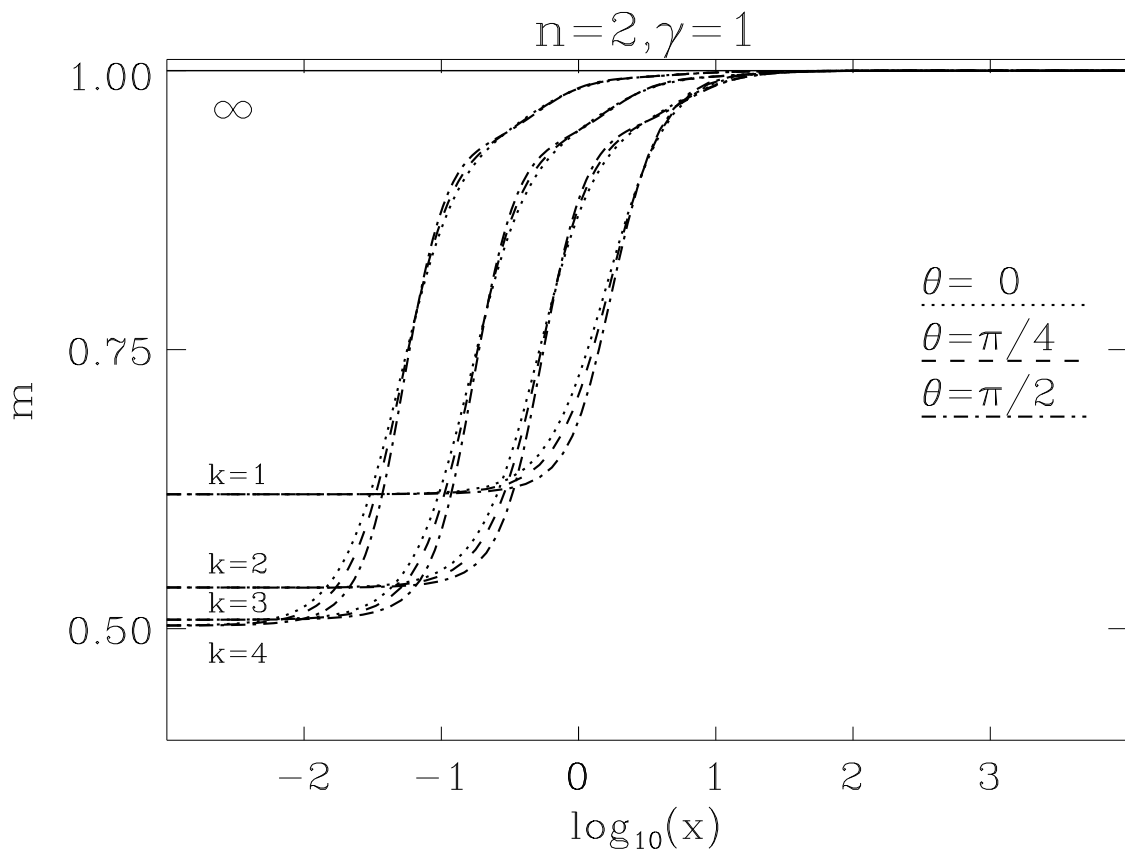


Fig. 18b
Same as Fig. 18a for the metric function m .

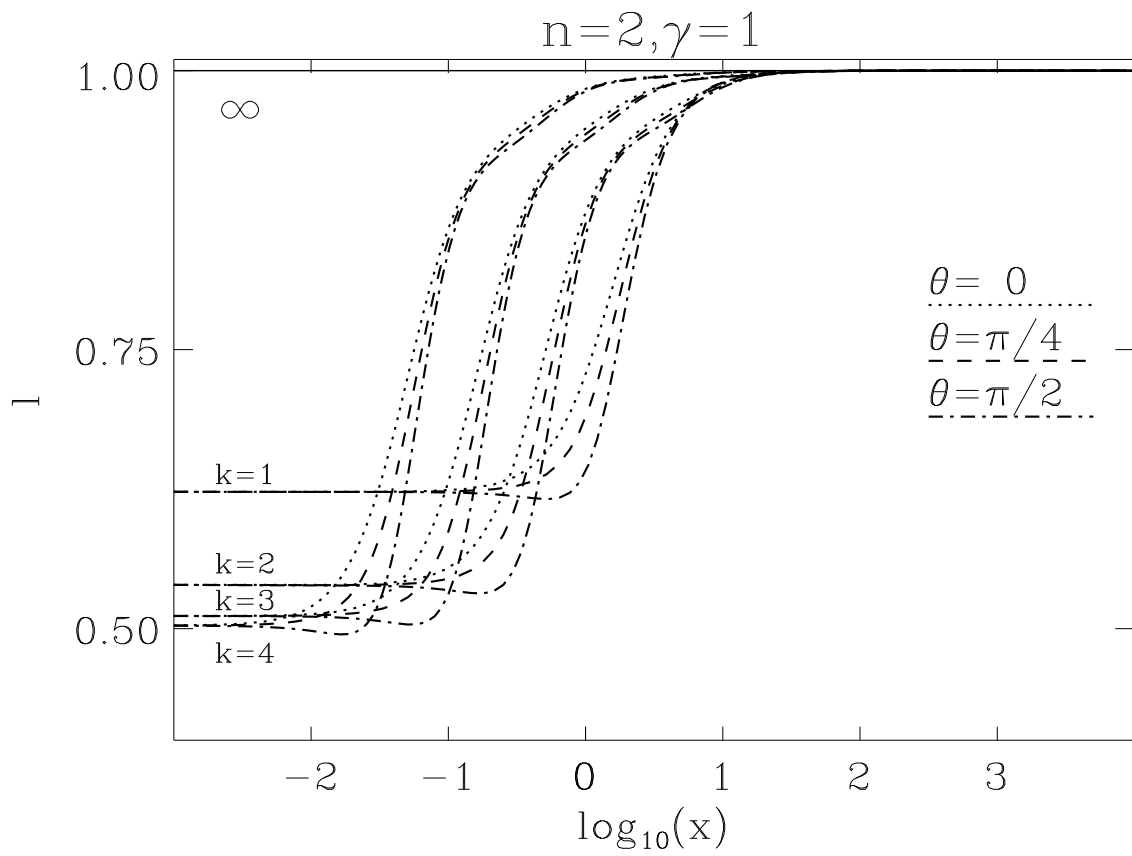


Fig. 18c
 Same as Fig. 18a for the metric function l .

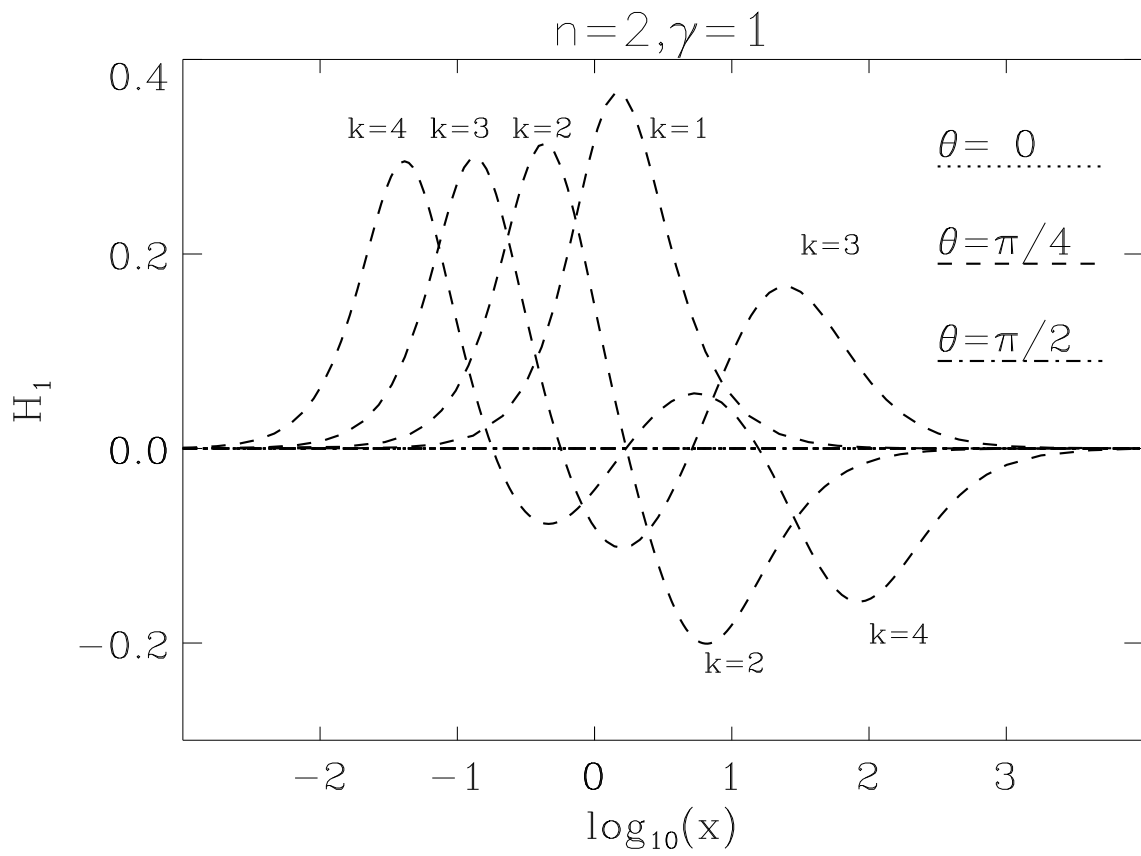


Fig. 19a
Same as Fig. 18a for the gauge field function H_1 .

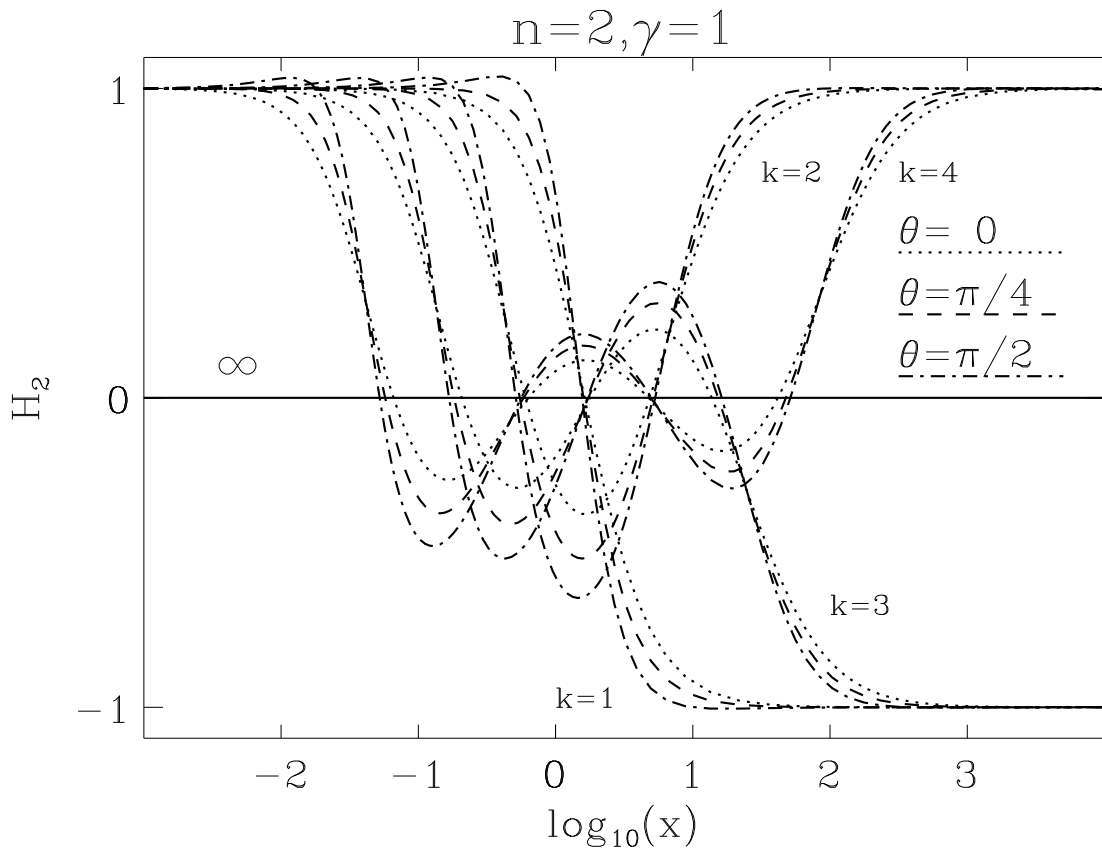


Fig. 19b
Same as Fig. 18a for the gauge field function H_2 .

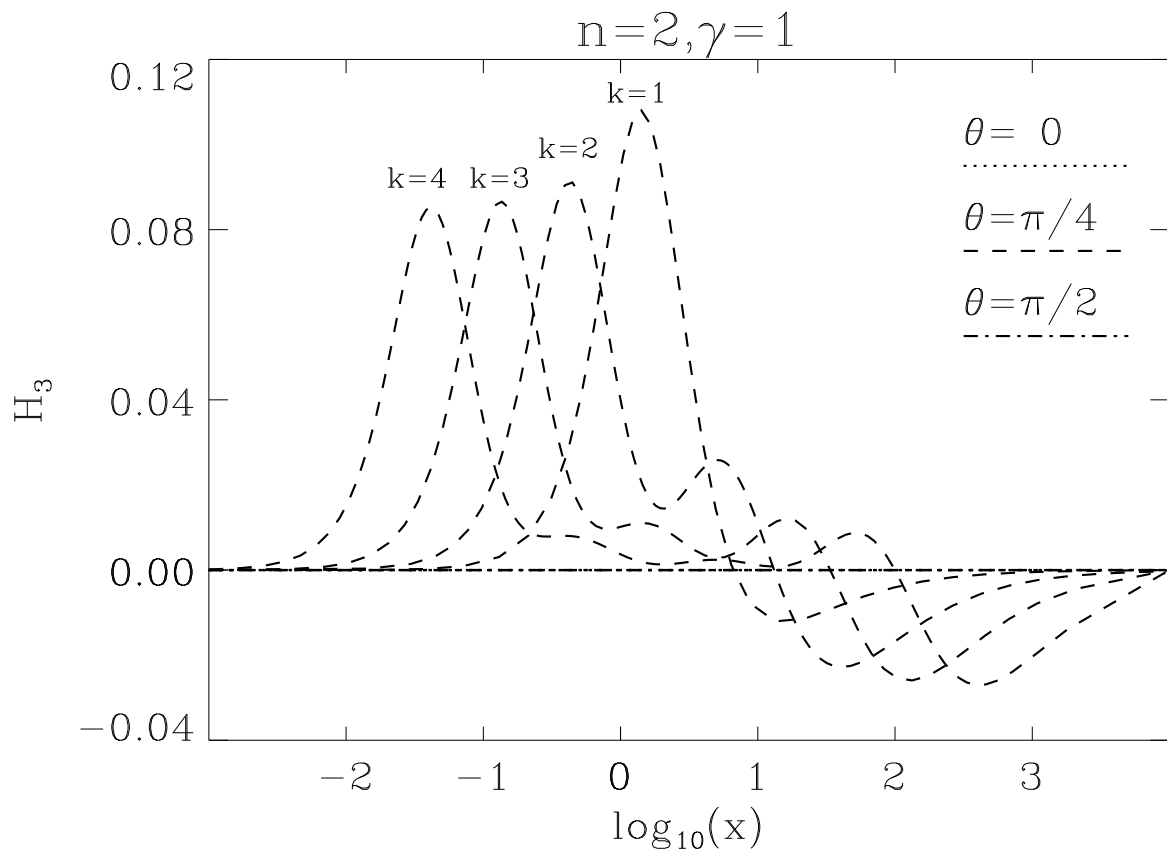


Fig. 19c
 Same as Fig. 18a for the gauge field function H_3 .

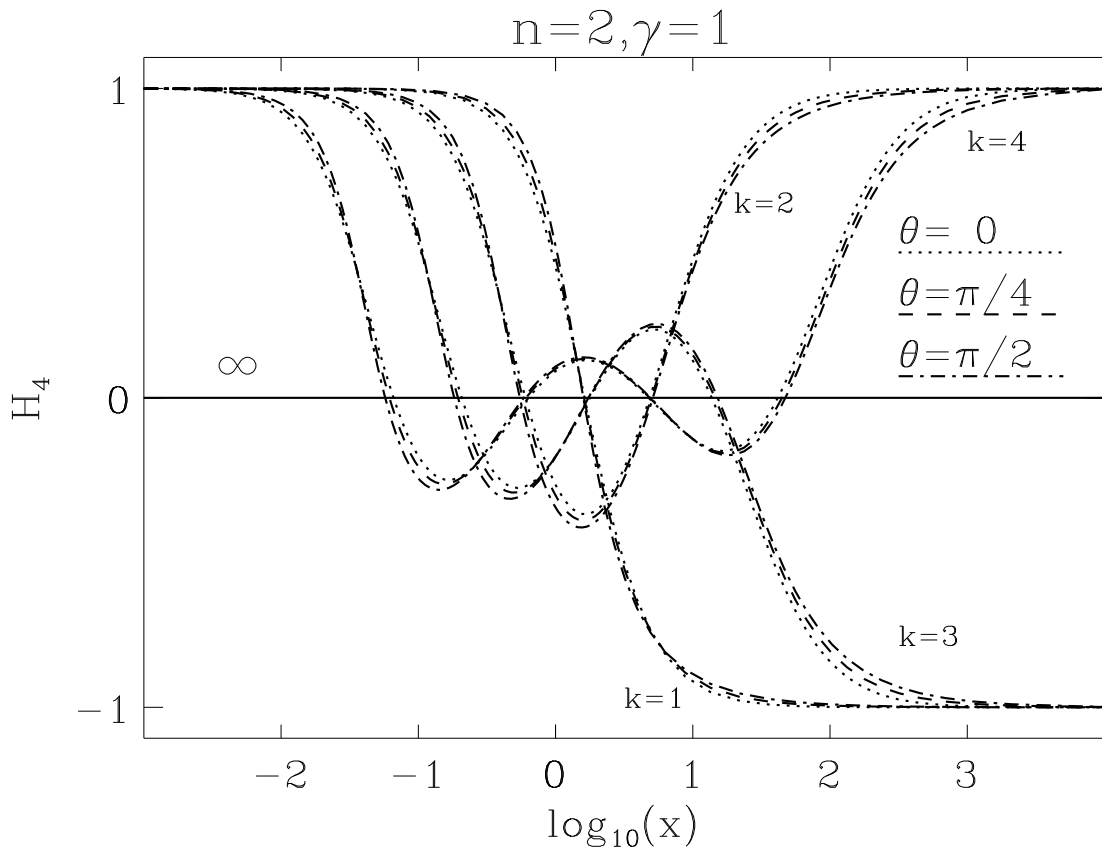


Fig. 19d
 Same as Fig. 18a for the gauge field function H_4 .

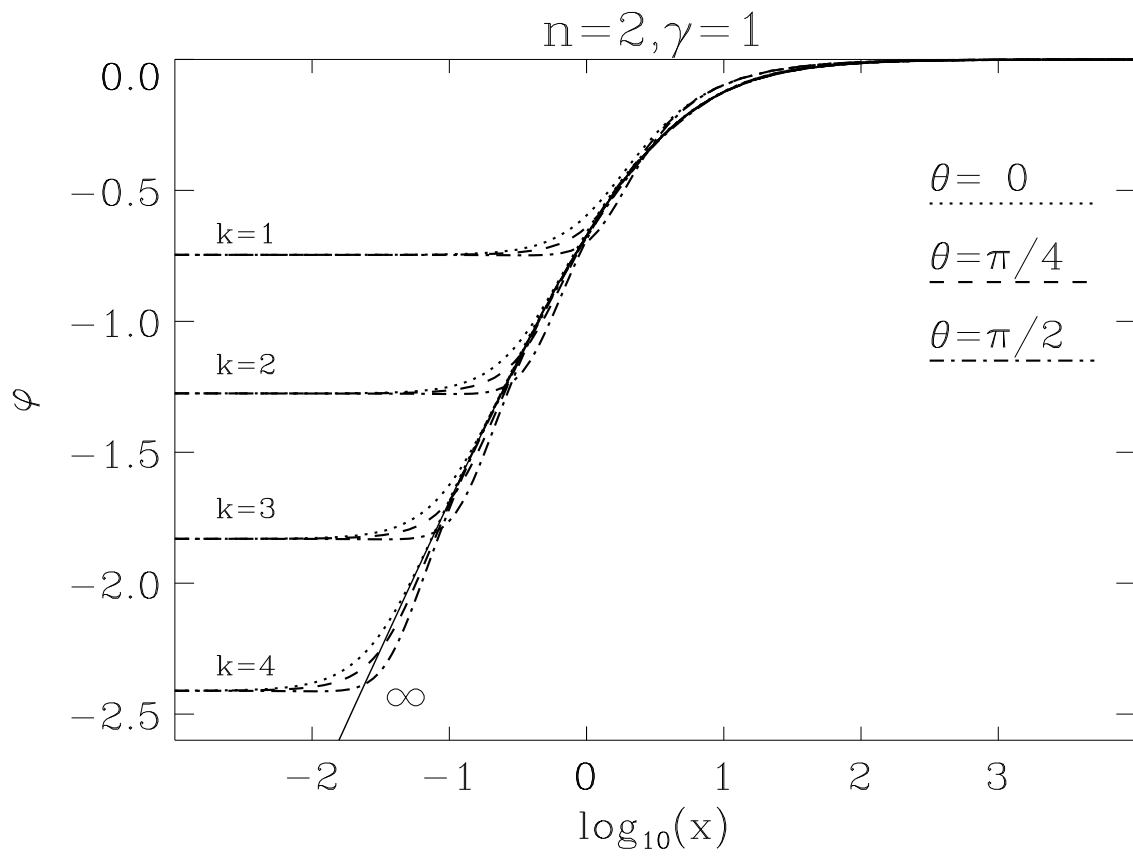
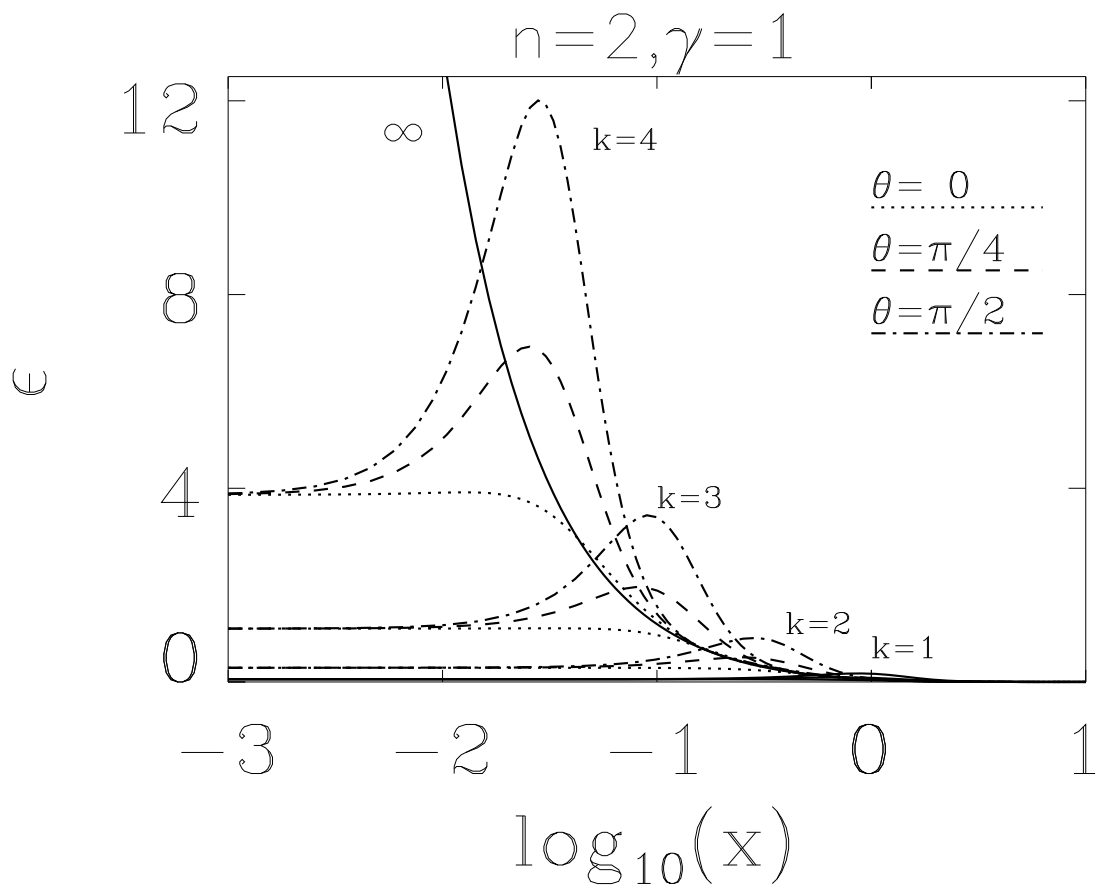


Fig. 20
Same as Fig. 18a for the dilaton function φ .



Same as Fig. 18a for the energy density of the matter fields ϵ .

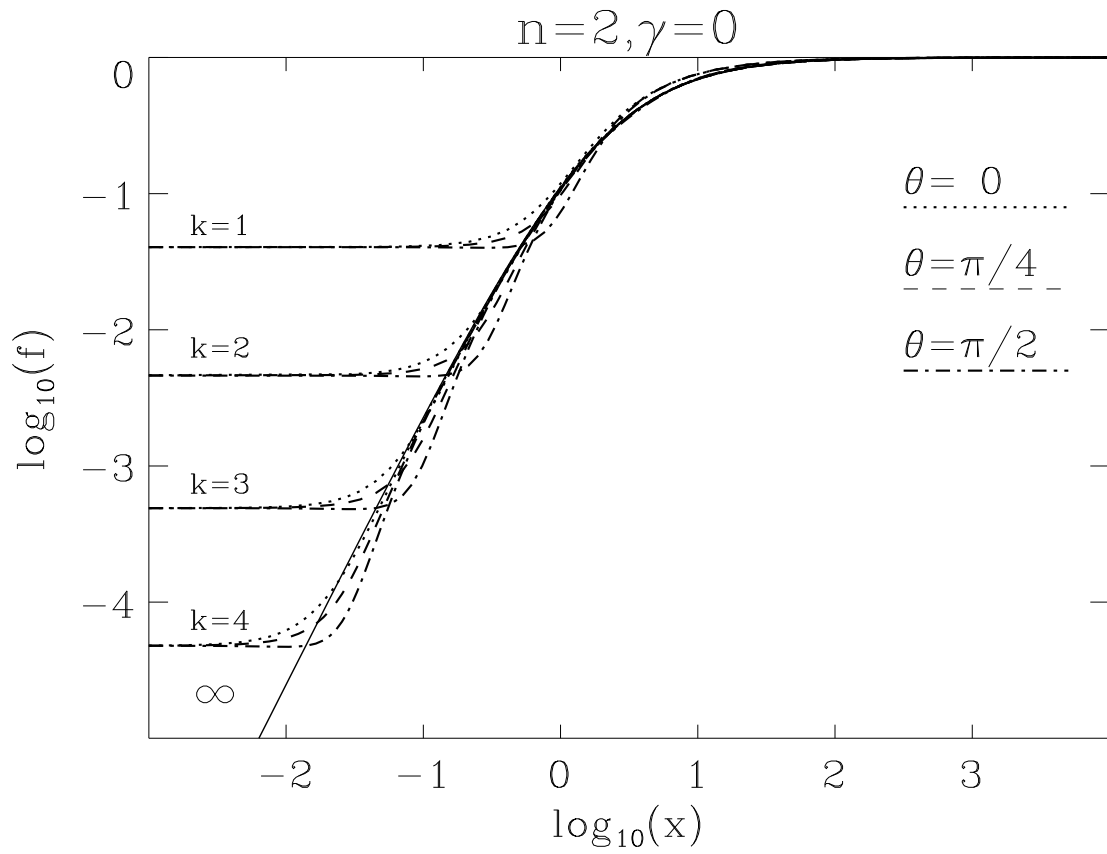


Fig. 22a

The metric function f of the EYM solutions with $n = 2$, and $k = 1 - 4$ is shown as a function of the coordinate x for the angles $\theta = 0, \pi/4$ and $\pi/2$. Also shown is the metric function of the limiting RN solution.

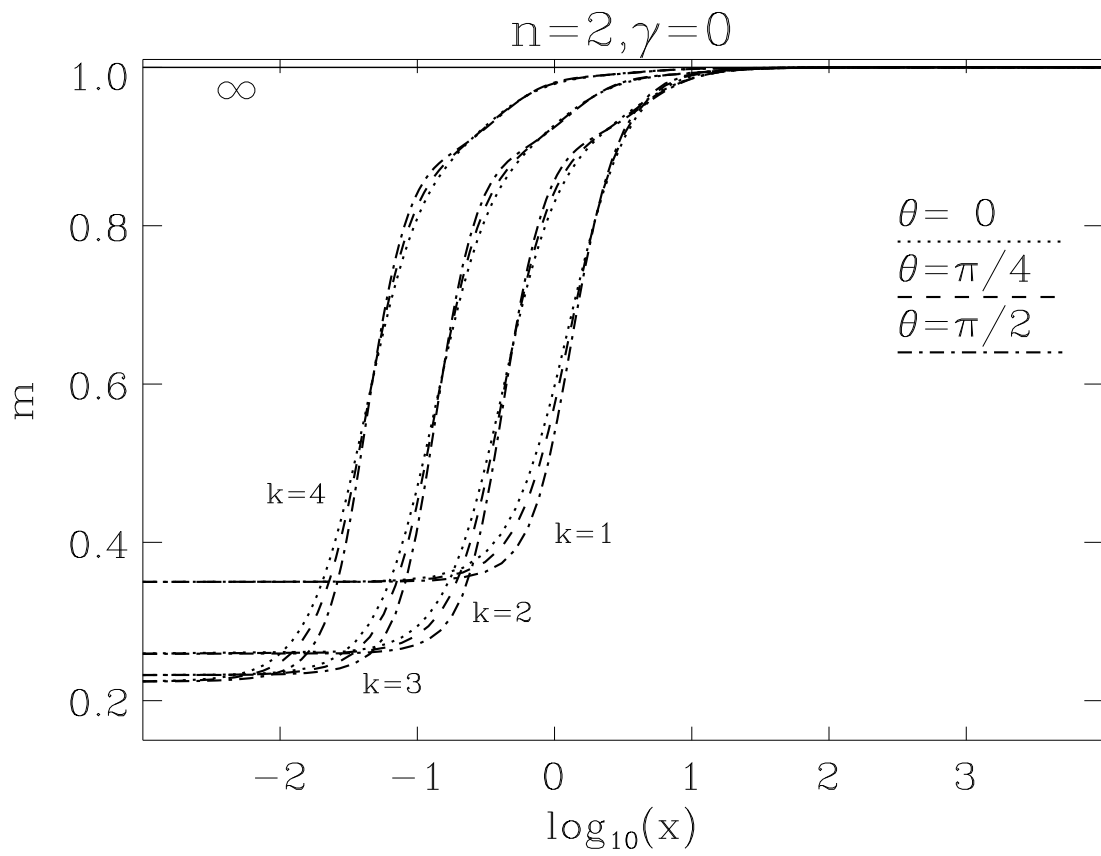


Fig. 22b
Same as Fig. 22a for the metric function m .

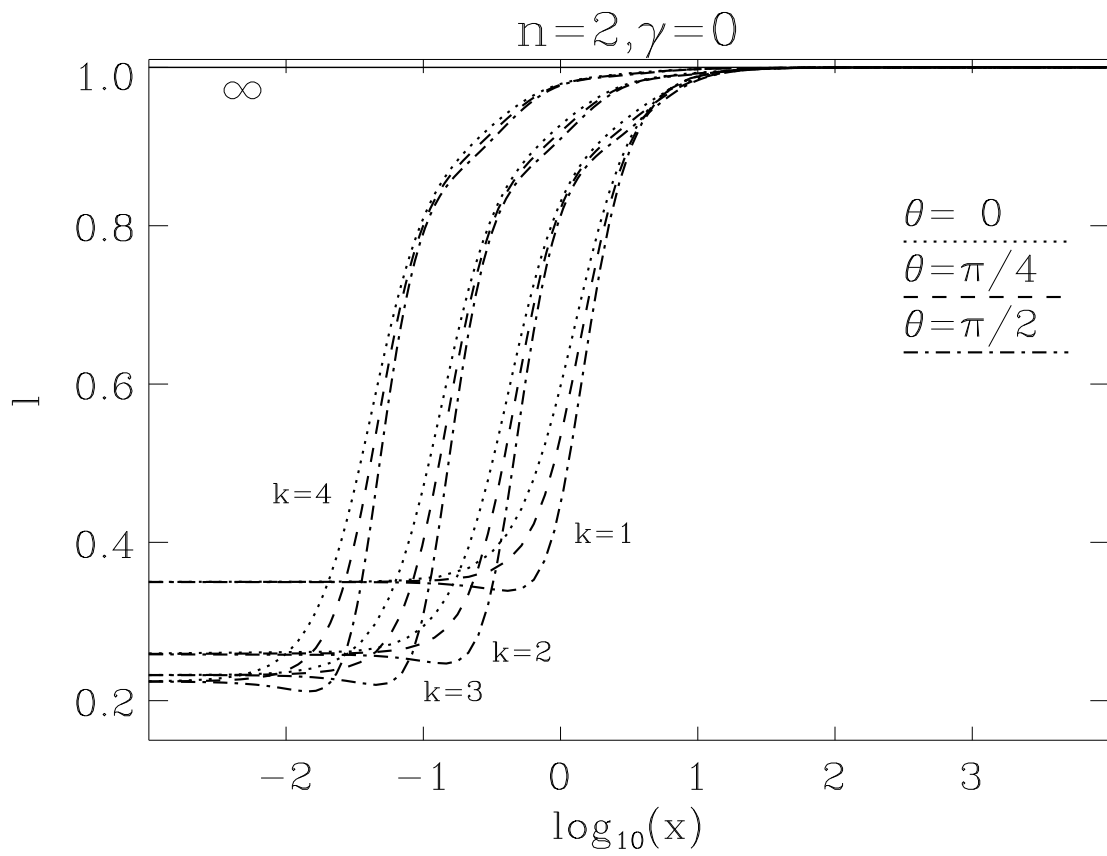


Fig. 22c
Same as Fig. 22a for the metric function l .

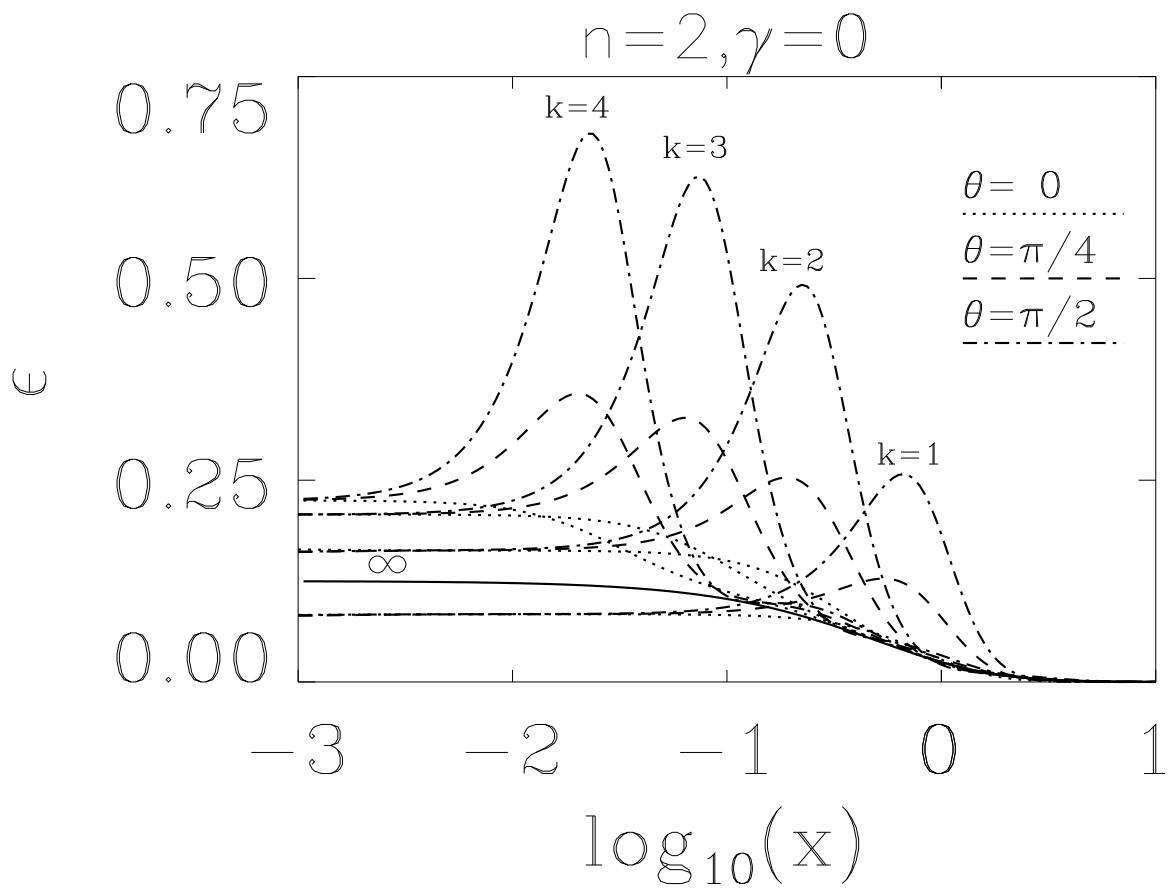


Fig. 23

Same as Fig. 22a for the energy density of the matter fields ϵ .

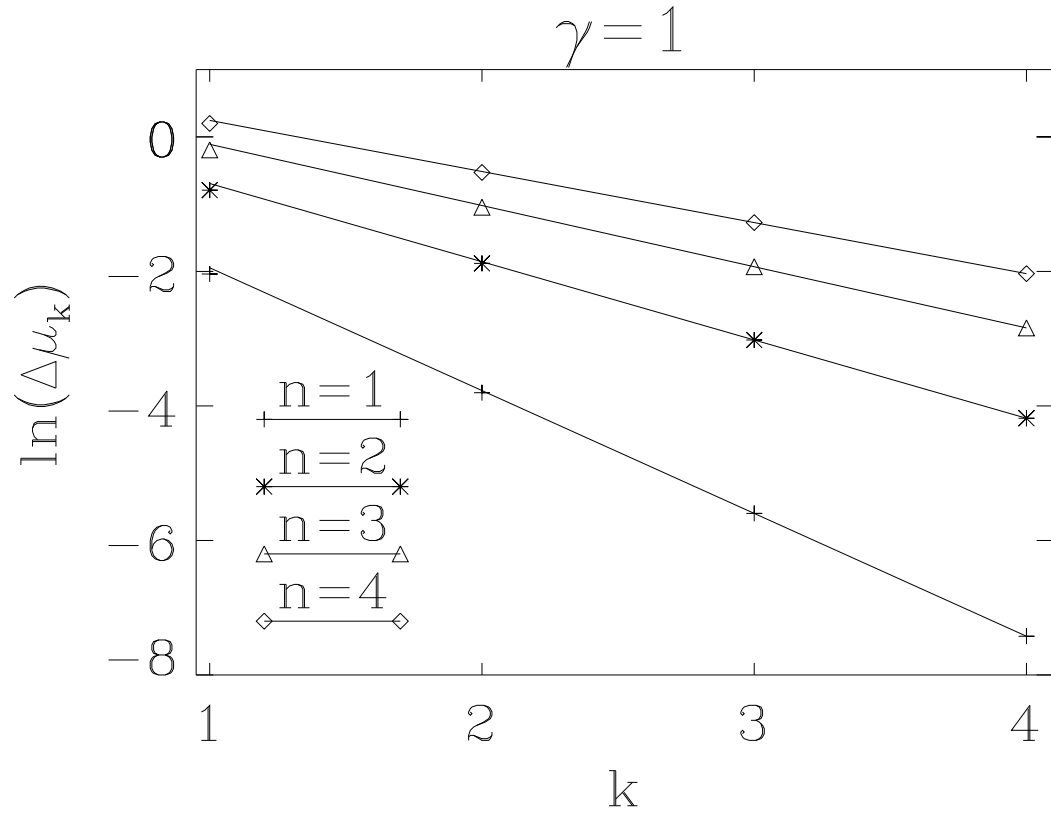


Fig. 24a

The logarithm of the absolute deviation from the limiting solution $\Delta\mu_k = \mu_\infty(\infty) - \mu_k(\infty)$ for the EYMD masses as a function of the node number k with dilaton coupling constant $\gamma = 1$ for winding number $n = 1 - 4$. The straight lines are fitted to the data with $k = 3$ and $k = 4$.

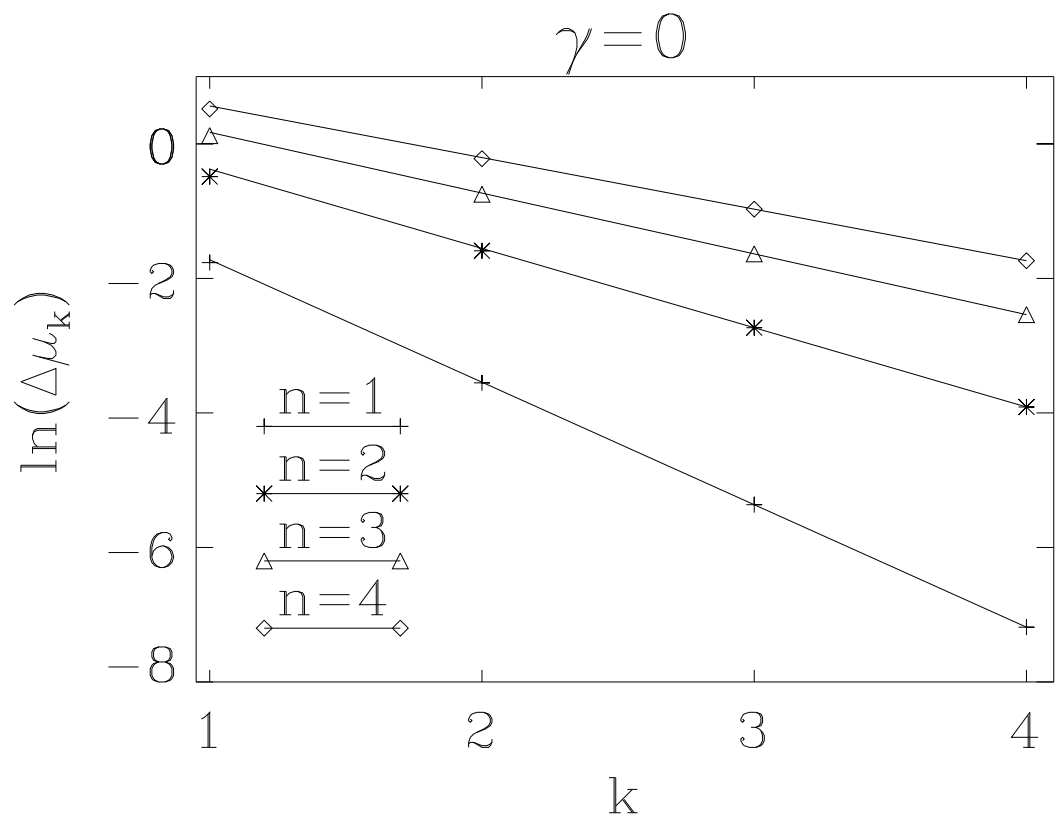


Fig. 24b
Same as Fig. 24a for the EYM solutions, i. e. $\gamma = 0$.